DEVELOPMENT OF NOVEL EMBEDDED DSP ARCHITECTURE FOR NON-INVASIVE GLUCOSE ANALYSIS

Thesis submitted to Goa University

for the award of the degree of

Doctor of Philosophy

In

Electronics

By

Jivan Shrikrishna Parab

Supervisor
Prof. G. M. Naik

Department of Electronics
Goa University, Goa-403206

JULY 2010

Dedicated with love to my family

Shri.Shrikrishna Ganesh Parab

Smt.Shilpa Shrikrishna Parab

Miss.Jyoti Shrikrishna Parab

Miss.Jagruti Shrikrishna Parab

Statement

I hereby state that this thesis for Ph.D degree on **"Development of Novel Embedded DSP Architecture for Non-Invasive Glucose Analysis"** is my original contribution and the same has not been submitted on any occasion for any other degree or diploma of this University or any other University / Institute. To the best of my knowledge, the present study is the first comprehensive work of its kind in the area mentioned. The literature related to the problem investigated has been cited. Due acknowledgements have been made wherever facilities and suggestions have been availed of.

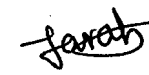

Place: Goa University
Date: 28/7/2010

(J. S. Parab)
Candidate

Certificate

This is to certify that the thesis entitled **"Development of Novel Embedded DSP Architecture for Non-Invasive Glucose Analysis"**, submitted by Mr. Jivan Shrikrishna Parab, for the award of the degree of Doctor of Philosophy in Electronics, is based on his original and independent work carried out by him during the period of study, under my supervision. The thesis or any part thereof has not been previously submitted for any other degree or diploma in any University or institute.

2/8/2010

Place: Goa University
Date: 2/8/2010

(Prof. G. M. Naik)
Research Guide

The changes suggested by examiners have been incorporated

CERTIFIED TRUE COPY

9/4/2011
(External Examiner)

guide 9/4/11

ACKNOWLEDGEMENTS

This work is based on research conducted between August 2006 to May 2010 at the Electronics Section, Department of Physics, Goa University. The study was supported by the Indian Council of Medical Research (ICMR). Many people have contributed to the writing of this thesis, and therefore deserve to be mentioned.

It gives me great pleasure to express my deep sense of gratitude towards my research guide Dr.Gourish M. Naik, Professor & Head, Department of Electronics, Goa University, under whose able guidance and constant inspiration enabled me to complete my thesis. It has been an honour and a great privilege that I got this opportunity to work under him. I also express my sincere appreciation for his endless support, encouragement, great inspiration, ideas and comments throughout the completion of my research.

Thanks to Dr. Rajendra S. Gad, Associate Professor, Department of Electronics, Goa University for helping me in designing the Multivariate model to predict the glucose concentration in whole blood. I am grateful to Dr.R.K.Kamat for having inspired me to take up research in the area of embedded biomedical field and guiding me to write research papers which were published in reputed journals.

I acknowledge the advice and the assistance received from Prof. K. S. Rane, Dean, Faculty of Natural Science and Prof. J.A.E. Desa, Head, Department of Physics. I would also like to acknowledge the technical advice given by subject experts Dr. Prashant Potnis, Head, Technology department, Syngenta Pvt. ltd and Dr.R.B.Tangsali, Associate Professor, Physics Department ,Goa University during the various phases of my research work. I would like to extend my thanks to Dr. Y.S. Valaulikar, Department of Mathematics, Goa University, for helping me in understanding the concept of Partial Least Square Regression (PLS).

I am thankful to Dr. Kaustubh Priolkar & his research group from the department of Physics for providing valuable support with regard to FTIR spectrophotometer to record the spectras of blood constituents. I am thankful to Dr.Bhagat Singh, Goa Medical College, for providing me with various blood constituents samples to calibrate the Multivariate model.

I would like to express my gratitude to Mr. Jaiprakash Kamat and Mr. Agnelo Lopez for helping me to build the embedded board, that allowed me to run my experiment; without their help, I would have not completed my research.

I would also appreciate the efforts taken by Brenda Nazareth for proof reading my thesis. Special thanks go to Research Scholars of our Department, Francis Fernandes, Ingrid Anne Nazareth, Vinaya Gad, Sulaxana Vernekar and Mruga Phaldesai.

I enjoyed every moment which I experienced during my research work which transformed me to the present form. I thank all my colleagues for giving me valuable suggestions towards the completion of this research work.

I express my deep sense of gratitude to my sisters Jyoti and Jagruti, for their patience and understanding as well as taking much of the responsibilities at home. I shall forever remain indebted to my parents for the long hours that I owed them, I have spent for the thesis. I will be failing in my duties, if I do not mention the support and encouragement which I received from my friends Samir Patil, Siddharth Sawant, Rupesh, Anuj, Kunal, Roy, Caje, Rodney, Ribert, Jesni, Jaimala, Yogan, Mamata, Mahesh, Kaustubh, Seshu and Sapana.

Finally, I wish to express my gratitude to God, whose presence has given me strength to finish the research work.

Jivan S. Parab,

July 2010

TABLE OF CONTENTS

4. SOFT-CORE FOR NON-INVASIVE GLUCOMETER

5. MULTIVARIATE DATA ANALYSIS

LIST OF TABLES

LIST OF FIGURES

ABBREVATIONS

A/D: Analog to Digital converter

ADP: Adenosine Diphosphate

ARM: Advanced RISC Machnine

ASHA: Accredited Social Health Activists

ATP: Adenosine Triphosphate

BEMR: Bio-Electromagnetic Resonance

CI: Confidence Interval

CIE: International Commission on Illumination

DSP: Digital Signal Processing

EDA: Electronic Design Automation

EGA: Clark Error Grid Analysis

FDA: Food and Drug Administration

FPGA: Field Programmable Gate Array.

FT-IR: Fourier Transform Infrared Spectroscopy.

Hb: Deoxyhaemoglobin

HbO_2: Oxyhaemoglobin

HDL: Hardware Descriptive Language

IDE: Integrated Development Environment

IDF: International Diabetics Federation

IEC: International Electrotechnical Commission

IP: Intellectual Property

InGaAs: Indium Galium Arsenide

LASER: Light Amplification by Stimulated Emission of Radiation

LE: Logic Elements

LUT: Lookup table

MAC: Multiply and Accumulate

MIPS: Million Instructions Per Second

MTBF: Mean Time Between Failure

MVSPC: Multivariate Statistical Process Control

NDEP: National Diabetes Education Program

NIDDM: Non-insulin-Dependent Diabetes Mellitus

NRHM: National Rural Health Mission

PCA: Principal Component Analysis

PCR: Principal Component Regression

PhRMA: Pharmaceutical Research and Manufacturers of America

PLSR: Partial Least Square Regression

PMT: Photo multiplier tube

QTH: Quartz Halogen Tungsten

RISC: Reduced Instruction set computing

RMSE: Root Mean Square Error

SEC: Standard error of calibration

SEP: Standard error of prediction

SNR: Signal to Noise Ratio

SOC: System On Chip

SOPC: System on programmable chip

VHDL: Very-high-speed integrated circuit HDL

WHO: World Health Organization

PREFACE

This thesis is about the "Development of Novel Embedded DSP architecture for Non-Invasive Glucose Analysis". This architecture is developed using Altera NIOS II soft-core platform designed using Altera DE2 board having target as CYCLONE II (EP2C6) to estimate the level of blood glucose in the human body non-invasively by using the NIR radiation in the range 2.0 μm to 2.5 μm. PLSR model, based on SIMPLS algorithm, is also developed in C language and ported on NIOS II platform to estimate the glucose concentration.

In this thesis, Chapters I & II emphasize the need to develop blood glucose measuring technique non-invasively and describe other techniques presently being used to quantify glucose. The working principles of different radiation based techniques of measuring glucose are described and reasons for choosing NIR based methods for the research work are explained.

Chapter III gives the methodology to design an embedded DSP platform for blood glucose analysis non-invasively and highlights the spectrophotometer design based on embedded system. It also discusses about the selection of light source, sample holder, detector and signal conditioning circuit.

Chapter IV describes the design of FPGA soft-core processor for non-invasive glucose analysis. Here various possibilities of FPGA selection are explained and Altera FPGA is used to design the embedded platform for blood glucose measurement non-invasively.

Chapter V discusses about the Multivariate Data Analysis. Here the designed PLSR model is tested and verified for different multivariate problems.

Chapter VI gives the results obtained. The standard glucose solution mixed with other influential variants normally found in the blood tissue, were used to test the reliability and the accuracy of the designed system. The results obtained were subjected to RMSE, EGA and correlation coefficient.

Jivan S Parab,
July 2010

LIST OF PUBLICATIONS

International /National Journal :

1. **Parab.J.S**, Gad.R.S, Naik.G.M, **"Noninvasive Glucometer Model Using PLSR technique for Human Blood Matrix"**, Journal of Applied Physics(JAP), AIP Publishing, Issue 10, volume 107,May 2010,pp104701(1-5).

2.**Parab.J. S**, Gad.R.S, Naik.G.M, **" Implementation of DSP algorithms on reconfigurable embedded platform"**, Journal of Electrical and Electronics Engineering Research (JEEER), Volume 1(1),November 2009, pp 023-029.

3. **Parab.J. S**, Paliekar R.S, Naik.K.V, Kamat.R.K. & Naik.G.M, **"Heterogeneous Embedded system with 'Microcontroller-CPLD' based shared memory interface for sensor application"**, Sensor Review,Emerald U.K, Issue: 4, Volume 25, september 2005, pp.287 - 291.

4. **Parab .J.S**, R. S. Gad, G.M .Naik **"NIOS II based platform for Blood Glucose Analysis "** International journal of VLSI Design, Hindawi publishers,USA, Accepted.

5. S. R. Vernekar, **Parab .J.S**, R.S.Gad, G.M.**Naik " Precision Farming for high yield: SoC based low cost instrumentation"** International journal of VLSI Design, Hindawi publishers,USA, Accepted.

6. **Parab.J. S**, Gad.R.S, Naik.G.M " Multivariate system spectroscopic model using Lorentz Oscillators and PLSR analysis", Review of Scientific Instruments, AIP Publishing, Under Review.

7. **Parab .J.S**, R. S. Gad, G. M. Naik, **"Design of NIOS II Soft-core for flash based Matrix manipulation"**, Institution of Electronics and Telecommunication Engineers (IETE) Journal of Research , Under Review.

Papers presented in International/National seminars:

1. **J.S.Parab**, R. S. Gad, G. M. Naik," **Development of Online Embedded Reconfigurable, Real Time FPGA based Unit for Medical application"** UGC sponsored National Seminar on "Emerging trends and Development in Embedded system", Goa, 13th & 14th March 2007.

2. **J. S. Parab**, R. S. Gad, G. M. Naik, **"Implementation of Signal processing Algorithms on Soft -core platform"** UGC Sponsored National Seminar on Recent Advances in Sensors and Instrumentation,NSRASI-07,Shankarrao Mohite Mahavidhyalaya, Akluj, Maharastra,15th & 16th October, 2007.

3. R. S. Gad, **J. S. Parab**, S. Sawant, G. M. Naik, **"Design of Dual Stage Monochromator for Non-Invasive Glucometer using embedded control"** National Conference on Sensors, NCS05, Thapar Institute of Engineering and Technology, Punjab, 25th & 26th November 2005.

4. **J. S. Parab**, R. S. Gad, G. M. Naik, S. S. Sawant, **"Development of Novel Embedded DSP architecture for Non-Invasive glucose analyses"**,NSIAE-2006,Chopda, Maharastra, 28th & 29th January 2006.

5. R. S. Gad, **J. S. Parab**, G. M. Naik **"Brain–computer interfaces using Near Infra Red technique"** NSIAE-2006, Chopda, Maharastra,28th & 29th January 2006.

6. R. S. Gad, **J. S. Parab**, G. M. Naik, **"Estimation of Blood Glucose Electronically using PLS Technique"** UGC Sponsored National Seminar on Recent Advances in Sensors and Instrumentation, NSRASI-07, Shankarrao Mohite Mahavidhyalaya, Akluj, Maharastra ,15th & 16th October 2007.

7. **J. S. Parab**, R. S. Gad, G. M. Naik," **Computerized Biosignal Detection"**, UGC Sponsored National Seminar on Recent Advances in Sensors and Instrumentation, NSRASI-07, Shankarrao Mohite Mahavidhyalaya, Akluj, Maharastra, 15th & 16th October 2007.

8. H.S.Gad, **J. S. Parab**, R. S. Gad, G. M. Naik **"Bi-Variants Eco-system entropy model using Lorentz oscillator"** organized by Mulsi Institute of Technology of Research (MITR), Pune, Maharastra, 16th -18th February 2009.

9. **J. S. Parab**, R. S. Gad, G. M. Naik," **FPGA based Wireless Data Acquisition System for Weather Radar Application"**,National Conference on Unthethered Commmmunication , IET West zone ,Goa,21st August 2006.

10. **J. S. Parab**, R. S. Gad, G. M. Naik **"Soft-core based embedded platform for Non-Invasive Glucose analysis"**,4th annual National symposium on on VLSI & EMBEDDED SYSTEM, Goa Chapter , 5th February 2010.

11. S.Vernekar , **J. S. Parab**, G. M. Naik **"Use of Electronic Instrumentation in preceision farming"** 4th annual National symposium on on VLSI & EMBEDDED SYSTEM, , Goa Chapter, 5th February 2010.

12. V.R.Gad , F.F. Fernandes, **J.S Parab**, G.M Naik **"Wireless TCP/IP control softcore based SOC platform for Smart Appliances"**, IEEE conference on New Generation Wireless communication technology organised by communication of society and L&T institute of technology, Mumbai,Maharashtra, 30th - 31st October 2009.

13. N.Shrivastava, G.Naik, B.Harmalkar, A.Sawant, **J. S. Parab**, R. S. Gad **"Strip Base Resistive Glucometer using ARM LPC2138"**, 4th annual National symposium on VLSI & EMBEDDED SYSTEM, Goa Chapter, 5th February 2010.

CHAPTER 1

INTRODUCTION

1.1Introduction

"Man may be the captain of his fate, but he is also the victim of his high blood sugar".[1] Over the last century, human behaviour and lifestyles have changed, resulting in a dramatic increase of diabetes over the world. Especially the past two decades have seen an explosive increase in the number of people diagnosed with diabetes as well as obesity. Diabetes itself may not be a serious disease but the long-term complications associated with the disease like eye damage which leads to Blindness, Kidney damage, Loss of feeling in the extremities, Nerve damage, Slow healing of wounds, Amputations of toes, feet or legs and often most seriously Cardiovascular Diseases. It is clear that the tight control of blood glucose level will lower the risk of complications. Many of the complications do not show up until after many years, even decades of having these diseases. They usually develop silently and gradually over the time. Talking or thinking about long term complications and the cost required to tackle the disease can be scary. It can be tough for anyone to change their lifestyle today, to decrease the risk of health problems that may not appear for decades. A healthy diet, regular physical activity, maintaining a normal body weight and avoiding tobacco use, can prevent or delay the onset of diabetes. In order to detect diabetes, it is necessary to measure the blood glucose level by using the various techniques discussed in Chapter 2. This trend of increasing prevalence of diabetes and obesity has already imposed a huge burden on health care systems and this will continue to increase in the future.[2] Due to the surge of the 'diabetes' disease, many technological players put their efforts to design a user friendly module either in invasive or non-invasive mode. It is evident that there is a need for good instrumentation development to monitor blood glucose non-invasively. Thus the problem was formulated to develop various skills leading to blood glucose analysis using a reconfigurable embedded system platform.

1.2 Worldwide Diabetics Breakdown

Diabetes touches almost every family at some time or the other. Most people are familiar with the long-term complications of the disease. If patients adhere strictly to a proper diet, exercise, medication and check their blood glucose regularly, they are able to maintain their health, and indeed, lead relatively normal lives.

Based on the survey done by the International Diabetes Federation (IDF) on October 2009, it is estimated that 285 million people around the world have diabetes. This total is expected to rise to 438 million within 20 years. Each year a further 7 million people develop diabetes. In 2007, survey showed that India had the largest number of people with diabetes (40.9 million) followed by China (39.8 million), the United States (19.2 million), Russia (9.6 million) and Germany (7.4 million).[3][4][5][6]

By 2025, the largest increase in diabetes prevalence will take place in developing countries that is due to socio-economic disparities in the world and diabetes is more due to stress and associated life style. The survey done by IDF on Worldwide Prevalence of Diabetes Mellitus (DM), 2009, is given in Table 1.1. From the Table 1.1 it is clear that Western Pacific region (WP), South East Asia region (SEA) and Europe region(EUR) have the most diabetes affected people. Out of 59 billion affected diabetes people in SEA region, major affected population is in India i.e. 51 billion.

Diabetes is the sixth leading cause of death in the United States and a leading cause of heart disease and stroke. In 2005, 1.1 million people died from diabetes. Almost 80% of deaths occurring from diabetes in low and middle income countries. Almost half of deaths occur in people under the age of 70 years. World Health Organization (WHO) projects that deaths from diabetes will double between 2005 and 2030. As per IDF, every 10 seconds two people develop diabetes and a person dies from diabetes-related causes.[7] Due to increase in

the diabetes at such an alarming rate, all the countries should take necessary initiative to reduce the onset of this disease.

Table 1.1: Worldwide Prevalence estimates of Diabetes Mellitus (DM),2009

2009	Population (20-79)	Diabetes prevalence adjusted to		Number of people with DM (000's) in the 20-79 age-group							
Region	000s	National population	World population	Rural	Urban	Male	Female	20-39	40-59	60-79	Total
AFR	378,550	3.2%	3.8%	3,891	8,198	6,193	5,896	4,062	5,146	2,873	12,089
MENA	344,469	7.7%	9.3%	8,098	18,548	13,260	13,386	6,127	13,742	6,777	26,646
EUR	646,367	8.6%	6.9%	Not available	Not available	27,787	27,600	4,516	20,812	30,059	55,388
NAC	319,893	11.7%	10.2%	1,137	6,505	17,378	19,984	4,162	15,431	17,769	37,362
SACA	286,922	6.3%	6.6%	2,117	15,842	8,100	9,858	2,226	8,974	6,758	17,958
SEA	837,732	7.0%	7.6%	33,512	25,150	31,620	27,042	12,577	28,819	17,266	58,662
WP	1,530,822	5.0%	4.7%	29,031	34,144	37,712	38,997	10,505	39,336	26,868	76,709
Totals	4,344,755	6.6%	6.4%	77,785	108,387	142,050	142,764	44,176	132,260	108,370	284,814

AFR: Africa region, *MENA: Middle East North Africa region,* ***EUR:*** *Europe*
NAC: North America and Carribean region, *SACA: South and cetral American region*
SEA: South East Asia region, *WP: Western Pacific region*

Initiatives adopted

Almost 24 million people, or about 8 % of the population, currently have diabetes in US. There is no question that every community needs to take action, to prevent this epidemic from spreading. Americans of all ages, races, and ethnic groups are vulnerable, and it is especially a topic of concern for older adults. More than 12 million adults aged 60 and older have diabetes.

The answer to control this silent killer lies in awareness, education, early diagnosis, and proper treatment. The National Diabetes Education Program (NDEP) - a joint program of the National Institutes of Health and the Centers for Disease Control and Prevention, have created "The Power to Control Diabetes Is In Your Hands", an awareness campaign to help older adults with diabetes and their loved ones to learn how to manage the disease, live

longer and healthier lives. The outreach effort focuses on the importance of promoting a comprehensive approach to control diabetes by managing blood glucose (blood sugar), blood pressure, and cholesterol, taking prescribed medications, making healthy food choices, and engaging in regular physical activity. The campaign also provides important information about Medicare benefits available to people with diabetes.

The global diabetes community including IDF member associations, diabetes organizations, NGOs, health departments, civil societies, individuals and companies develop an extensive range of activities, tailored to a variety of groups. Activities organized each year include Radio and television programmes, sports events, free screenings for diabetes and its complications, public information meetings, poster and leaflet campaigns, Diabetes workshops and exhibitions, press conferences, Newspaper and magazine articles.

Looking at figures given in Table 1.1, Government of India started National Diabetes Control Programme. India is also planning a compulsory diabetes check for people above forty years in rural areas. Accredited Social Health Activists (ASHA) is a scheme to facilitate mandatory check-up of the rural population above the age of 40 years for diabetes as well as hypertension. Health infrastructure developed through National Rural Health Mission (NRHM) can be leveraged for combating diabetes in India which has the largest number of diabetics in the world. The health ministry plans to rope in six lakh ASHAs.

1.3 Diabetes overview:

Diabetes Mellitus, more commonly known only as diabetes is a chronic disease that occurs either when the pancreas does not produce enough insulin or when the body cannot effectively use the insulin it produces.[8] Insulin is a hormone that regulates blood sugar. Hyperglycemia, or raised blood sugar, is a common effect of uncontrolled diabetes and over

a period of time, leads to serious damage to many of the body's systems, especially the nerves and blood vessels.

1.3.1 Types of Diabetes:

There are many types of diabetes that affect different kinds of individuals and are treated in slightly different ways. **Type 1 diabetes** (previously known as insulin-dependent, juvenile or childhood-onset) is the most serious type and affects 5 – 10 % of the diabetic population. It is a disease that usually develops during childhood or adolescence and is characterized by a severe deficiency of insulin secretion, resulting from atrophy of the islets of Langerhans, and causes hyperglycemia. **Type 2 diabetes** (formerly called non-insulin-dependent (NIDDM) or adult-onset) is most common form of diabetes which affects 90-95% of the diabetes population. This is a common form that develops especially in adults and most often in obese individuals and that is characterized from hyperglycemia resulting from impaired insulin utilization coupled with the body's inability to compensate with increased insulin production.[9] **Gestational diabetes** is hyperglycemia with its onset first recognized during pregnancy.

1.3.2 Causes and Symptoms of Diabetes

Causes:

Hereditary or Inherited Traits, Increasing Age, Poor Diet (Malnutrition Related Diabetes), Obesity and Fat Distribution, Sedentary Lifestyle, Stress, Drug Induced (clozapine, olanzapine, risperidone, quetiapine and ziprasidone), Infection to pancreas, Sex (Diabetes is commonly seen in the elderly, especially males), Hypertension, high serum lipids and lipoproteins are the causes of diabetes.

Symptoms of Diabetes:

In both types of diabetes, signs and symptoms are more likely to be similar as the blood sugar is high, either due to less or no production of insulin, or insulin resistance. In any case, if there is inadequate glucose in the cells, it is identifiable through certain signs and symptoms. These symptoms are quickly relieved and also reduce the chances of developing serious health problems once the diabetes is treated. Common symptoms of diabetes are Nausea, Vomiting causing fast weight loss, Increased fatigue, Polydipsia, Polyuria, Polyphegia, weight fluctuation, blurry vision, irritability, infections and poor wound healing.

1.3.3 Physiological Aspect

Glucose is the most essential energy carrier in the human organism. Glucose level in blood levels preceding a meal (preprandial) are less than 100 mg / dL (5.5 mmol / L) in plasma and 89 mg / dL (4.9 mmol / L) in whole blood or capillary. After eating (postprandial) those values should not exceed 140 mg / dL (7.8 mmol / L) in plasma and 125 mg / dL (6.9 mmol / L) in whole blood or capillary, as shown in Table 1.2.[10] D-Glucose can be found in two different stereo isomers, i.e. the α and the β anomeric form, whose structure can be seen in Figure 1.1.[11]

The sugar concentration in blood is controlled by the pancreas. In pancreas there are clusters of cells called islets of Langerhans, which are formed by alpha or beta types. Alpha clusters produce the hormone glucagon, which raises the level of blood sugar. Beta cells produce insulin, which is responsible for helping the body to transform glucose into energy which helps to maintain the normal glucose level in blood.

Table 1.2: Glucose level consequences in whole blood.

mmol/l	mg/dL	Interpretation
2.0	35	extremely low, danger of unconsciousness
3.0	55	low, marginal insulin reaction
4.0 -6.0	70-100	normal preprandial in nondiabetic
8.0	150	normal postprandial in nondiabetic
10.0	180	maximum postprandial in nondiabetic
15.0	270	a little high to very high depending on patient
16.5 -20.0	300 -360	danger
22	400	max mg/dL for some metres and strips
33	600	high danger of severe electrolyte imbalance

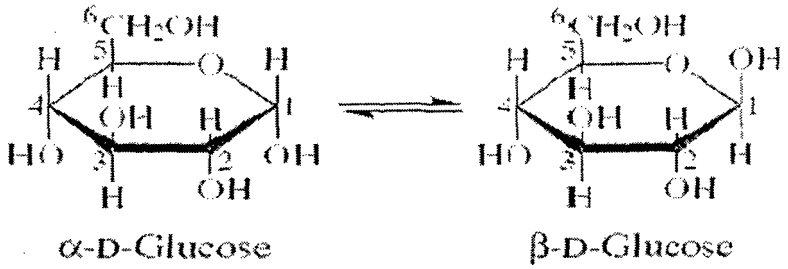

Figure 1.1: Glucose molecule structure.

1.3.4 Treating Diabetes

There is no permanent cure to diabetes, but people with diabetes can lower the occurrence of these and other diabetes complications by controlling blood glucose, blood pressure, and blood lipids.[12]

- Diet plays a significant role in controlling the diabetes. The diabetic diet may be used alone or else in combination with insulin doses or with oral hypoglycemic drugs.
- To survive, people with Type 1 diabetes must have insulin delivered by injection or a pump.

- Many people with diabetes also need to take medications to control their cholesterol and blood pressure.

Self-management education or training is a key step in improving health outcomes and quality of life. Common oral drugs used to control diabetes are metformin, gliclazide, glitazones, Exenatide (Byetta), Sitagliptin (Januvia), Less common drugs are meglitinides, amaryl, Xenical, glitazone . Keeping in mind the complications of high blood glucose, doctors are now advising patients to take insulin injection for control of glucose in blood. Apart from oral tablets many physicians recommend insulin to control the diabetes. There are various types of insulin like:

Rapid onset-fast acting insulin: Since it is fast acting, it starts working within 1 to 20 minutes. It is clear in appearance and its peak time is about one hour later and lasts for 3 to 5 hours. The two rapid onset-fast acting insulin types currently available are:

- Novo Rapid (Insulin Aspart)
- Humalog (Lispro)

Short acting insulin: It looks clear and begins to lower blood glucose levels within 30 minutes so one needs to take the injection half an hour before eating. Short acting insulin has a peak effect of four hours and works for about six hours. Short acting insulin types, currently available include:

- Actrapid
- Humulin
- Hypurin Neutral (bovine highly purified beef insulin)

Intermediate acting insulin: Intermediate acting insulin looks cloudy. They have either protamine or zinc added to delay their action. This insulin starts to show its effect about 90 minutes after it is injected and has a peak of 4 to 12 hours and lasts for 16 to 24 hours. Intermediate acting insulin presently available with protamine includes:

- Protaphane
- Humulin NPH
- Hypurin Isophane (bovine)

Mixed insulin: Mixed insulin is cloudy in appearance. It is a combination of either a rapid onset - fast acting or a short acting insulin and intermediate acting insulin. Its advantage is that two types of insulin can be given in one injection. When it shows 30 / 70, it means 30 % of short acting insulin is mixed with 70 % of intermediate acting insulin. The mixed insulin currently available includes:

- NovoMix30
- Humalog Mix 25
- Mixtard 30/70 , Mixtard 20/80

Long acting insulin: There are two kinds of long acting insulin available in market, both with clear appearance.

- Lantus
- Levemir – (It has a relatively flat action and can last up to 24).

Apart from Allopathic treatment to control the diabetes, ayurvedic and yoga treatments are also found effective to control the blood glucose within the normal range.

Natural way of Diabetes Control and Treatments

In Ayurveda, diabetes is known as **Madhumeha** and is classified as a kapha type of disorder. Ayurveda identifies 20 types of diabetes - 4 die to Vata, 6 results from Pitta, and 10 are caused by Kapha. Some of the most useful Herbs for the Treatment of Diabetes are the following: Bitter Gourd (Momordica charantia), Bael (Aegle marmelos), Gurmar Leaves (Gymnema sylvestrae), Fenugreek (Trigonella foenum graecum), Turmeric (Curcuma longa), Onion (Allium cepa), Nayantatra (Vinca rosa), Neem (Azadirachtha indica), Garlic (Allium sativum) and Sagar gota (Ceasalpinia crista).

Ancient way of Diabetes Treatment

In the last few years different diabetic treatment methods have been used to control diabetes. While many nutritionists suggested different techniques for dieting, many doctors also recommended regular exercise to control sugar level. However, recent studies have shown that yoga too can produce major health benefits for diabetic's patient. Yoga has shown some beneficial results in controlling diabetes. Not long ago, many people were familiar with yoga as a succession of movements or poses. But today, it has emerged as one of the most convenient options to control diabetes.

The yoga exercise involves positions tailored to treat certain conditions, as well as meditation and relaxation. Yoga can stimulate the pancreas and insulin production. Regular practice of yoga actually reduces the blood sugar levels, blood pressure and the rate of progression to the complications. While most diabetics need to lose or at least maintain a certain weight limit, yoga is an excellent choice to accomplish these twin goals. The symptoms are also reduced to a large extent and so also are the number of diabetes related hospital admissions. Apart from this, some studies have also shown that certain yoga poses have the effect of massaging or stretching certain internal organs which actually lead to the increase of insulin production to maintain the glucose level.[13]

1.4 Economic impact of diabetes?

Diabetes is one of the biggest health challenges of the 21st century. Diabetes and its complications have a significant economic impact on individuals, families, health systems and countries. Diabetes is one of the costliest health problems in the world. The IDF statistics says that the direct annual healthcare cost of diabetes in 2007 globally for people aged 20 – 79 is 232 – 422 billion US dollars. It is predicted that healthcare cost will increase to 303 – 559 billion dollars by 2025. According to the WHO, direct healthcare costs of diabetes-related illnesses range from 2.5 % to 15 % of a country's annual healthcare budget, depending on local diabetes prevalence and the sophistication of treatment available. There are also indirect costs to be taken into account: lost productivity due to the inability to work, sickness, absence, disability, premature retirement or premature death. They are harder to estimate, but can be even more significant than the direct medical costs. Total costs of lost production due to diabetes problems may be as much as five times the direct healthcare cost of diabetes treatment. Families too suffer loss of earnings as a result of diabetes and its consequences.

WHO estimates that diabetes, stroke and heart disease together will cost about 555.7 billion US dollars (433 billion Euros) in China over the next 10 years, 303.2 billion dollars (236 billion Euros) in the Russian Federation, 336.6 billion dollars (263 billion Euros) in India and 49.2 billion dollars (38 billion Euros) in Brazil. These estimates are based on lost productivity, resulting primarily from premature death.

These costs are directly related to the medical complications associated with chronic hyperglycemia. Early detection and tight glycemic control are paramount to controlling the costs of the diabetes epidemic.[14] Over a year of testing at least twice per day, the average patient will spend $730 on test strips alone. By 2010 end, 14.5 million people will be

diagnosed with costs near $156 billion, and in 2020 an estimated 17.4 million people will be diagnosed with costs amounting to nearly $192 billion.[15] Despite a fragile economy, America's pharmaceutical research and biotechnology companies invested a record $65.3 billion last year in the research and development of new life-changing medicines and vaccines - an increase of more than $1.5 billion from 2008, this is according to the analysis done by the Pharmaceutical Research and Manufacturers of America (PhRMA) and Burrill & Company. Private sector has shown little interest in investing in R&D in India. The government continues to bear most of the burden, with industry chipping in with 10 to 12 %. The average R&D expenditure is around 2 % of the turnover as per a study covering 150 companies. Investment in pharmaceutical R&D has been rising steadily. From Rs 220 crores in 1997 - 98, R&D expenditure rose to Rs 260 crores in 1998 - 99 and Rs 320 crores in 1999 – 2000, Rs 1,500 crores in 2005 and 500 crores in 2009. R&D is increasingly becoming an area of focus for Indian pharmaceutical companies and most of the big players are spending about 6 - 7 % of their revenue on R&D activity. This is low as compared to the global average of 12 - 16 %. **If simple, inexpensive, reliable tests were available, they could make those measurements better and as often as required. This implies the potential for the blood glucose analysis. Hence Glucose was identified as a constituent of the human whole blood, for analysis.**

1.5 Energy Source for Life

Self-organization is a process of attraction and repulsion, in which the internal organization of a system is maintained. The concept of self-organization is central to the description of biological systems, from the sub cellular to the ecosystem level. The concept of entropy and the second law of thermodynamics suggest that systems naturally progress

from order to disorder. If so, how do biological systems develop and maintain such a high degree of order? The general kinds of processes involved in the energy cycle are: 1) **Synthetic Work:** Both plants and animals must make the complex molecules necessary for life. One example is the production of DNA - your genetic material; 2) **Electrical Work:** Each of our cells has an electric potential associated with it, this potential, or voltage, helps to control the migration of ions across the cell membranes. A major example of electrical work is in the operation of the nerves. Electrical energy transformation is essential for sensing your environment as well as for reacting to that environment in any way; 3) **Mechanical Work:** Most easily visualized is the mechanical work associated with the moving of our muscles. This muscle movement is very important and requires a lot of energy. The source of this energy is Adenosine Triphosphate (ATP). The distribution of glucose in a body is shown in Figure 1.2.

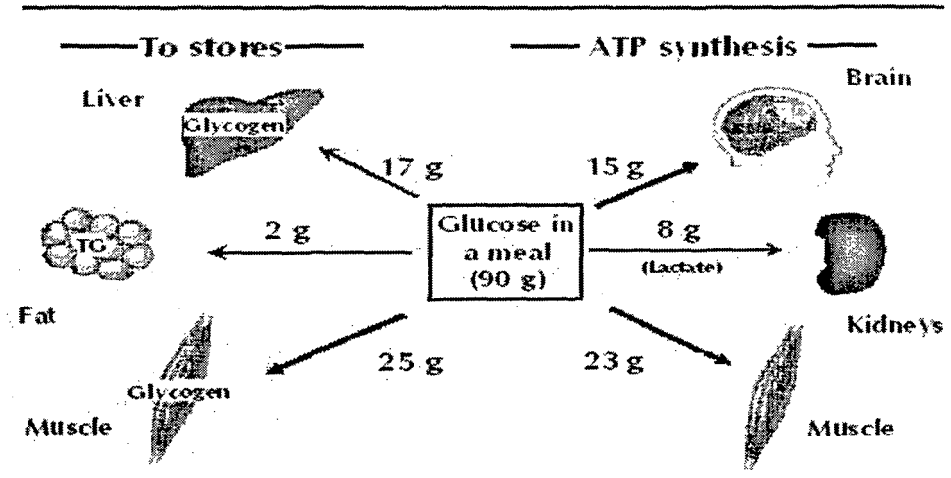

Figure 1.2: Distribution of glucose after meal.

1.5.1 An Energy Cell

A fascinating parallel between plant and animal life is in the use of tiny energy factories within the cells to handle the energy transformation processes necessary for life. In plants, these energy factories are called chloroplasts. They collect energy from the sun and

use carbon dioxide and water in the process called photosynthesis to produce sugars. Animals can make use of the sugars provided by the plants in their own cellular energy factories, the mitochondria. These produce a versatile energy currency in the form of ATP. ATP is considered by biologists to be the energy currency of life. It is present in the cytoplasm and nucleoplasm of every cell and essentially all the physiological mechanisms that require energy for operation obtain it directly from the stored ATP.[16] As food in the cells is gradually oxidized, the released energy is used to re-form the ATP so that the cell always maintains a supply of this essential molecule. In animal systems, the ATP is synthesized in the tiny energy factories called mitochondria. The most prominent roles of the cell mitochondrion are the production of ATP and regulation of cellular metabolism. Living cells use oxygen as a part of cellular respiration to produce energy, through the pathway of chemical conversion of carbohydrates, fats and proteins, into carbon dioxide and water. However, the mitochondrion has many other functions in addition to the production of ATP. Of course, the role they play as cellular furnaces by converting nutrients and oxygen into energy is immensely important.

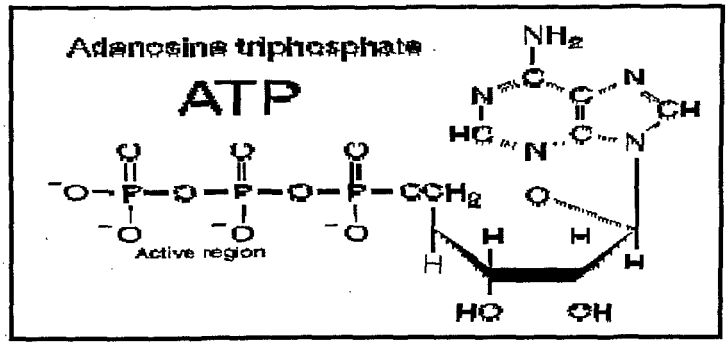

Figure 1.3: Structure of adenosine triphosphate.

The structure of ATP shown in Figure 1.3 has an ordered carbon compound as a backbone, but the part that is really critical is the phosphorous part - the triphosphate. Three phosphorous groups are connected by oxygen to each other, and there are also side oxygen

connected to the phosphorous atoms. If you remove just one of these phosphate groups from the end, so that there are just two phosphate groups, the molecule is much stable. This conversion from ATP to ADP (Adenosine Diphosphate) is an extremely crucial reaction for supplying energy for life processes. Living things can use the ATP like a battery. The ATP can power the needed reactions by losing one of its phosphorous groups to form ADP, but you can use food energy in the mitochondria to convert the ADP back to ATP, so that the energy is again available to do the needed work. In plants, sunlight energy can be used to convert the less active compound back to the highly energetic form and animals use the energy from high energy storage molecules.

1.5.2 Overview of Glucose Metabolism

Metabolism is the set of chemical reactions that occur in living organisms in order to maintain life. These processes allow organisms to grow and reproduce, maintain their structures, and respond to their environments. Figure 1.4 shows a very simplified model of the glucose metabolism. The digestive tract breaks down most of the carbohydrates in the food into glucose and releases it into the blood stream. Glucose is stored in the liver as glycogen and released again if the blood glucose drops too low. The extraction of glucose from the blood stream by the liver requires insulin, which suppresses indirectly the inverse process and the release of glucose by the liver. Most cells, including muscle cells, need insulin to absorb glucose from the blood stream. The central nervous system and the red blood cells rely completely on glucose for their energy supply, but fortunately do not require insulin to metabolize it. Glucose is lost in urine (renal clearance) if the blood glucose level increases above the renal threshold. The glucose metabolism and blood glucose level in a healthy person are kept within tight tolerances and are controlled by the secretion of insulin by the beta-cells of the pancreas.

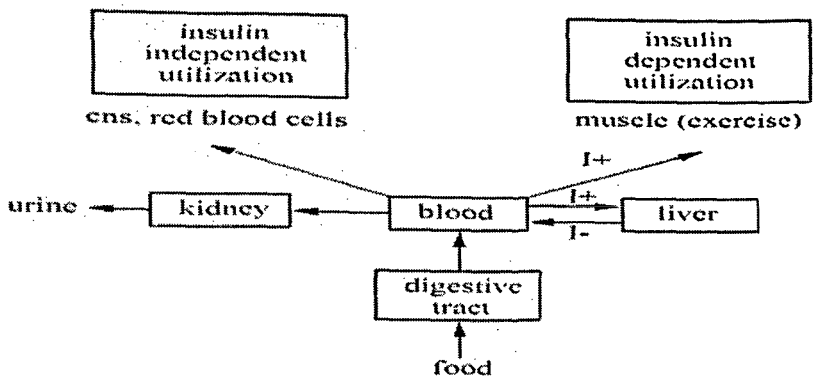

Figure 1.4: A simplified model of the glucose metabolism.

The arrows indicate the transport of glucose. I+ and I- indicate glucose transports which are promoted and inhibited respectively, by insulin in the blood.

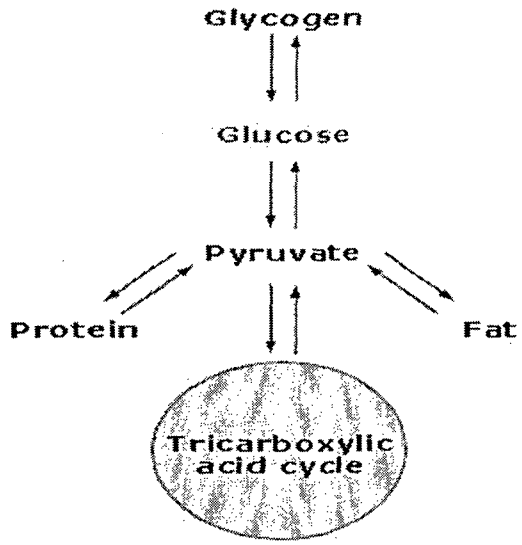

Figure 1.5: Glucose metabolism.

Figure 1.5 shows the glucose metabolism in human body. Glucose is used for many purposes in the body. It can be converted into energy via pyruvate and the Tricarboxylic Acid (TCA) cycle, as well as being converted to fat (long-term storage) and glycogen (short-term storage). Some amino acids may also be synthesized directly from pyruvate; thus, glucose may also indirectly contribute to protein synthesis. Metabolism is usually divided into two categories: Catabolism and Anabolism. Catabolism breaks down large molecules,

for example to harvest energy in cellular respiration. Anabolism, on the other hand, uses energy to construct components of cells such as proteins and nucleic acids. Catabolism and anabolism of glucose is shown in Figure 1.6.

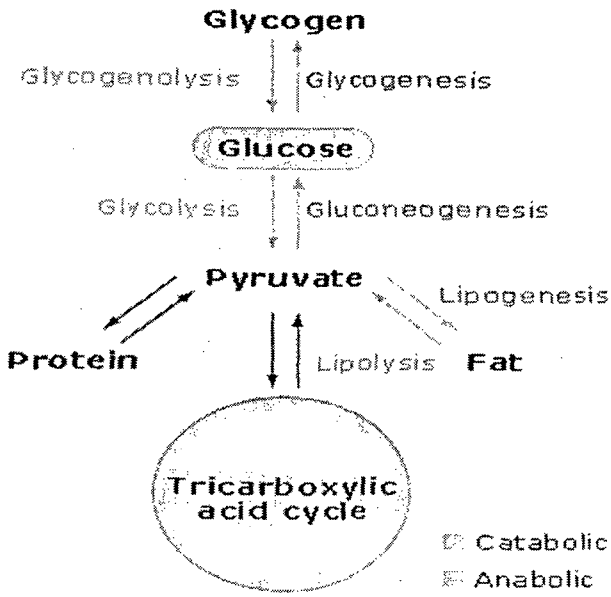

Figure 1.6: Anabolism and catabolism of glucose.

Glucose metabolism involves both energy-producing (catabolic) and energy-consuming (anabolic) processes. Glucagon is the main hormone opposing the action of insulin and is released when food is scarce.[17] The speed of metabolism and the metabolic rate also influences how much food an organism will require. Most of the structures that make up animals, plants and microbes are made from three basic classes of molecules: amino acids, carbohydrates and lipids (fats) as shown in Table 1.3. These macromolecules are essential parts of all living organisms. Some of the most common biological polymers are listed in the table below.

Table 1.3: Basic type of molecules and their polymer forms

Type of molecule	Name of monomer forms	Name of polymer forms	Examples of polymer forms
Amino acids	Amino acids	Proteins (also called polypeptides)	Fibrous proteins and globular proteins
Carbohydrates	Monosaccharide	Polysaccharides	Starch, glycogen and cellulose
Nucleic acids	Nucleotides	Polynucleotide	DNA and RNA

1.5.3 Normalization of glucose in body:

Insulin and glucagon are hormones found in the body that maintain an exceptionally tight range of blood sugar levels in the body. The production of glucagon and insulin by the pancreas is the determining factor in whether or not an individual has diabetes, hypoglycaemia, or another blood sugar problem. As shown in Figure 1.7, the level of blood glucose in the body determines whether the pancreas secrete glucagon or insulin. As the blood glucose level in the body increases, the amount of insulin secreted by the pancreas increases and as the blood glucose level decreases, the insulin secretion also decreases.

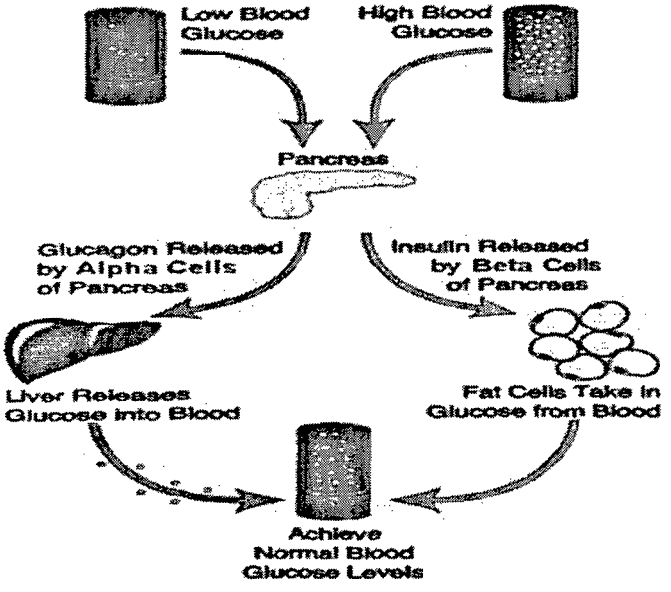

Figure 1.7: Process of normalizing blood glucose levels in the body

Some cells in the body such as muscle cells, red blood cells and fat cells absorb glucose out of the blood to lower high blood glucose levels to a more normal range. When blood glucose is low, such as during exercise or between meals, the pancreas secretes glucagon into the body. This secretion affects the liver and causes it to release stored glucose to raise the blood glucose level in the body to a normal range. A normal blood glucose range is from 70 - 110 milligrams per deciliter (mg / dL). Hypoglycaemia occurs when the blood glucose level falls below 70 mg / dL, hyperglycaemia occurs when the level exceeds 180 mg / dL and an individual is diagnosed with diabetes when the level exceeds 200 mg / dL after drinking a glucose enriched drink.[18]

1.6 Role of blood as Transporting Media

Blood is a specialized body fluid that delivers necessary substances to the body's cells. Blood performs many important functions within the body including the Supply of oxygen to tissues, Supply of nutrients such as glucose, amino acids and fatty acids (dissolved in the blood or bound to plasma proteins), Removal of waste such as carbon dioxide, urea and lactic acid, Immunological functions, including circulation of white blood cells and detection of foreign material by antibodies, Coagulation, which is a part of the body's self-repair mechanism, Messenger functions, including the transport of hormones and the signaling of tissue damage, Regulation of body pH (the normal pH of blood is in the range of 7.35 - 7.45) and Regulation of core body temperature & Hydraulic functions.

Blood Constituents in Healthy Body

Blood tests are an essential diagnostic tool to identify diseases. Blood is made up of different kinds of cells and contains other compounds, including various salts and certain

proteins. Blood tests reveal details about these blood cells, blood compounds, salts and proteins. The liquid portion of the tested blood is called plasma. The remaining liquid is called serum, which can be used in chemical tests and in other blood tests to find out how the immune system fights diseases.

Most blood tests fall within one of two categories: Screening and Diagnostic. Screening Blood tests are used to detect a disease when there is little or no evidence that a person has a suspected disease. For e.g. measuring cholesterol levels help to identify one of the risks of heart disease. These screening tests are performed on people who may show no symptoms of heart disease, as a tool for the physician to detect a potentially harmful and evolving condition. Diagnostic Blood tests are utilized when a specific disease is suspected to verify the presence and the severity of that disease.

The average adult has a blood volume of roughly 5 liters, composed of plasma and several kinds of cells. These formed elements of the blood are erythrocytes (red blood cells), leukocytes (white blood cells) and thrombocytes (platelets). By volume the red blood cells constitute about 45 % of whole blood, the plasma constitutes about 55 % and white cells constitute a minute volume.

About 55% of whole blood is blood plasma, a fluid that is the blood's liquid medium, which by itself is straw-yellow in colour. The blood plasma volume totals around 2.7 - 3.0 liters in an average human. It is essentially an aqueous solution containing 92 % water, 8 % blood plasma proteins and trace amounts of other materials. Plasma circulates dissolved nutrients such as glucose, amino acids and fatty acids (dissolved in the blood or bound to plasma proteins) and removes waste products such as carbon dioxide, urea and lactic acid. The infrared wavelength spectroscopy has high water absorption. The multivariate system of the complex blood matrix consists of 118 constituents, having

overlapping signatures, complicates the ensemble under the multivariate system. Table 1.4 shows the Blood test reference range chart.

Table 1.4: Blood test reference range chart

Test	Reference Range
17 Hydroxyprogesterone (Men)	0.06-3.0 mg/L
17 Hydroxyprogesterone (Women) Follicular phase	0.2-1.0 mg/L
25-hydroxyvitamin D (25(OH)D)	8-80 ng/mL
Acetoacetate	<3 mg/dL
Acidity (pH)	7.35 - 7.45
Alcohol	0 mg/dL (more than 0.1 mg/dL normally indicates intoxication) (ethanol)
Ammonia	15 - 50 µg of nitrogen/dL
Amylase	53 - 123 units/L
Ascorbic Acid	0.4 - 1.5 mg/dL
Bicarbonate	18 - 23 mEq/L (carbon dioxide content)
Bilirubin	Direct: up to 0.4 mg/dL Total: up to 1.0 mg/dL
Blood	8.5 - 9.1% of total body weight
Calcium	8.5 - 10.5 mg/dL (normally slightly higher in children)
Carbon Dioxide Pressure	35 - 45 mm Hg
Carbon Monoxide	Less than 5% of total haemoglobin
CD4 Cell Count	500 - 1500 cells/µL
Ceruloplasmin	15 - 60 mg/dL
Chloride	98 - 106 mEq/L
Complete Blood Cell Count (CBC)	Tests include: haemoglobin, haematocrit, mean corpuscular haemoglobin, mean corpuscular haemoglobin concentration, mean corpuscular volume, platelet count, white blood cell count.
Copper	Total: 70 - 150 µg/dL
Creatine Kinase (CK or CPK)	Male: 38 - 174 units/L Female: 96 - 140 units/L
Creatine Kinase Isoenzymes	5% MB or less
Creatinine	0.6 - 1.2 mg/dL
Electrolytes	Test includes: calcium, chloride, magnesium, potassium, sodium
Erythrocyte Sedimentation Rate (ESR/Sed-Rate)	Male: 1 – 13 mm/hr Female: 1 - 20 mm/hr

Glucose	Tested after fasting: 70 - 110 mg/dL
Hematocrit	Male: 45 – 62 % Female: 37 – 48 %
Haemoglobin	Male: 13 - 18 gm/dL Female: 12 - 16 gm/dL
Iron	60 - 160 µg/dL (normally higher in males)
Iron-binding Capacity	250 - 460 µg/dL
Lactate (lactic acid)	Venous:4.5-19.8mg/dL Arterial: 4.5 - 14.4 mg/dL
Lactic Dehydrogenase	50 - 150 units/L
Lead	40 µg/dL or less (normally much lower in children)
Lipase	10 - 150 units/L
Zinc B-Zn	70 - 102 µmol/L

Lipids

Cholesterol	Less than 225 mg/dL (for age 40-49 yr; increases with age)	
Triglycerides	10 - 29 years	53 - 104 mg/dL
	30 - 39 years	55 - 115 mg/dL
	40 - 49 years	66 - 139 mg/dL
	50 - 59 years	75 - 163 mg/dL
	60 - 69 years	78 - 158 mg/dL
	> 70 years	83 - 141 mg/dL
Liver Function Tests	Tests include bilirubin (total), phosphatase (alkaline), protein (total and albumin), transaminases (alanine and aspartate), prothrombin (PTT)	
Magnesium	1.5 - 2.0 mEq/L	
Mean Corpuscular Haemoglobin (MCH)	27 - 32 pg/cell	
Mean Corpuscular Haemoglobin Concentration (MCHC)	32 - 36% haemoglobin/cell	
Mean Corpuscular Volume (MCV)	76 - 100 cu µm	
Osmolality	280 - 296 mOsm/kg water	
Oxygen Pressure	83 - 100 mm Hg	
Oxygen Saturation (arterial)	96 - 100%	
Phosphatase, Prostatic	0 - 3 units/dL (Bodansky units) (acid)	
Phosphatase	50 - 160 units/L (normally higher in infants and adolescents) (alkaline)	
Phosphorus	3.0 - 4.5 mg/dL (inorganic)	

Platelet Count	150,000 - 350,000/mL	
Potassium	3.5 - 5.0 mEq/L	
Prostate-Specific Antigen (PSA)	0 - 4 ng/mL (likely higher with age)	
Proteins		
Total	6.0 - 8.4 gm/dL	
Albumin	3.5 - 5.0 gm/dL	
Globulin	2.3 - 3.5 gm/dL	
Prothrombin (PTT)	25 - 41 sec	
Pyruvic Acid	0.3 - 0.9 mg/dL	
Red Blood Cell Count (RBC)	4.2 - 6.9 million/µL/cu mm	
Sodium	135 - 145 mEq/L	
Thyroid-Stimulating Hormone (TSH)	0.5 - 6.0 µ units/mL	
Transaminase		
Alanine (ALT)	1 - 21 units/L	
Aspartate (AST)	7 - 27 units/L	
Urea Nitrogen (BUN)	7 - 18 mg/dL	
BUN/Creatinine Ratio	5 – 35	
Uric Acid	Male	2.1 to 8.5 mg/dL (likely higher with age)
	Female	2.0 to 7.0 mg/dL (likely higher with age)
Vitamin A	30 - 65 µg/dL	
WBC (leukocyte count and white blood cell count)	4.3-10.8 × $10^3/mm^3$	
White Blood Cell Count (WBC)	4,300 - 10,800 cells/µL/cu mm	

These values vary somewhat among laboratories, due to methodology and even geography. Blood tests, blood testing methods and quality vary widely in different parts of the world and in different parts of many countries, due to the characteristics in the population. Both racial blood differences and ethnic blood characteristics are among other factors. The American system generally uses mass per unit volume, while SI uses moles per unit volume.

1.7 A Brief History of Blood Glucose Monitoring:

Urine based monitoring

The disease diabetes has been known since ancient times, as the level of blood glucose rises above the normal range, kidneys pass the glucose into urine. In ancient times the Chinese used to test for the disease by checking if ants were attracted to sugar in a patient's urine. Testing urine for diabetes has been done over a century (prior to modern chemical techniques, tasting of a urine sample was even considered a valid test). In 1941, the Ames Division of Miles Laboratories (the division name reportedly came from that of the president, a physician named Walter Ames Compton), in Elkhart, Indiana, introduced a tablet based on a standard test for certain sugars involving copper sulphate, called Benedict's solution. One of these "Clinitest" tablets could be added to a few drops of urine and noting the colour change from bright blue to orange, was compared to a series of printed colours on the instruction sheet and the approximate level of glucose in the urine was estimated.[1] Urine testing for glucose, however, has very serious problems. When a person first develops diabetes, the level of glucose in urine is a reasonable indication of excessive amounts in the blood; however, because both normal and low blood glucose levels result in no glucose in urine, it is never possible to assess low blood levels using urine tests. As the disease progresses over a period of time, it becomes much less reliable as a marker of high blood glucose. Even otherwise, it's never an accurate measurement, and even though improved testing devices ("dipsticks") have been developed over the years, it's never been more than a "semi-quantitative" test.

---

[1] Believe it or not, these tablets are still available even after sixty years, although it's likely that, in the U.S. at least, more of them are used in commercial wineries to detect small amounts of sugar in wine than for urine glucose testing.

Blood based Monitoring

To get accurate values, it is necessary to measure the amount of glucose in the blood itself, and this is done in doctors' offices and laboratories. In order to maintain healthy levels of glucose, there has always been a need for simple, accurate tests that could be performed at home. In 1964, after developing many dipstick tests for urine, Ernest Adams of Ames developed a practical test strip for measuring glucose in blood, and it was named Dextrostix (shown in Figure 1.8). Instead of using a chemical reaction to measure glucose, as Clinitest had done, Dextrostix used a biochemical reaction, with an enzyme called glucose oxidase, which reacts with glucose to produce hydrogen peroxide. The hydrogen peroxide produced a colour from another chemical called o-tolidine and the amount of colour on the strip after exposing it to a drop of blood was a good measure of the amount of glucose present. The amount of colour was simply compared to a series of printed colours on the label and the glucose concentration was estimated by colour comparison. The procedure was not trivial, but could be mastered by most people for home use.

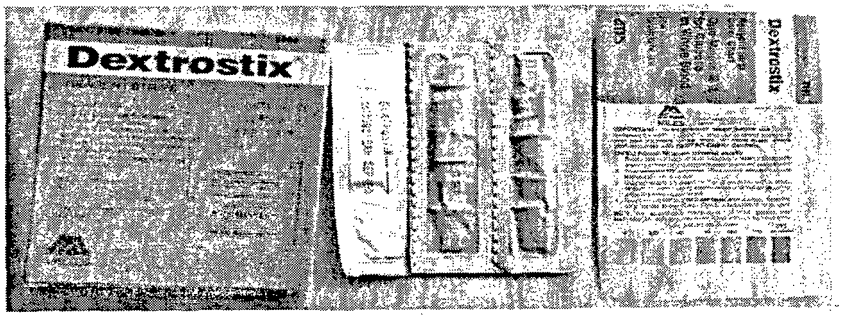

Figure 1.8: Photo of Dextrostix reagent strip

The limitations to this approach are the timing and manipulation involved, as its visual acuity and the ability to perceive colour accurately decreases with age. Since people with diabetes are especially prone to cataracts, those who most needed to perform the test were least able to perform it without assistance. As it turned out, strips 'Dextrostix' were good enough that better accuracy could be obtained by making an electronic measurement of

the amount of colour in the strip, and at least three meters were developed to do so. The first was developed at Ames by Anton Clemens and called the Ames Reflectance Meter[2] (shown in Figure 1.9), or A.R.M. According to interviews with Clemens, he was ordered to drop the project several times but somehow managed to bring it to the market, and the first electronic blood glucose device could be purchased in about 1970 for about $400.

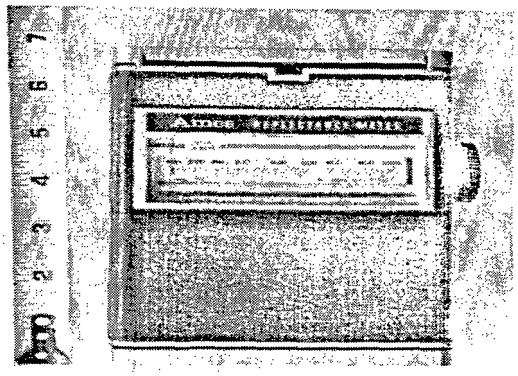

Figure 1.9: Ames Reflectance meter

Unfortunately it had some reliability problems, mostly from its rechargeable lead-acid batteries, and its use did not become widespread. The next electronic strip reader appeared in about 1972, called the Eyetone, and was manufactured by a Japanese company, Kyoto Dai-ichi (which later changed the company name to Ark-Ray). It also read Dextrostix, but used a plug-in AC adapter for power instead of batteries. In about 1979, Kyoto Dai-ichi introduced an improved Dextrostix meter with a digital readout, called the Dextrometer.

Boehringer Mannheim, which had developed a parallel blood glucose test strip for visual colour comparison called the Chemstrip bG, kept pace by introducing a meter to read

[2] Interestingly, LifeScan's original business plan was to produce test strips for use in meters offered by other companies. The irony of this became evident when two companies began to sell strips in 1993 that worked in LifeScan's One Touch meters. Since the strips infringed LifeScan's patents, extended patent infringement litigation, resulted in their effective removal from the market, but not before one of the companies sold over $100 million worth of test strips in just a year.

the strips, the Accu-Chek bG in about 1982. The Chemstrip bG was preferred by many over Dextrostix because the blood could be wiped off the strip (with a cotton ball) after a minute's contact instead of washing off with water. Later versions of the meters were called Accu-Chek in the U.S. and "Reflolux"overseas.

LifeScan entered the market in about 1981, with a meter (first called Glucocheck, then GlucoScan) developed in England by Medistron and test strips developed in Japan by the Eiken corporation—the first product in which the meter was not preceded by a strip intended for visual comparison.

Some of the early GlucoScan meters had their own reliability problems, but they sustained the company until it was purchased by Johnson & Johnson in 1986 and it introduced radically new technology in 1987 with the One Touch meter and strip.

Photometric based meter was called the Exactech, with a strip developed in England, manufactured by MediSense and marketed originally in the U.S. by Baxter, it came in the form of either a slim pen or a credit card sized, thin plastic package. Early versions of the device had both accuracy and reliability problems, which hampered its early market acceptance.

1.8 Global approach in Blood Glucose Monitoring

Because of the market and demand for glucose monitoring due to the surge of the diabetes disease, many technological players put their efforts to design a user friendly module either in invasive or non-invasive mode. Following are the major groups (shown in Table 1.5) who tried to establish glucose monitoring due to its potential in physiological measurements. Table 1.5 is categorized under two categories i.e. Invasive and Non-Invasive Techniques and different techniques used to achieve the goal.

Table 1.5: Worldwide groups working in Glucose measurement techniques.

Sr. no.	Invasive Techniques	Groups	Source
1	Dermis glucose	Advanced BioSensors Inc	http://www.advancedbiosensors.com/
2	Blood glucose monitoring products	Agamatrix Inc.	http://www.agamatrix.com/wavesense_continuous.shtml
3	R1000 insulin pump	Animas Corp	http://www.animascorp.com/products/pr_glucosesensor.shtml
4	Opto-electronic	Gluko MediTech AG,	http://www.pagebleu.com/stratcom/level1/prod1298.htm
5	Glucose-sensing polymer	GluMetrics LLC	http://www.glumetrics.com/.
6	Implantation under the skin	GlySens Inc.	http://www.jacobsschool.ucsd.edu/alumni/profiles/winter99.shtml
7	Gluco Pack, can be Fitted onto regular cell phones	HealthPia America	http://www.healthpia.us/
8	GM 300 blood glucose meter	Invictus Scientific Inc.	http://invictusscientific.com/
9	Minimally-invasive continuous glucose sensor	iSense Corp.	http://www.isensecorp.com/
10	Micro-needle	Kumetrix Inc.	http://www.lein-ad.com/
11	Minimally invasive	MicroSense International LLC	http://jamesvsherer.hubnew.com/microsense-international-llc-announces-key-addition-to-clinical-advisory-board/
12	Carbon nanotube technology	MysticMD Inc	http://www.mysticmd.com/.
13	Dual electrode system	Nellcor	US Patent application 20070032717
14	Microsensor for injection under the skin	Osmolife A/S	http://www.lifecare.no/
15	Highly integrated blood glucose	Pelikan Technologies Inc	http://pelikantechnologies.com/
16	Sensor injected into the fatty layer	Sensors for Medicine and Science Inc.	http://www.s4ms.com/
17	A glucose biosensor patch with RF transmitter	Sontra Medical Inc.	http://www.sontra.com/
18	Interstitial fluid	SpectRx Inc	http://www.spectrx.com/
19	Implantable glucose biosensor	Synthetic Blood International	http://www.sybd.com/
20	Non-toxic	Technical Chemicals & Products Inc.	http://www.techchem.com/
21	Disposable, miniaturized electrochemical sensor	TheraSense Inc	http://abbottdiabetescare.com/freestylenavigator/qa.aspx.
22	Implanted glucose sensor	Zyvex Corporation	http://www.hoise.com/vmw/07/articles/vmw/LV-VM-06-07-5.html

	Non-Invasive Techniques	Groups	Source
1	Onset of hypoglycemia in people with type 1	AiMedics Pty Ltd	AiMedics.com
2	Glucose monitor	Argose Inc.	http://www.diabetesmonitor.com/meters.htm
3	Innovative method	ArithMed GmbH	http://www.arithmed.de/
4	Radio waves	Bioject Inc.	http://www.bioject.com/
5	Diasensor 1000	Biocontrol Technology Inc.	http://www.highbeam.com/doc/1G1-17551919.html
6	Glucose monitoring	Biopath Research Inc.	http://goliath.ecnext.com/coms2/product-compint-0000641308-page.html
7	Fusion Sensor Technology	Biopeak Corporation	http://www.biopeak.com/
8	Blood glucose monitor	Biosign Technologies Inc.	http://biosign.com/
9	Optical glucose sensor	BioTex Inc.	http://www.biotexmedical.com/
10	Glucoband	Calisto Medical Inc.	http://www.calistomedical.com/eng/?p=main
11	Mid infrared sensing technology and microfluidic blood sampling	Cascade Metrix	http://www.cascademetrix.com/
12	Laser finger perforator	Cell Robotics International Inc.	http://www.cellrobotics.com/lasette/home.html
13	Non-invasive biochemical analysis	ChemImage Corporation	http://www.chemimage.com/
14	Contact lenses	CIBA Vision	http://www.msnbc.com/news/591718.asp?0dm=C12LH#BODY.
15	Optical hypoglycemia detector	Cybiocare	http://www.cybiocare.com/index.html
16	Radio frequency	Diabetex International Corp.	http://www.diabetexintl.com/
17	Continuous blood glucose monitor	Diametrics Medical Inc	http://www.diametrics.com/
18	Spectroscopic techniques and signal analysis methods	Fluent Biomedical Corp.	http://www.fluentbio.com/
19	Optics based	Fovi Optics Inc.	http://www.fovioptics.com/
20	Ocular (Eye) glucose measurement	Freedom Meditech Inc.	http://biz.yahoo.com/bw/070201/20070201005077.html?.v=1
21	Dream Beam Analyzer	Futrex Inc.	http://www.futrex.com/
22	Microscatter technology, optical coherence tomography and low coherence interferometry	GlucoLight Corporation	http://mjschurman.web.aplus.net/Gluco_home.htm .
23	Photoacoustic	Glucon Medical Ltd	http://www.glucon.com/

24	Wearable blood glucose monitor	GlucoSense Inc.,	http://www.gen3.com/glucosense/
25	Detect physiological parameters	Hitachi Ltd.	http://www.hitachi.com/New/cnews/040223.html
26	Glucose monitor biosensor	Hypoguard	http://www.medisys-group.com/intro/products/hypo/1-2.htm
27	Blood glucose levels from the eardrum using the body's natural heat emission, or thermal radiation	Infratec Inc	http://care.diabetesjournals.org/cgi/content/full/25/12/2268
28	Spectroscopy and chemometrics	InLight Solutions Inc	http://www.inlightsolutions.com/
29	Suction of interstitial tissue fluid	Institut für Chemo- und Biosensorik	http://www.glucose-monitor.com/
30	Bloodless glucose meter	Integ Inc.	http://www.integonline.com/
31	Ultrasound, conductivity, and heat capacity, GlucoTrack	Integrity Applications	http://www.integrity-app.com/
32	Near infrared (NIR)	International Diagnostic Technologies Inc	http://www.idtscience.com/
33	Combination of Raman based spectroscopy and a proprietary tissue modulation process	LighTouch Medical Inc	http://www.lightouchmedical.com/
34	Spectroscopically analyzing	Luminous Medical	http://www.luminousmedical.com/
35	D-PAL	MedApps Inc.	http://www.medapps.net/Documents/AZRepOct052006.pdf
36	Photoacoustic spectroscopy	Nexense Ltd	www.diabetesmonitor.com/meters.htm
37	Near infrared light	NIR Diagnostics Inc	http://www.cmetele.com/
38	Visible light spectrometry	The Non Invasive Blood Glucose Project	http://www.nibgm.co.za/
39	Mid infrared for non-invasive glucose detection in the conjunctiva of the eye.	Oculir Inc	http://www.sagehealthcare.com/people/burd.shtml
40	Mid-infrared radiation spectroscopy	OptiScan Biomedical Corp.	http://www.ieee.org/organizations/pubs/newsletters/leos/apr98/midinfrared.htm
41	Innovative electro-optical technology	OrSense Ltd	http://www.orsense.com/home.html
42	Radio wave impedance spectroscopy	Pendragon Medical Ltd	http://www.pendragonmedical.com/

43	Interstitial fluid using silicon-based MEMS technology	Phoenix Biosystem	http://www.ardesta.com/1network/netcom11.asp
44	Apply a film to their finger	Pindi Products	http://www.pindi.com/
45	Interstitial fluid	PowderChek Diagnostics	http://www.mendosa.com/meters.htm
46	Fluorescence Resonance Energy Transfer	PreciSense	http://www.precisense.dk/
47	Proprietary photonic technology	QStep Technologies Inc	http://www.qstep.com/
48	Enhance blood glucose	Rosedale Medical Inc	Pequot Ventures
49	Diffuse reflectance near-infrared spectroscopy chemometric analysis	Sensys Medical	http://www.sensysmedical.com/home.html
50	Impedance spectroscopy	Solianis Monitoring AG	http://www.solianis.com/cms/index.php?id=1,2,0,0,1,0
51	Terahertz radiation	Spire Corp	http://www.spirecorp.com/
52	Fluorescence spectroscopy	VeraLight Inc	http://www.veralight.com/
53	Optical characteristics of the eye	Visionary Medical Products Corporation	http://www.vmpc.com/
54	Near-infrared technology	VivaScan Corporation	http://www.vivascancorporation.com/
55	Disposable skin patch will measure glucose in the sweat.	VivoMedical Inc	http://www.vivomedical.com/

CHAPTER 2

REVIEW OF PAST WORK IN THE AREA

2.1 Review of Blood Glucose Analysis Techniques

Blood glucose analysis techniques are categorized as Spectroscopic Techniques, Trans-Dermal and Trans-Membrane Techniques, Techniques using Body Extracts, Radio Frequency / Impedance measurement, Microporation, Optical Coherence Tomography (OCT) and Thermal Techniques.

2.1.1 Spectroscopic Techniques

Introduction: Spectroscopic techniques are used to determine the presence or concentration of a substance by measuring how it interacts with light. When light is absorbed while passing through a material, the amount of depletion of the light is measured and is termed as "absorption." (This is the inverse of the amount of light passed through, which is referred to as "transmittance").

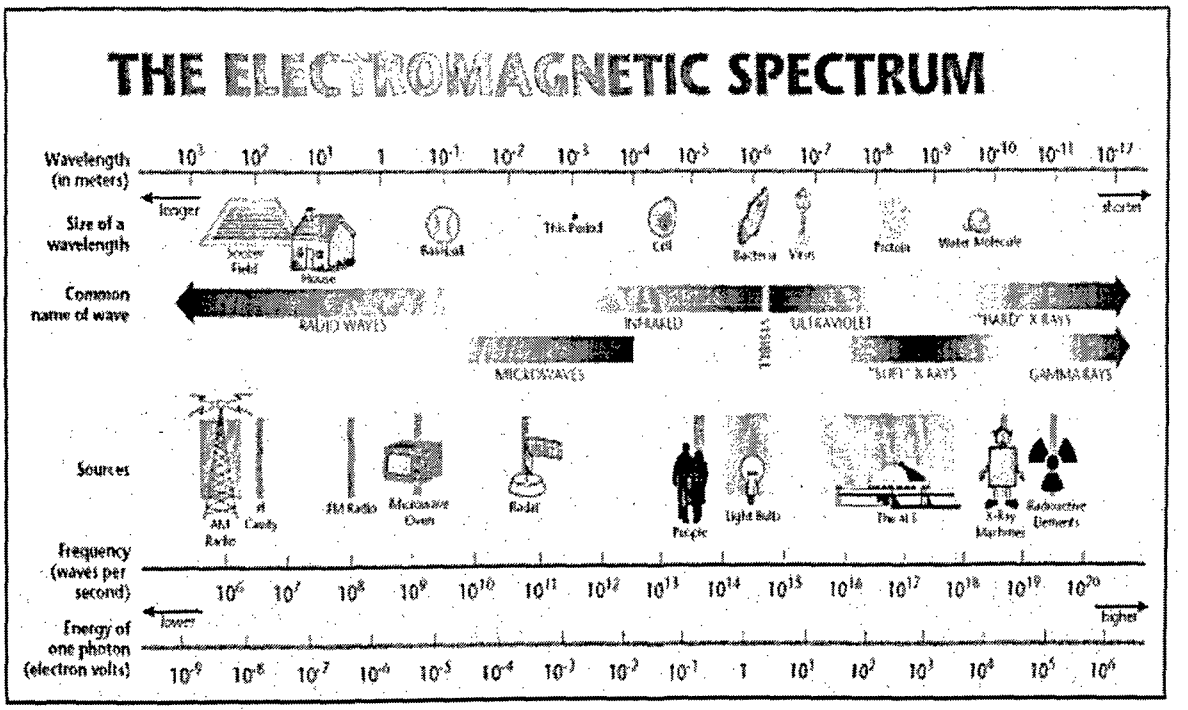

Figure 2.1: Electromagnetic spectrum.

Under certain circumstances, substances can also give off light, and this is called "emission." When the amount of absorption, transmission, or emission is plotted against wavelength, the resulting curve is referred as "spectrum." Each material shows a specific and reasonably unique spectrum, depending on its chemical structure, physical state, and temperature, but the amount of information contained in the spectrum can vary tremendously from one region to another as shown in Figure 2.1.

In the NIR or MIR region, water has a very intense absorption, and small amounts of it can be easily detected. Most of the tissues of the body are too thick to make reliable transmission measurements at the wavelengths that need to be used for glucose, so an alternative technique called "Reflectance" is employed. Here, the light is directed at the surface of tissue, travels some distance into it, and some (usually small) percentage back-scatters. To complicate matters, there are several kinds of reflectance: "Specular Reflectance", where the light bounces off a shiny surface, as in a mirror, and "Diffuse Reflectance", where the light is scattered before it comes back. Glossy white paint acts a lot more like a mirror, and the light primarily bounces off at the same angle it hits, resulting in Specular Reflectance (Figure 2.2a). Flat white paint on a smooth wall yields diffuse reflectance with a reflectance profile termed "Lambertian," where the reflected light is distributed over a full 180 degrees from the surface (Figure 2.2b). "Tissue Reflectance" is even more complex, since light penetrates to a depth where there are many surfaces (collagen fibers, cells) which scatter the light, and the result is a kind of a "Glowball" of reflected light that comes back from layers beneath the skin (Figure 2.2c). The technique is complicated because the top surface of the skin also exhibits some Specular Reflectance and since this light has not interacted significantly with the tissue, it contains almost no information about glucose.

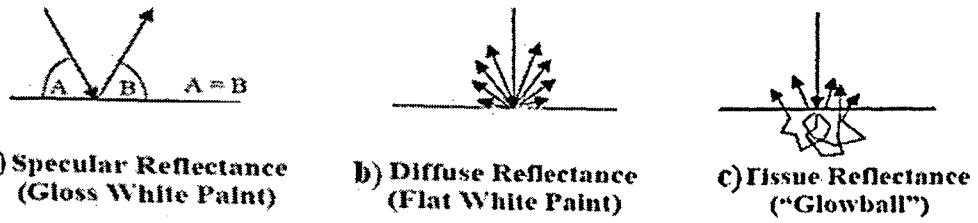

Figure 2.2: Types of reflectance

NIR Technique

The most frequently-attempted region is NIR spectroscopy. Anyone who has held a flashlight under his fingers in a dark room will notice a red light (and the invisible band just above it in wavelength called NIR light) will pass through a considerable thickness of skin and tissue. The light that gets through contains the signature of various constituents during the passage.

Light of higher wavelength, usually termed "MIR" is strongly absorbed by water, which constitutes a very large percentage of all tissues, and generally cannot penetrate to greater depth. The MIR region is quite sensitive and contains a great deal of information about the structure of chemical compounds, so much so that it is often termed the "fingerprint" region of the blood spectrum. The NIR region, where light does penetrate tissue to a greater extent, has more of what might be called "glimmers and ghosts" of structural information. The bands here are called "overtone and combination" bands, and their intensity is greatly reduced below those in the MIR. For practical purposes, NIR light is defined as wavelengths of light between 700 nm and 2500 nm, which is the same as 0.7 to 2.5 μm or "microns." Visible light, generally considered being 400 to 700 nm, but the region below 700 nm contains no glucose information and can safely be eliminated in the search for glucose. The ultraviolet region below 400 nm is even more opaque, and almost no light at

these wavelengths can pass through the tissue, as light is absorbed and scattered by the tissue.

The researcher who plans to use NIR region for analysis has to take care of 2 problems carefully. First, since the signal related to glucose is quite weak, researchers working in this area have to rely on sophisticated mathematical techniques to establish correlation between their measurements and reference values. Known to chemists as "chemometrics" and to mathematicians as "multivariate techniques", these approaches generally try to separate the variation within a data set into a series of components or curve shapes which account for decreasing amounts of the observed variability.

Mid-Infrared spectroscopy

The MIR is usually considered to be light with wavelengths 2.5 to 16 μm. The equivalent region is about 600 to 4000 cm^{-1}. Any material with a temperature above absolute zero emits "blackbody" radiation, and the wavelength region is determined by the object's temperature. Since the glucose molecule absorbs and emits in this region, there is a possibility that variations in the amount of emitted light could contain glucose information. An early investigator who proposed this was Jacob Wong of Santa Barbara, California.

Stimulated Emission spectroscopy (Raman)

These are spectroscopic techniques that attempt to use the interaction of two wavelengths of light in either the NIR or MIR regions. They have been investigated by researchers at Georgia Tech, and by Jacob Wong. Raman spectroscopy has been used mainly for vibration band assignment and qualitative analysis. Instrument complexity and difficulties with calibration delayed its acceptance as a quantitative analytical tool.[19][20] The advent of holographic optical elements and Charge-Coupled Device (CCD) cameras has

allowed the design of fast Raman spectrometers with which the spectrum is acquired over a wide range of wave numbers and averaged in ≤ 30 s. Chemometric methods have allowed ease of generating training sets for subsequent prediction of concentration. Long wavelength solid state lasers have helped shifting the excitation wavelength to the NIR, thus reducing the fluorescence background from biological samples. These advances in hardware and data analysis methods made the measurement of the concentration of a weak Raman scatterer, with a lowest limit of detection (LOD), comparable to other spectroscopic techniques.[21]

Raman spectroscopy offers several advantages for the measurement of glucose. Raman bands are specific to glucose molecular structure. The fundamental vibrations are monitored in Raman spectra and thus are sharper and have less overlap compared with NIR combination bands, and water has a low Raman cross-section as opposed to its high IR absorption. It is possible to detect glucose by monitoring the 3,448 nm C-H stretch band or the C-O and C-C stretch Raman bands at 11,111 - 8,333 nm, which represents a finger-print for glucose.

Photo Acoustic Spectroscopy (PAS)

PAS is based on ultrasonic waves created by tissue absorption of pulsating light.[22] When laser beams meet cells, heat is generated causing pressure variations in the sample. These acoustic signals can be detected through a piezoelectric transducer and with the specific incident wavelengths, reflect optical properties of glucose in blood.[23] PAS, a non-invasive glycemic monitoring device, like the Aprise from the Glucon Company, is already available in the market.[24] Although this method was shown to correlate with blood sugar levels, it is still necessary to improve the reproducibility and sensitivity in order to decrease interferences from other substances. This is a scientifically fascinating but so far not a practically useful technique. When materials absorb visible light, they give it off as heat,

through an energy conversion system called "vibronic coupling," where light (more energetic photons) absorbed by a material is given off as infrared or heat energy (less energetic photons).

Evanescent Wave Spectroscopy (EWS)

Evanescent spectroscopy developed by VivoMedical, works on the principle that when light is reflected from the interface between any two materials of different refractive indices, the light penetrates to a depth of approximately one-half wavelength of the light (for green light of 550 nm, the penetration is about 275 nm into the second material). Although this approach has been attempted several times, in Japan and elsewhere, the thickness of skin everywhere on the body is too great to allow the light to interact with glucose.[25] The Cupertino California startup called MedOptix (since renamed VivoMedical) sought to overcome this problem by measuring glucose in the extremely thin layer of sweat that forms on skin before it evaporates.

Fluorescence

It is known that glucose levels in tears reflect concentrations similar to those in blood therefore fluorescence is also a sensing technology for painless monitoring.[26] This system can track blood glucose with an approximate 30 minutes lag time and does not suffer interference from fluctuations in the light intensity of the ambient surrounding. The photonic sensing is done with polymerized crystalline colloidal arrays which respond to different concentrations through diffraction of visible light.[27]

Thermal Emission Spectroscopy (TES)

Thermal emission spectroscopy measures IR signals generated in the human body as a result of glucose concentration changes. One promising application of this technology uses a similar concept used in standard clinical tympanic membrane thermometers, with the addition of specific wavelengths for glucose fingerprint (9.8 μm and 10.9 μm). This membrane information is important, because it shares the blood supply with the center of temperature regulation in the hypothalamus. In addition, signals from blood vessels in this organ have to cross a smaller path length than in skin or oral mucosa sites. A prototype was calibrated and tested in patients demonstrating reproducibility and predicting glucose concentrations with a mean error of 12 mg / dL.[28]

2.1.2 Trans-Membrane and Trans-Dermal Techniques

Trans-Membrane: The Retina

If the eye is the window to the soul, why not the same, be the best place to find glucose? In addition to the aqueous humor attempts, the optical clarity of the eye has tempted many investigators to seek glucose there, especially in the retina. Attempts to make NIR measurements of glucose in the retina have produced universally discouraging results, and also the attempts to find glucose within the blood vessels visible on the retina have not yielded any success. There are several major complications, such as limitation to the amount of light that can be safely put into the eye. Only a fraction of 1 % of the light is reflected from the retina or its vessels. More significantly, in order to make a glucose measurement in retinal vessels (this would almost certainly be a spectroscopic method, and most likely NIR), it is necessary to look at the path the measuring light would need to travel and what it holds. The light must pass through several millimeters of the aqueous humor, where the glucose is likely to vary somewhat more slowly than in blood, and varies much more slowly in 20 ml

of vitreous humor. Finally, the regions of the NIR spectrum that are most specific for glucose are wavelengths where the allowed intensity in the eye is severely restricted by safety considerations. An interesting approach, also sponsored by LifeScan, was investigated by RetiTech. Advanced methods, but still related to the eye, are techniques that have been patented which make use of vision changes to estimate glucose. After many hours of high glucose levels, the lens of the eye swells and changes the focal point of the eye. An early approach used a series of parallel lines with varying separation to estimate the glucose level—the smallest pair that the user could resolve was the approximate glucose level. Others have made measurements of the refractive correction of the eye and related that to glucose levels. Unfortunately, this approach seems to work effectively only at high levels (after quite a delay), and has not yet been found to be accurate enough for general use.

Trans-Dermal: Reverse Iontophoresis

This is another non-invasive technology, developed at the University of California, San Francisco and Cygnus Therapeutic Corporation in Redwood City, CA, and had nothing to do with light. Rather, the approach measured sugar levels transdermally with a device called a GlucoWatch. The method of iontophoresis has been used for many decades and utilizes electrical current to deliver charged drug compounds through the skin. Non-invasive monitoring, however, uses transport of glucose in the opposite direction (from the skin outward), therefore this process has been called 'Reverse Iontophoresis'.[29] The GlucoWatch monitor is a wrist-watch glucose control device manufactured by Animas Technologies that utilizes this technique with two independent potentiostat circuits.[30] This measurement is possible because neutral molecules, such as glucose, are extracted through the epidermis surface via this electro-osmotic flow to the iontophoretic cathode, along with Na+ ions. Glucose concentrations extracted through the skin with mA currents are in μmolar

ranges. In this electrode, blood sugar is collected in hydrogel discs containing the enzyme Glucose Oxidase (GOD).

The government approved a wristwatch-looking device that uses tiny electric currents to monitor diabetes. The reality of the device was quite different from the advance press. The amount of current required to pull glucose out of the skin was enough to cause reddening and burning of the skin (sometimes even blisters), and the accuracy was not good enough to allow it to be used reliably, even as an alarm for low glucose values and therefore the approval was withdrawn.

In case of transdermal monitoring, parameters such as sweating, skin color, surface roughness, tissue thickness, breathing artifacts, blood flow, body movements, ambient temperature, pressure, and sample duration also influence the results.[31]

Sub-Dermal

Companies or groups have investigated the use of a "reporter molecule," placed just under the skin, which are sensitive to glucose and reports the concentration by changing colour or varying its fluorescence.

2.1.3 Techniques using Body Extracts

Glucose measurements were tried non-invasively with the extracts which were easily accessible and produced in relative abundance, like saliva, urine, sweat, tears, ear wax and nasal exudates. The latter two are not valid markers of glucose, primarily because of the time period over which they are produced and the fact that they are not always available for examination.

2.1.4 Radio Frequency / Impedance measurement

Impedance measurements using radio frequency (or other frequency ranges) have appeared occasionally over the years. One group in Switzerland, Pendragon, made a big splash and presented several posters at scientific meetings before crashing in flames when the technique was shown not to provide reproducible results. Another that has recently appeared is the Glucoband developed by Calisto Medical. It uses bio-electromagnetic resonance phenomenon and will be in the form of a wristwatch. Bio-Electromagnetic Resonance (BEMR™) technology is based on the detection of a change of electrical impedance in the human body caused by an externally applied glucose-specific electromagnetic wave ('Glucose signature').[32] Each concentration of Glucose solution has its unique electromagnetic molecular self-oscillation signature-wave - 'glucose signature'. Human body is experiencing BEMR when a signature-wave matching any internal molecular self-oscillation wave is applied. Due to the BEMR, the body is changing its electrical impedance.

2.1.5 Microporation

SpectRx, headquartered in Norcross, Georgia, began life as Laser Atlanta, and has been interested in non-invasive glucose measurements. Their first approach, which was licensed for some time to Boehringer Mannheim (Roche), involved measuring the amount of cross linking in the lens of the eye. This process is a consequence of both ageing and diabetes, and they initially thought it might be reversible enough to track glucose levels. Studies showed that it was essentially irreversible, and could not respond to even weekly changes in glucose levels, let alone those occurring in just a few minutes. SpectRx has developed a device called "BiliChek" which non-invasively monitors bilirubin in the skin, especially in babies with jaundice. Bilirubin (a breakdown product of haemoglobin) can be

measured through the skin because of its intense yellow-green colour. They moved on to a system they termed as "microporation," wherein a laser beam creates very small holes in the skin, through which interstitial fluid can be collected and analyzed for glucose with an electrochemical sensor.[33] It is touted as a "continuous" monitor, but the need to find new sites to create the holes would not allow continuous monitoring at one site for very long. In practice, a dye which absorbs NIR light is applied to the skin, and a laser burns off the top layer of skin. Abbott invested in the technology for a year or two, but apparently decided it was not a practical approach.[34]

2.1.6. Optical Coherence Tomography (OCT)

This is a powerful imaging technique which allows investigators to effectively see several mm below the surface of opaque tissue, is being explored by GlucoLight in Bethlehem, under a license agreement from the University of Texas. A number of patents have appeared with hopeful descriptions of how the technique might allow the determination of glucose, but so far it has not delivered the promised glucose measurements.[35]

2.1.7 Thermal Techniques

In addition to OptiScan, where the temperature of tissue was manipulated in an attempt to cause a variation in the optical emission of glucose in the infrared, a number of patents have appeared, owned by Hitachi, in which glucose is determined by measuring the temperature of the fingertip, supposedly as a result of variation in metabolic activity with varying glucose levels.[36] The first to appear indicated that the fingertip temperature would be a good indication of glucose.

2.2 Light Absorption Spectroscopy

Spectroscopy measurement can be done basically through absorption, scattering and emission approaches. Scattering spectroscopy, such as Raman spectroscopy, measures physical electromagnetic properties by analyzing the amount of light that a substance scatters at certain wavelengths, incident angles, and polarization angles. Emission spectroscopy reads light spectra radiated by the substance, whose energy can result from sources, such as temperatures or chemical reactions. Absorption spectroscopy quantifies the concentrations of substances through the detection of transmitted or reflected photons, which have the same wavelength as the incident beam. In this thesis only absorption effect is described since all assays were done based on this phenomenon.

Principle:

The Beer-Lambert Law describes the attenuation of incident light (I_0) crossing a material with absorbing properties, as seen in Figure 2.3.[37] When an incident beam (I_0) enters the sample, the intensity of transmitted light (I) decreases exponentially as shown in Equation 2.1.

$$I = I_0 \cdot e^{-\varepsilon(\lambda) \cdot c \cdot L} \qquad 2.1$$

Where:

I → intensity of transmission light;

I_0 → intensity of incident light;

ε → absorptivity (extinction coefficient) of the substance at a specific wavelength, mol^{-1} cm^{-1} (1/mol centimeters);

c → concentration of absorbent, mol (mol);

L → optical path length in the medium, cm (centimeters).

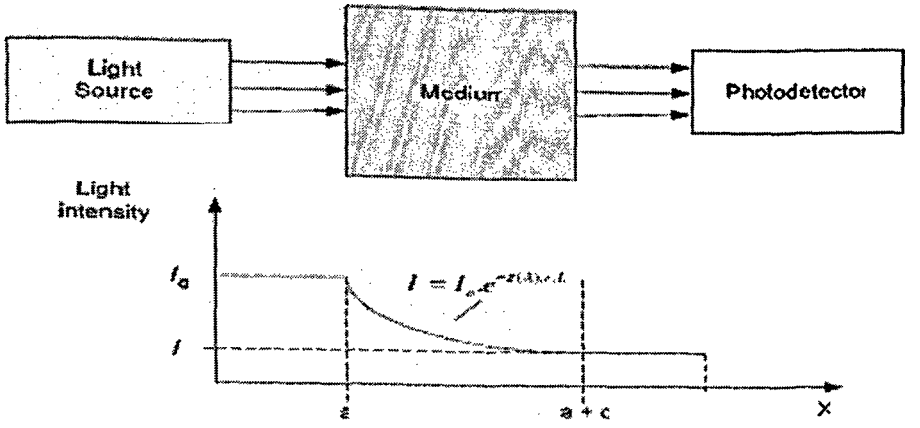

Figure 2.3: Beer-Lambert Law, relationship that relates the absorption of light to the properties of the material penetrated .

The transmittance (T) of light crossing a medium with an absorbance substance is the ratio of transmitted light (I) to the incident light (I_0), and absorbance is the negative natural logarithm of the transmittance, as shown in Equation 2.2.[38]

$$A = -\ln T = -\ln \frac{I}{I_0} = -\varepsilon(\lambda)cL \qquad 2.2$$

where:

A →absorbance, AU (absorbance unit);

T → transmittance, no units;

Even if absorption of light in a medium occurs in different sections of the medium of lengths L1, L2,....Ln, the Beer-Lambert Law is still valid (Equation 2.3).

$$AI = \varepsilon_1(\lambda)c_1L_1 + \varepsilon_2(\lambda)c_2L_2 + ... + \varepsilon_n(\lambda)c_nL_n \qquad 2.3$$

2.2.1 Near Infrared Spectroscopy:

NIR Spectroscopy is a spectroscopic method which uses the near infrared region of the electromagnetic spectrum. NIR can penetrate relatively deep into biological soft tissues. The NIR absorption property of tissue varies with tissue constituents especially water, fat, collagen, and their combination ratio. Most biological soft tissues have a relatively low light absorption property in the visible and NIR spectral regions. This spectral region is known as a "tissue optical window" or "therapeutic window".[39] Outside this region, light is greatly absorbed by tissue pigments (such as haemoglobin and melanin). It offers several advantages over MIR spectroscopy in a non-invasive glucose monitoring system, e.g., less background interference due to water absorption as shown in Figure 2.4, absorbance due to skin is negligible in that range and penetration depths are greater at the shorter wavelengths, which is necessary for monitoring blood glucose in capillaries and glucose in interstitial fluid and tissue.

The use of NIR spectroscopy has emerged since the 1970's as a technique for on-line monitoring and process control.[40] Within the biomedical field, vibrational spectroscopy is emerging as a potential diagnostic tool with many diverse applications.[41] The increasingly prevalent disease diabetes mellitus has created a demand for continuous non-invasive monitoring of blood glucose concentration. Therefore, methods to do so based on a variety of techniques, including near and mid infrared spectroscopy, has been sought intensively in latter years.[42][43][44][45][46][47][48][49][50][51] [52]

NIR Absorption of Water & Glucose

Water

Water, the major component of biological tissues, accounts for 60% to 80% of total body mass.[53] The water content varies with tissue type and it is age and gender-dependent.

For example, the brain of a new-born comprises of 90% water by mass, whereas the water content in an adult skeletal muscle is around 74%. Water is considered to be one of the most important chromophores in tissue spectroscopic measurements because of its high concentration in most biological tissue. The absorption spectrum of water is shown in Figure 2.4 over the wavelength range 200 – 10,000 nm and on an expanded scale from 650 to 1050 nm.[54] Between 200 and 900 nm there exists a region of relatively low absorption. Above 900 nm the absorption coefficient increases rapidly to a peak at about 970 nm, and following a minor trough continues to increase at longer wavelengths into the MIR. The region of low absorption acts as a 'window' of transparency, allowing NIR spectroscopic measurements through several centimeters of tissue.

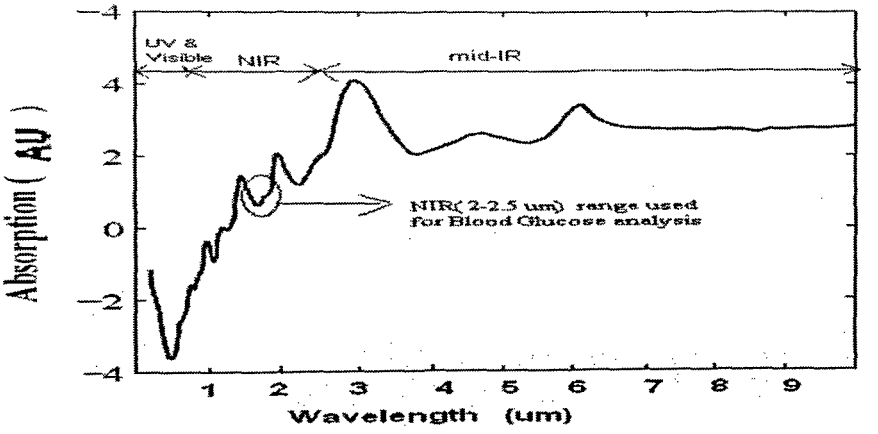

Figure 2.4: Water Absorbance spectra.

The intensity of the NIR absorption bands for water is sensitive to solute concentration and temperature.[55][56][57] It decreases as solute concentration increases because of the change in the molar ratio of water. This is referred to as water displacement. The physical properties of aqueous solutions have been determined from the temperature

dependent on the intensity of the 1400 nm band.[58][59] A similar temperature sensitivity of the NIR absorption of water is observed in the tissue.[60]

The fundamental IR absorption bands of glucose have been reported in solid pellets and in solution.[61][62][63][64][65] The strongest bands that can generate intense combinations and overtones are the broad OH stretch at 2,857 nm and the CH stretch vibrations at 3,377 and 3,393 nm. Possible combination bands are a second OH overtone band at 939 nm (3νOH) and a second harmonic CH overtone band at 1,126 nm (3νCH). A first OH overtone band can be assigned at 1,408 nm (2νOH). The 1,536 nm band can be assigned an OH and CH combination band (νOH + νCH). The 1,688 nm band is assigned as a CH overtone band (2νCH). Other bands at > 2,000 nm are possibly combinations of a CH stretch and a CCH, OCH deformation at 2,261 nm (νCH + νCCH, OCH) and 2,326 nm (νCH + νCCH, OCH). The presence of the CCH, OCH ring deformation component confers some glucose specificity on these bands. The calculated NIR overtones and combination spectra of glucose overlap with several (more intense) combinations and overtone bands of water, fat and haemoglobin absorption bands. These are the major potential interferences with the Non invasive determination of glucose. NIR (2000–2500 nm) spectrophotometric determination of glucose has been achieved in aqueous media. [66][67][68][69][70][71][72]

Nevertheless, background absorption caused by water in the MIR region is too distractive to permit non-invasive tissue measurements. In the NIR region, however, glucose has relatively large absorption at wavelengths between 1500 ~ 1800 nm and 2100 ~2200 nm. The background absorption caused by water in tissue is around ~1mm^{-1}, which enables light to propagate a few hundreds of micrometers into the skin. This propagation may reach all the way to the dermis, where glucose is dissolved in blood and interstitial fluid.

Glucose

Glucose has three regions that are generally accessible: **1)** The combination region: 2000 – 2500 nm; **2)** The first overtone region: 1,540 – 1,820 nm; and **3)** The short-wavelength NIR region: 700 – 1,330 nm. Glucose has three absorption bands in the combination region (centered at 2,100, 2,270, and 2,320 nm as shown in Figure 2.5). Although glucose absorption bands are difficult to measure in the short-wavelength NIR owing to their extremely low absorptivities, bands centered at 760, 920, and 1,000 nm are reported.

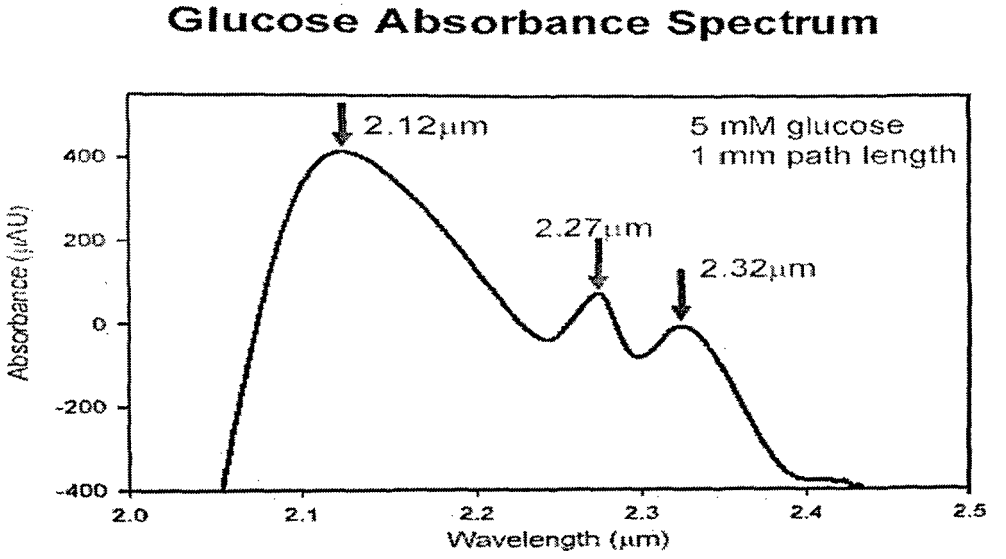

Figure 2.5: Absorption spectra of glucose in NIR

Glucose measuring unit

The standard unit for measuring blood glucose is mmol / L (same as millimolar, mM). The U.S. is the only country in the world to use mg / dL.

To convert blood glucose readings:

- Divide the mg / dL figure by 18 (or multiply by 0.055) to get mmol / L.
- Multiply the mmol / L figure by 18 (or divide by 0.055) to get mg / dL.

2.3 Optical Properties of Human Tissue and Blood

Light can penetrate deep enough into the tissue to allow a spectral measurement or a therapeutic procedure. Optical imaging and non-invasive diagnosis of the human body depends strongly on the optical and physical properties of skin and blood. The composition and morphology of the skin is very complicated. Therefore, to build a reasonable optical model of the skin, its composition and structure must be studied.

2.3.1 Structure & Composition of Skin Tissue

The structure and properties of skin vary considerably in different parts of the body. A typical structure of skin is shown in Figure 2.6, while Table 2.1 and Table 2.2 list the average elemental composition and the biochemical composition, respectively.[73] The skin is usually divided into three layers, namely, the epidermis, dermis, and subcutaneous fat, each with their own sub-layers. The outermost layer of the epidermis is composed of a relatively thin, but rough, protective top layer of dead and dry skin cells, known as the stratum corneum or horny layer. The remainder of the epidermis, including the stratum lucidum, stratum granulosum and stratum spinosum, is made up of cells called keratinocytes as well as melanocytes, which are pigment cells responsible for skin pigmentation. The thickness of the epidermis varies from 0.1 mm in the eyelids to nearly 1 mm on the palms and soles. The dermis consists of a variety of cells, fibres, amorphous ground substance, nerves, oil glands, sweat glands, blood vessels and hair roots. Its upper layer is called the papillary dermis and contains the vascular network and sensory nerve endings, whereas the deeper layer, referred to as reticular dermis, consists mainly of a loose connective structure and epithelial-derived structures such as glands and follicles. The thickness of the dermis varies from 0.3 mm in the eyelids to about 3 mm in the palm and soles. Subcutaneous fat is composed of fat cells,

which form a cushioning layer between the skin and the deeper muscles. It also has abundant blood content.

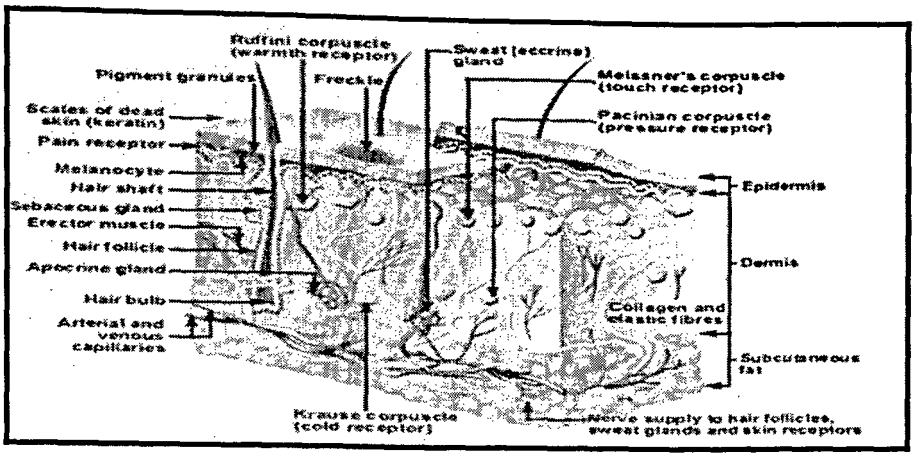

Figure 2.6: Structure of human skin.

Table 2.1: Average elemental composition of the skin, percentage by mass

O	C	H	N	Na	Mg	P	Cl	K
59.4 69.5	25 ~ 15.8	10~10.1	4.6 ~ 3.7	0.2	0.1	0.2	0.3	0.1

Table 2.2: Percentage constituents of adult human skin

Water	Protein	Lipid	Ash
8.6 ~ 72.1	22 ~ 27.2	5.2 ~ 13.5	0.7

2.3.2 Optical Absorption by skin tissue

Being composed of water as well as proteins and lipids, the chemical make-up of the skin influences its optical absorption properties. Water absorbs photons at wavelengths longer than the MIR range, while proteins are strongly absorbed in the UV and Violet region (Figure 2.7). Fortunately, the optical absorption capacity of water, proteins and lipids is small in the red and NIR region. This region, known as the "tissue optical window", has a range 600 nm to 2,300 nm and the light can penetrate to a depth of a few hundreds of

micrometers to a few mm into the skin tissue.[74] As a result, it can be exploited for a variety of purposes, including diagnosis, imaging or therapy.

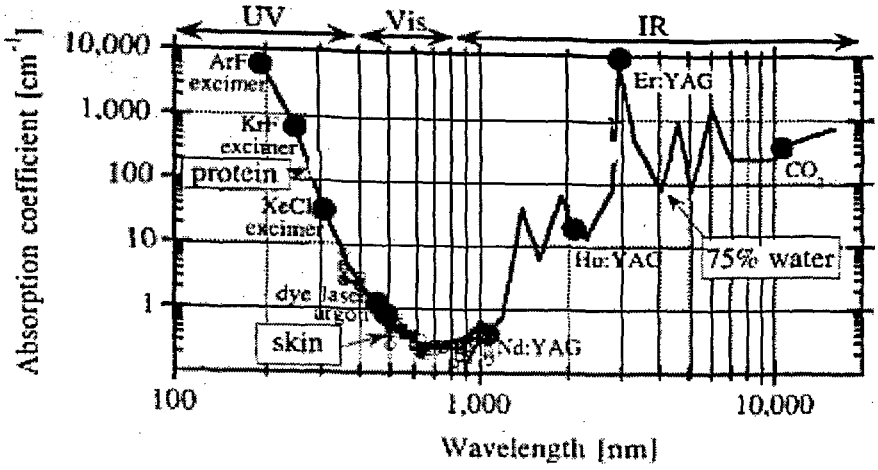

Figure 2.7: The absorption spectrum of tissues.

At the shorter wavelengths of the tissue optical window, from 600 nm to 1,100 nm, the most important photon absorbing chromophores are blood and melanin. Water becomes dominant at incident wavelengths longer than 1,150 nm. The epidermis does not contain any blood and its water content is also much lower that of the dermis. However, the stratum granulosum and stratum spinosum comprises of some melanocytes, including melanin, which is involved in skin pigmentation. Because the absorption capacity of melanin is stronger than that of blood and water, it is the dominant source of absorption in the epidermis at shorter NIR wavelengths. The volume fraction of melanosomes in the epidermis can vary from 1.3 ~ 6.3 % for light-skinned adults, 11 ~ 16% for well-tanned adults and 18 ~ 43 % for darkly pigmented Africans. The blood content of the dermis is about 0.2 ~ 5 %, representing the main source of absorption at wavelengths shorter than 1100 nm. If the optical wavelength exceeds the NIR range, water content becomes an important consideration in terms of optical absorption. It is a well-known fact that the measured values of absorption coefficient of a tissue are different *in-vitro* and *in-vivo*

measurements. This can be explained on a number of grounds: first, soaking the tissue sample in saline prior to an in-vitro measurement may alter its optical properties, and increase the amount of reflectance. Also other kinds of tissue treatments, including freezing, drying, heating or deforming, may change the optical properties of the sample. Secondly, measuring and calibration procedures may introduce an error into the determined values for diffuse reflectance and total transmittance. Thirdly, the use of simplified calculation methods may result in an incorrect interpretation of the measured data, as in the case of internal reflectance at tissue boundaries.

2.3.3 Variants in Human Tissue

There are various variants which affect the spectra of glucose; some of the variants along with their absorption spectra are listed below:

Haemoglobin

Within the window of transparency for water the most dominant absorption of NIR light is by haemoglobin in its various forms. Haemoglobin is carried in red blood cells, or erythrocytes, and constitutes approximately 40 – 45 % of whole blood. It is responsible for delivering oxygen from the lungs to the body tissues and returning waste gases, such as carbon dioxide, to the lungs to be exhaled. Haemoglobin consists of the protein globin bound to four 'haem' groups. Each 'haem' group contains an iron atom at the centre of a ring-like structure. In the oxygenated state haemoglobin is known as oxyhaemoglobin (HbO_2). The de-oxygenated form, with no oxygen molecules attached, is known as deoxyhaemoglobin (Hb).

The absorption spectra of oxy and deoxyhaemoglobin, shown in Figure 2.8, differ significantly, particularly in the red region of the visible and the NIR.[75] This difference in absorption explains the visible colour difference between venous and arterial blood. Arterial blood is usually about 98% oxygen saturated in adults.

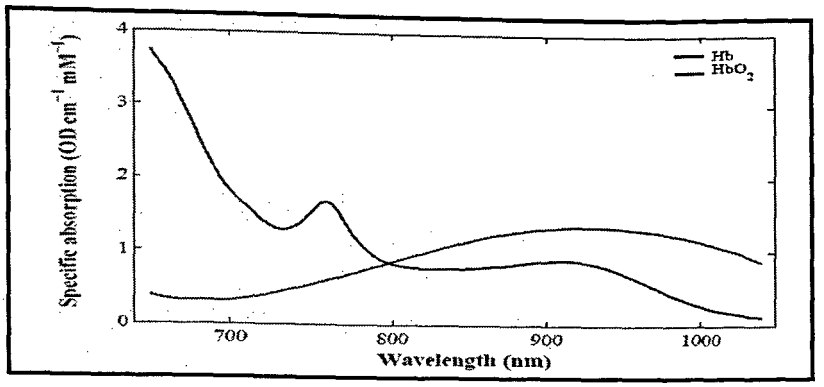

Figure 2.8: Absorption spectra of Hb and HbO2 in the NIR

Lipids

Most of the lipid in the body exists in the form of triglycerides (neutral fats) and is found in subcutaneous tissues and around internal organs. The lipid content in the brain, which also contains steroidal lipids, varies with age from 2.6 % in the new-born to 11.6 % in the adult. In adipose tissue, found in the sub-dermis, the lipid concentration is again age and gender dependent, in the range 23 – 47 % for new-born infants and 68 – 87 % for adults . The importance of lipid as an absorber in NIR spectroscopy depends upon the tissue in question. Since the water content is much greater than the lipid content in the brain, absorption due to lipid may be insignificant. In the forearm, however, the lipid content is seen to be highly variable, depending on the fat-to-muscle tissue ratio, in which case lipid absorption may well be significant in spectroscopic measurements.[76]

2.4 Why Non Invasive Glucose Technique?

As home blood glucose monitoring became a more common place from the early 1980s through the early 21st century, there was still resistance to its acceptance by many people, largely for the reason that, no matter how fast the test or how small the blood drop was, there was no way to obtain a sample other than to stick a needle-sharp lancing device into part of the body to get blood. For all but a few, this causes pain, fear, apprehension,

revulsion or other negative emotions, and many people just will not do it! The reason they cannot, is that this has turned out to be one of the most difficult, recalcitrant, obstreperous and devious problems that has ever challenged science and engineering.

Before blood glucose testing at home became common, the only lancing device available was a sharp piece of stamped steel that made a painful and fairly deep cut in the fingertip. In parallel with the development of blood glucose meters, lancing devices also evolved. Both small, disposable units and reusable "pens" with replaceable tips became commercially available, and they had the added advantage of sharp point being hidden from the view. In the blood glucose monitoring industry, it is well accepted that there are three "C" terms that drive people's willingness to test: Cost, Comfort and Convenience. Non-Invasive monitoring of glucose has been of particular interest because of the pain associated with invasive self-monitoring. Ease of use and reduction of pain can encourage more frequent testing and hence tighter control of the glucose concentration. A large number of Non-Invasive glucose patents lack scientific rigour and some may be based on wrong or unproven assumptions. Several recent reviews have discussed the importance of Non-Invasive glucose testing.[77][78][79][80][81] The limits of detection and quantification, the standard deviation of the measurement, the accuracy, and the total error of Non-Invasive measurement need to correlate with self-monitoring devices and with measurements in the laboratory.

Present day requirements in medical field are that patients demand quick treatment for which fast diagnosis is important. Current pathological tests which are available to analyze blood glucose need to be simplified considering its long test time, trauma, infection, recurring cost and side-effects. Our main aim is to design a novel embedded DSP architecture to analyze the concentration of glucose in human blood non-invasively.

CHAPTER 3

METHODOLOGY

3.1 Objective

One of the important requirements in medical field is that patients demand quick treatment for which fast diagnosis is need of the hour. Current pathological tests which are available to analyze blood glucose needs to be simplified considering its long test time, trauma, infection, side effects and recurring costs. Also the technological trend is from In-vitro to In-vivo to In-silo wherein attempts are to embed signal-processing & data acquisition in the programmable devices. Our main aim is to design a novel embedded DSP architecture to analyze the concentration of glucose in human blood non-invasively. Various techniques are discussed in Chapter 2 like Diffuse Reflectance / Scattering, PAS, EWS, TES, Fluorescence, Raman Scattering, NIR etc. Although the non-invasive glucose measurement technique based on NIR Spectroscopy has been an active research area for over twenty years, a reliable monitoring method has not been established yet. The key problem is that the spectral variations due to glucose concentration are extremely small compared to that from other biological components. In addition, there are also some ambiguous time-dependent physiological processes, which make the explanation of the model more difficult, especially in the universal calibration. In order to design an instrumentation for glucose monitoring which will have accuracy close to that of established clinical methods, one needs a design circuitry which can enhance selective glucose concentration with high signal to noise ratio. Among the different techniques discussed, we have taken up NIR spectroscopy based technique for investigation to find the glucose concentration in blood with following objectives:

1. Design a novel embedded DSP architecture to analyze non-invasively the concentration of glucose in human blood.

2. Design of NIOS II soft-core processor based embedded system to control the system modules.

3. Spectral data processing using PLS technique based on SIMPLS and its implementation on NIOS II processor.

3.2 Methodology for Glucose Estimation

The proposed design for "Non-invasive blood glucose analysis" (Figure 3.1) consists of two parts namely computerized spectrophotometer and signal processing hardware. We have selected NIR detector in the range 2.0 μm - 2.5 μm for the reason explained at Section 2.2.1.

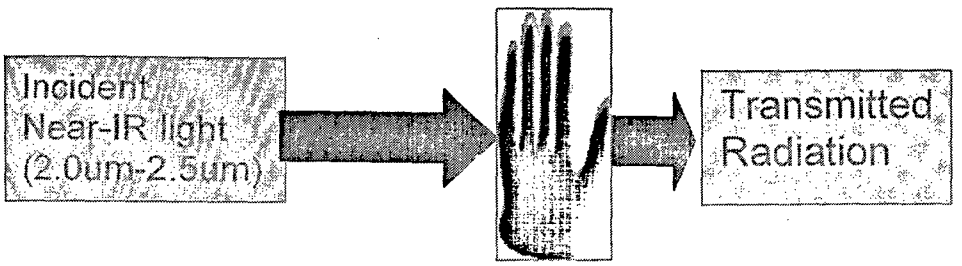

Figure 3.1: General Block Diagram of Non-invasive blood Glucose Analysis

The concept of such a measurement is to pass a beam of Near Infrared light (NIR) through a vascular region of the body and then extract the signal pertaining to glucose concentration by way of analyzing spectral information using the Novel embedded DSP architecture design, using Altera CYCLONE II FPGA. Good spectral signals and data processing algorithms are keys to the success. The spectra must possess sufficiently high SNR to provide reliable glucose-specific information and therefore data processing is needed to differentially enhance the spectral features of glucose from those originating from interfering matrix components and other spectral features. The processing algorithms consists of techniques like Correlation, Partial Least Square Regression (PLSR), Filter techniques etc. As the high speed non-invasive technique itself demands the analysis to be carried out without the chemical reagent or the physical separation, all required information should be obtained solely from the spectral data.

3.3 Spectrophotometer Design

There are various modules required to build the spectrophotometer like Sources, Detector and Accessories for IR Spectroscopy, monochromator, signal conditioning & signal processing.

Sources, Detector and Accessories for IR Spectroscopy:

IR radiations and detectors for these radiations have been relatively well standardized in the International Lighting Vocabulary published by the International Commission on Illumination (CIE) and the International Electrotechnical Commission (IEC) in 1987.

Sources

The most commonly used light source in the MIR region is a 'SiC' globar. This is a filament rod, heated to a temperature of about 800 °C by a current passing through it, which emits thermal radiation with a maximum intensity at approximately 4,800 nm. In the NIR region, QTH filament lamps are usually employed (m/s Newport Inc, USA, supplies several types of filaments rated at various operating voltages and watts as shown in Table 3.1). They have a temperature of about 2,500 °C, providing maximum intensity at 1,818 nm. The absorption of quartz in the MIR region prevents application of this light source in that spectral region. Various sources and their characteristics spectral irradiance is shown in Table 3.2.

Table 3.1: Various Lamps and their parameters (Source: Newport).

Lamp Wattage	DC Voltage (V)	Approximate Flux (Lumens)	Filament Size (WxH) (mm)	Filament Type	Colour Temperature (K)	Permissible Burning Position	Average Life (Hours)
10 W QTH	6	200	1.7 x 0.65	TC	3200	0 or 90Â°	100
20 W QTH	6	450	2.3 x 0.8	RD	3200	0 or 90Â°	100
45 W Calibrated QTH	6.8	705	4.75 H x 1.5 Dia.	CC	3200	0 or 90Â°	150
45 W QTH	6,8	705	4.75 H x 1.5 Dia.	CC	3200	0 or 90Â°	150
50 W, Short Filament	12	1600	3.3 x 1.6	RD	3300	0 or 90Â°	50
50 W Long Filament*	12	850	5.2 x 1.5	TC	3000	0 or 90Â°	3000
100 W QTH	12	3600	4.2 x 2.3	RD	3300	0 or 90Â°	50
200 W Calibrated QTH	30	5000	7.0 H x 3.6 Dia.	CC	3300	0 or 90Â°	50
200 W QTH	30	5000	7.0 H x 3.6 Dia.	CC	3300	0 or 90Â°	50
250 W QTH	24	10000	7.0 x 3.5	RD	3400	0 or 90Â°	50
600 W QTH	120	16500	4.0 x 13.5	CC	3200	Any	75
1000 W QTH	120	28000	5.0 x 18.0	CC	3200	Any	150
1000 W FEL QTH	120	27500	6.0 x 16.0	CC	3200	0 or 90Â°	300
1000 W Calibrated FEL QTH	120	27500	6.0 x 16.0	CC	3200	0 or 90Â°	150
1000 W FEL QTH	120	27500	6.0 x 16.0	CC	3200	0 or 90Â°	150

RD= Rectangular Dense, CC= Coiled Coil, TC Tight Coil

Table 3.2: Various sources and their characteristics spectral irradiance.

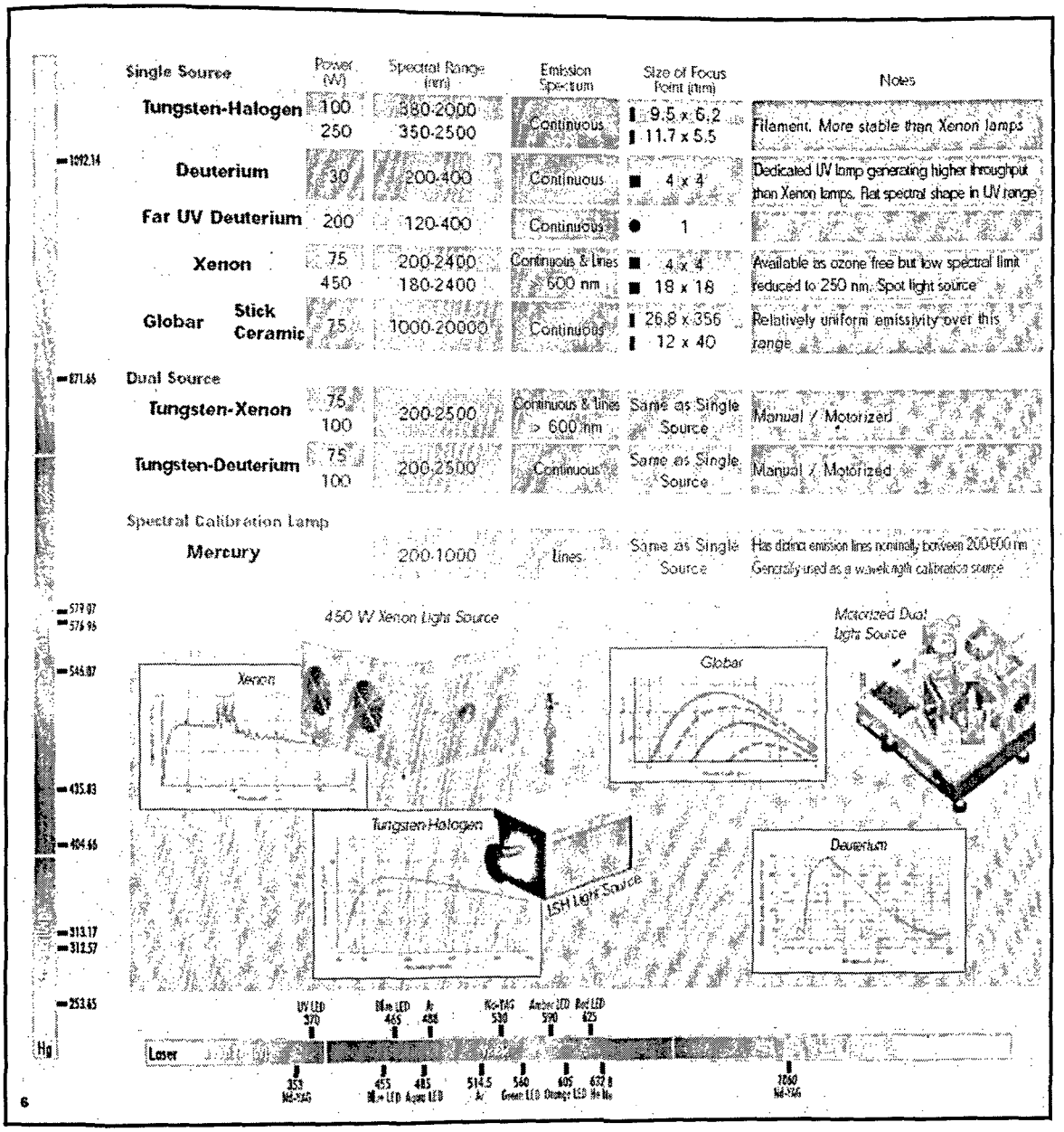

Monochromator Control Module

Fourier Transform (FT) spectroradiometers differ from the Variable Filter (VF) and monochromator based spectroradiometers not only due to different spectral band selector,

but there are also significant differences in the role of the optics. In case of VF and dispersive spectroradiometers, selection of the desired spectral band is done using convergent beams; while the interferometer is used in FT spectroradiometer which works with parallel beams. Next, the VF and the monochromator are self-contained blocks in the sense that major spectral characteristics do not depend very much on how one can irradiate the input slit of the monochromator and how one can collect the radiation from the exit slit of the monochromator (the filter output). FT spectroradiometers are characterized by very good spectral resolution and sensitivity, compared to any other types of spectroradiometers, which can be obtained by using the interferometer as a spectral selector. Better sensitivity originates from the fact that the detector is irradiated not only by the radiation from a desired narrow spectral band (the case of the VF and the dispersive spectroradiometers) but by a full spectrum of radiation coming to the interferometer input. This feature enables the design of high-speed, high spectral resolution FT spectroradiometers using standard or thermoelectrically cooled detectors (typically HgCdTe detectors) instead of bulky liquid nitrogen cooled detectors needed in the VF or dispersive spectroradiometers. However performance of the FT spectroradiometers can be severely reduced, even by a very small non-alignment of the optical system, which makes this type of spectroradiometers inherently sensitive to shocks and vibrations. Therefore for the last few decades, FT spectroradiometers were rather considered as laboratory type equipment that cannot be used in field applications. However, at present this opinion is changing as there are fully mobile FT spectroradiometers in the market. Majority of the commercially available spectroradiometers are systems enabling measurement of the spectral distribution of radiation emitted or reflected by a single spot and these systems can be termed as spot radiometers.

Material for Sample Holders

Various window materials and sample accessories (Table 3.3) used as in FT-IR spectrometers must be transparent to IR radiation. The most common materials are salts that are hygroscopic and therefore ill-suited for use in connection with aqueous solutions. Most beam splitters consist of a base of a material with a proper coating and FT-IR spectrometers are therefore either sealed, with a desiccant material within, or purged with dry air, free of water and carbon dioxide. These two gases have intense infrared absorption bands and the purge also has the purpose of reducing the concentration of these two gases. The most commonly used window material for measurements on aqueous solutions is 'CaF_2' which is sparingly dissolved by water and has an index of refraction which is close to that of water. Another commonly used material is 'ZnSe' which has a higher index of refraction. In the NIR spectral range, quartz and sapphire windows may be employed. They have the advantage of being hard and chemically inert.

Table 3.3: Infrared materials for windows.

Sr. No.	Material	Spectral range in nm	Refractive index at 10,000nm	Water solubility g/100g
1	KBr	204 - 28,985	1.52	53.5
2	Nacl	190 - 21,881	1.49	35.7
3	CaF2	125 - 9,000	1.39	0.0016
4	ZnSe	666 - 21,691	2.4	Insoluble
5	Sapphire	250 - 6,218	2.6	Insoluble
6	Suprasil 300	175 - 3,500	2.5	Insoluble
7	Diamond	333 - 333,333	2.4	Insoluble

Detectors

Wavelength 1,100 nm has a responsivity limit of popular 'Si' detectors. Similarly wavelength 3,000 nm has a long-wave responsivity limit of 'PbS' and 'InGaAs' detectors; wavelength 6,000 nm is a responsivity limit of 'InSb', 'PbSe', 'PtSi' detectors and 'HgCdTe' detectors optimized for 3,000 - 5,000 nm atmospheric window; and finally wavelength 15,000 nm is a long-wave responsivity limit of 'HgCdTe' detectors optimized for 8,000 - 12,000 nm atmospheric window. It may be noted that 'Ge' detector devices are not popular due to their high noise. Table 3.4 shows Values of the Energy Gap between the valence and conduction bands in semiconductors at room temperature.

Table 3.4: Values of the Energy Gap between the valence and conduction bands in semiconductors at room temperature.

Crystal	Eg(ev)	Crystal	Eg(ev)
Diamond	5.33	PbS	0.34 - 0.37
Si	1.14	PbSe	0.27
Ge	0.67	PbTe	0.30
InAs	0.33	CdS	2.24
InAs	0.33	CdSe	1.74
InP	1.25	CdTe	1.45
GaAs	1.4	ZnO	3.2
AlSb	1.6-1.7	ZnS	3.6
GaP	2.25	ZnSe	2.60
SiC	3	AgCl	3.2
Te	0.33	AgI	2.8
ZnSb	0.56	Cu2O	2.1
GaSb	0.78	TiO2	3

The above discussed detectors are quantum detectors and have non linear detection mechanism and therefore, if they are to be used for the instrumentation, a high level program is required to linearize them for various wavelength of interest. Therefore most of the spectrophotometer employ thermal detectors instead of quantum detectors despite of low efficiency as thermal detector have flat responsivity in the entire spectrum of interest. Some of the popular thermal detectors are described below.

Deuterated Triglycine Sulphate (DTGS) detector is the standard detector in most FT-IR instruments. This is a thermal detector, a so-called pyroelectric bolometer, which consists of a ferroelectric crystal which has a Curie point close to room temperature. The crystal therefore exhibits a large change in electrical polarizability when exposed to modulated radiation. By placing electrodes on the crystal faces, the crystal acts as a capacitor across which an AC voltage may be measured. This detector is very linear, stable and has a wide spectral range of operation.

Semiconductor based quantum detectors are used when increased sensitivity and low noise is required. In the MIR spectral region, the mercury cadmium telluride (HgCdTs) which is referred as 'MCT' detector is almost exclusively used. In the near infrared spectral region, 'InSb' and 'InAs' detectors which are employed, may be liquid 'N_2' or Peltier cooled. Compared with the 'DTGS' detector, these detectors have lower noise, higher sensitivity, but a narrower spectral range of operation. The levels of intensity that may be exposed are far lower than the 'DTGS' detector. The 'MCT' detector in particular has a non-linear behavior when exposed to higher levels of intensity. The difference in linearity between the 'MCT' detector in MIR and the 'InSb' and 'InAs' detectors in NIR may be understood from the structure of these detectors. In a semi-conductor structure with a conduction band separated from a valence band by a band-gap, a current can be measured, when free electrons are created in the conduction band by absorption of photons with

energies greater than the band-gap. A mid infrared detector has a small band-gap as it is required to detect radiation with low energies and thermal excitation creates a considerable number of electrons in the conduction band, even when the detector is cooled. The reservoir of electrons that may be excited by the incoming IR radiation is therefore small. This is illustrated in Figure 3.2. With too much light intensity reaching the detector, the reservoir is dried out and the detector saturates.

In comparison to MIR detectors, NIR detectors are required to detect much higher energies and consequently, it has a much larger band-gap. For this reason, thermal excitation does not create as much electrons in the conduction band as in MIR detectors. A higher incident flux of radiation is therefore permissible before saturation sets in. The use of dual-beam techniques where the intensity reaching the detector is twice as high as in the single-beam case is therefore much more limited by the 'MCT' detector in the MIR region than by the 'InAs' detector in the NIR region.

InGaAs Detector

Standard 'Si' detectors have a spectral range between 350 nm to 1,100 nm, and a UV enhanced type extends the range down to 200 nm in the ultraviolet. The Photomultiplier detectors are the most sensitive detectors for UV & Visible radiation.

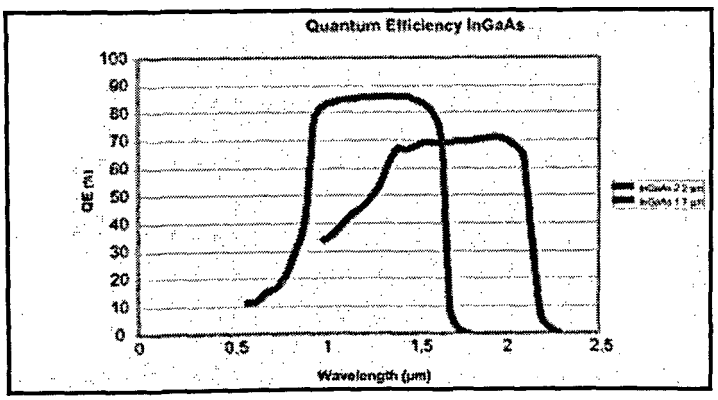

Figure 3.2: Spectral response of InGaAs detector: 1.7 µm and InGaAs 2.2 µm at +20°C. (InGaAs peak sensitivity moves approx. 1nm towards shorter wavelengths with 1°C cooling temperature.)

In fact they provide relatively noise free signal directly proportional to the incident light, with the sensitivity, several orders of magnitude greater than that of any system available. Operating on the principle of solid-state physics, semiconductor devices cover a much wider spectral range than PMT's. 'Ge', 'InGaAs' and 'InAs' are also quantum devices, with greater sensitivity in the infrared.

Signal Conditioning Techniques

The measurement of an absorption spectrum of an aqueous solution is mainly carried out using two different signal capturing techniques, namely using a transmission cell (Figure 3.3) or an Attenuated Total Reflection (ATR) cell (Figure 3.4). The transmission cell consists of two IR transparent windows, between which the aqueous solution is placed. The light ray of the interferometer then passes through the IR windows and the aqueous solution before reaching the detector. Transmission cells are well suited for near infrared spectroscopy of aqueous solutions. In this spectral region optimal path lengths are in the range of 0.5 – 10 mm and consequently much larger than the wavelength of the light. In the mid infrared region, the path length is in the range of 7 - 50 mm which is of the same order of magnitude as the wavelength of the light. This means that multiple reflections inside the transmission cell may cause fringe effects in the detector signal in the MIR region, but not in the NIR region. ATR is a capturing technique where light passes through a crystal or an IR optical fiber and is Totally Internally Reflected (TIR). The evanescent wave reaches into the sample and is altered by changes in the absorption and index of refraction of the sample.

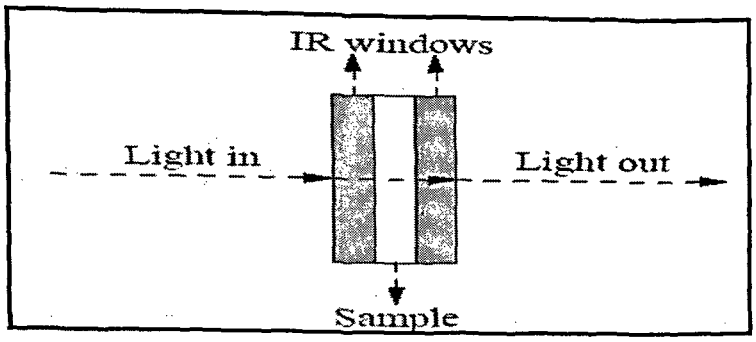

Figure 3.3: Transmission window for IR spectroscopy.

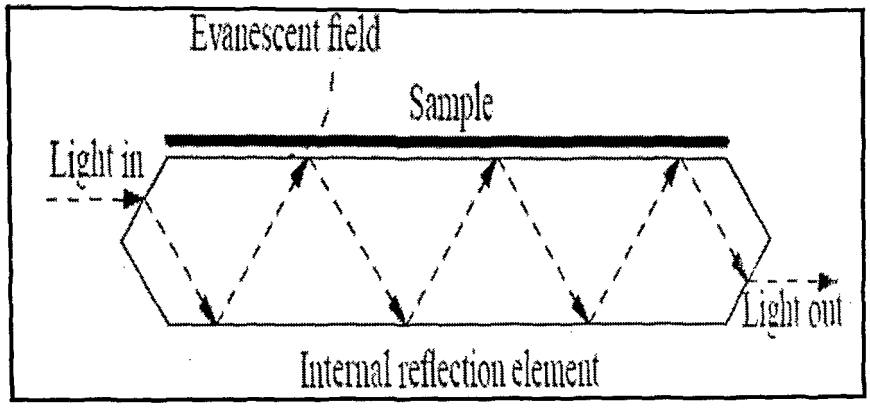

Figure 3.4: Attenuated total reflection (ATR) cell and Evanescent field.

Signal Processing

There are various signal processing technique like convolution, FFT, Filtering, least square regression techniques etc. We have planned to use filtering and PLSR regression techniques which are discussed in chapter 5. One can either use DSP processors or soft-core processors built on FPGA devices.

3.4 Actual Spectrophotometer Design

In the proposed spectrophotometer design QTH source is of 600 Watts (which can be modified for the 1000 Watts by selecting the filament type from the Table 3.1) output power. The monochromator can be designed for the required resolution (proposed 1 nm) wavelength. The monochromatic light output from the monochromator is then coupled to the sample in sample holder, which is then replaced with human tissue such as pinna, index finger etc and the transmitted light is coupled back to the dual channel photometer. The InGaAs thermal cooled detector is used which has sensitivity of pico-watts.

In order to design a spectrophotometer as shown in Figure 3.5 to record the spectral information, we have designed the entire unit around the Altera CYCLONE II FPGA. Design consists of CYCLONE II FPGA, QTH source, Monochromator, InGaAs detector and Newport power meter. Here we have selected QTH source which emits power of 600 Watts, The reason why we have selected QTH source is that it has a spectral range from 0.35 μm to 2.5 μm. The range in which we are interested to carry out the experiment for glucose analysis is from 2.0 μm to 2.5 μm and QTH source supports that spectral range.

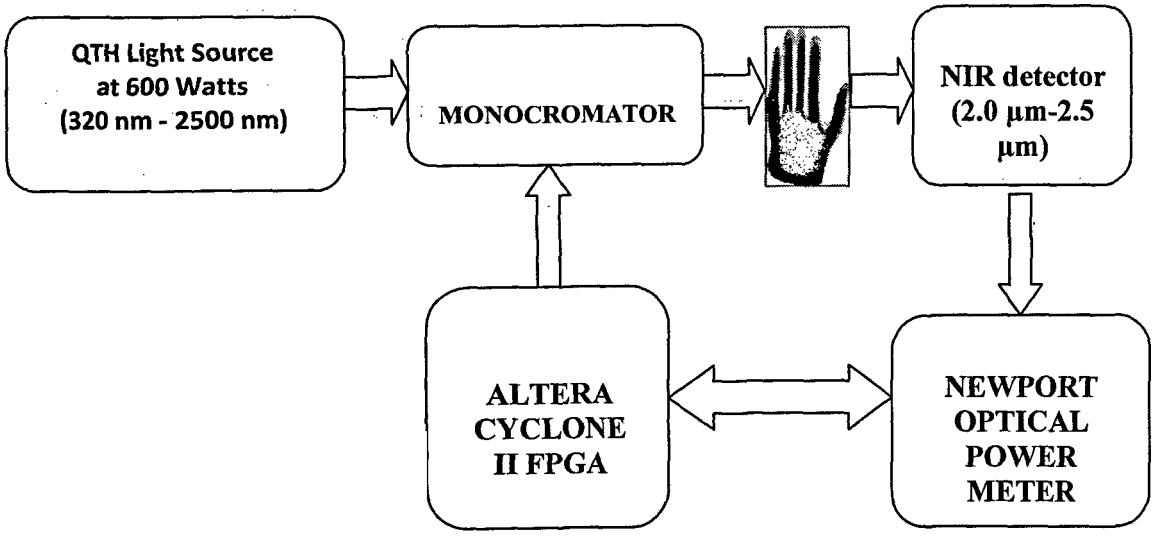

Figure 3.5: Schematic of digital spectrophotometer

The light from QTH source is guided through the fiber bundle for efficient coupling. We have also designed a monochromator having the resolution of 2 nm which selects the wavelengths in the range of 2.0 μm to 2.5 μm. This monochromatic light output is then coupled to human tissue (sample) such as palm, pinna, earlobe etc via a fiber bundle and light transmitted is coupled to thermal-cooled InGaAs detector, which is connected to dual channel photometer from Newport. Here Newport photometer is controlled by NIOS II processor. The reason for selecting thermal-cooled InGaAs detector is already explained in Section 3.3. Newport photometer 2935 has the sensitivity to detect the pico-watts power.

The main reason behind the designing of the above discussed spectrophotometer is that it is difficult to carry out the infrared spectroscopy experiments for the aqueous sample (such as blood) due to the unavailability of the sample holders. The sample holder like KBr , NaCl and CaF_2 (Table 3.3) are soluble in water which cannot be used to perform the experiments of the laboratory aqueous sample. Secondly, the ZnSe holders are very costly and are not available easily. The detected spectra are then passed on to the signal conditioning block wired inside the Altera CYCLONE II FPGA for further processing. Here we have used Newport power meter to standardize the design. The monochromator and power meter is controlled by the same Cyclone II FPGA used for signal processing. The details of the designed NIOS II soft-core interfaced with the power meter are given in Chapter 4.

3.5 System Design for Non Invasive Blood Glucose Analysis

The ultimate goal is to design a low cost portable instrumention for measuring the blood glucose. Keeping the portability and cost in mind, we have to redesign the block of spectrophotometer design by replacing the Newport power meter with InGaAs detector and A/D module. The detail block diagram design for Non invasive Glucose analysis is shown in Figure 3.6. Design consists of CYCLONE II FPGA, QTH source, Monochromator, InGaAs detector, ADC AD7891, Signal conditioning, Altera DE2 board with target as CYCLONE II, keypad and LCD panel. QTH emits in the spectral range of 0.35μm to 2.5μm but our area of interest is 2.0μm-2.5 μm since best possible glucose related information is available in this region; this selection is done with the help of monochromator controlled by NIOS II running on CYCLONE II FPGA. Monochromator so designed has a resolution of 1 nm which is satisfactory to carry out the experiment.

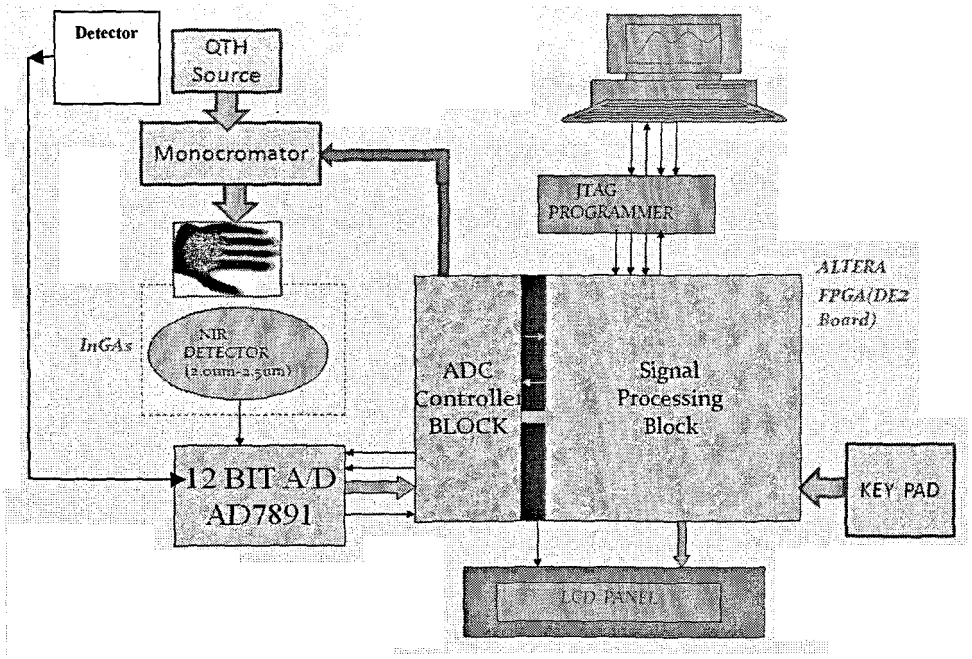

Figure 3.6: Block diagram of the Non-Invasive Glucometer

A specially designed worm-wheel arrangement was used for the fine and a good coupling ratio. The control unit for the coupling was designed using NIOS II running on CYCLONE II FPGA. The user-friendly interface was designed for entering the variables (like scan number and range of scanning) using the proprietary keypad.

The selected wavelength then passes through the tissue of the human body (such as palm, pinna or earlobe) and at the other side of the sample, NIR InGaAs detector is placed which detects the radiation transmitted through the tissue. Dual stage thermally cooled InGaAs sensor is selected for the setup and has power detecting capability up to 11 f Watt, which can take care of high attenuation of radiation in body tissue. To reduce the error in the source fluctuations, we are also monitoring the power emitted by the source using another detector and the output is given to the second channel of A/D 7891 after signal conditioning. If there is any change in the emitted intensity, the designed NIOS II soft-core processor takes the corrective action. The detected spectra contain the glucose signature and also the other interfering components overlapping the glucose spectra. The output of the detector is then passed though the first channel of signal conditioning & A/D stage. The digitized data is then passed onto Altera NIOS II processor running on CYCLONE II device. This digitized data is then passed through SIMPLS algorithm running on NIOS II processor. This algorithm predicts the concentration of Glucose in body tissue and displays the result on the LCD or computer screen. Detected spectra must possess sufficiently high SNR to provide reliable glucose-specific information and therefore the high level of data processing is needed to enhance spectral features of glucose from those originating from interfering matrix components like Alanine, Ascorbate, Triacetine, Urea, lactate, etc. The NIR spectra of these components and the information at multiple wavelengths required to identify glucose are shown in Figure 3.7.

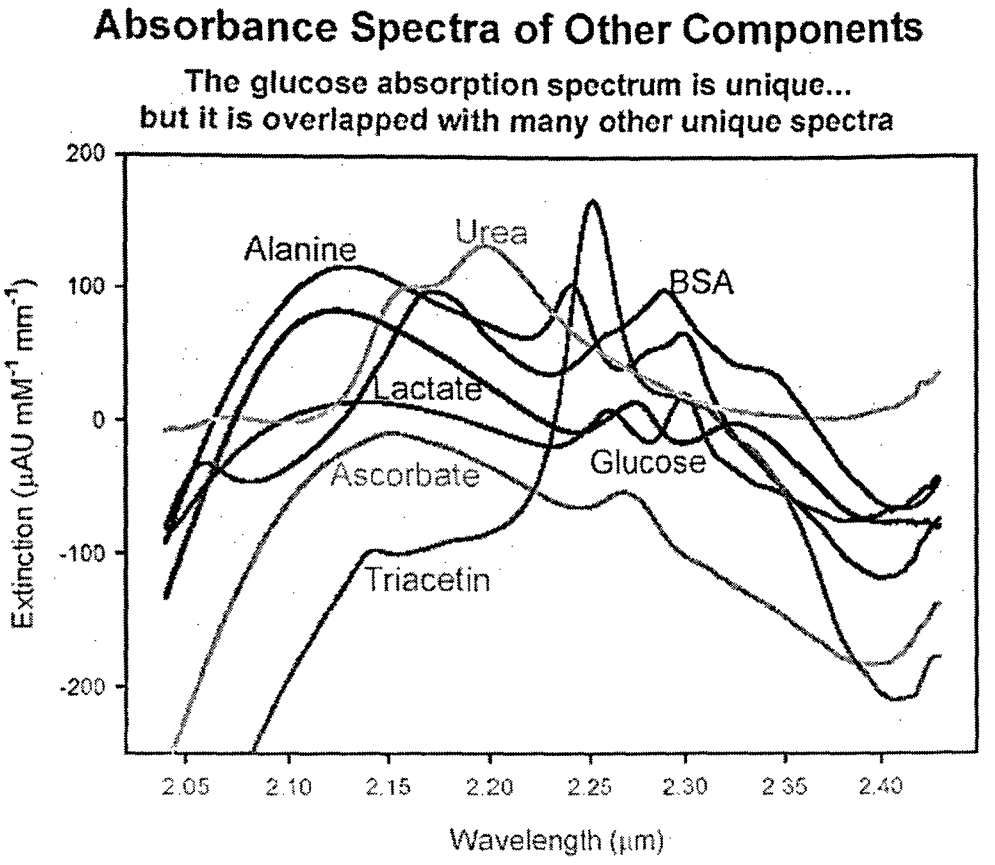

Figure 3.7: NIR spectra of various blood constituents.

The same system can be targeted to analyze other constituents in the blood by just developing the processing algorithms required to analyze the constituents without changing the hardware.

3.5.1 Altera NIOS II controlled Monochromator:

We have designed an Altera NIOS II soft-core on DE2 board to a controlled monochromator having the resolution of 1 nm. Flow chart of NIOS II based monochromator control is shown in Figure 3.8. Here the user has to enter the initial and final wavelengths by using the hex keypad interfaced to NIOS II. If the entered range is within the spectral range then the motor scans from the initial wavelength to the final wavelength with an increment value equal to resolution of the monochromator which is 1 nm. The return path can be

driven at a high speed by inserting a low delay in the path. Care should be taken in the program to reset the position of the motor to the initial position every time the monochromator is turned ON. The flowchart also guarantees the Reset position in case of POWER failure during the working of the monochromator.

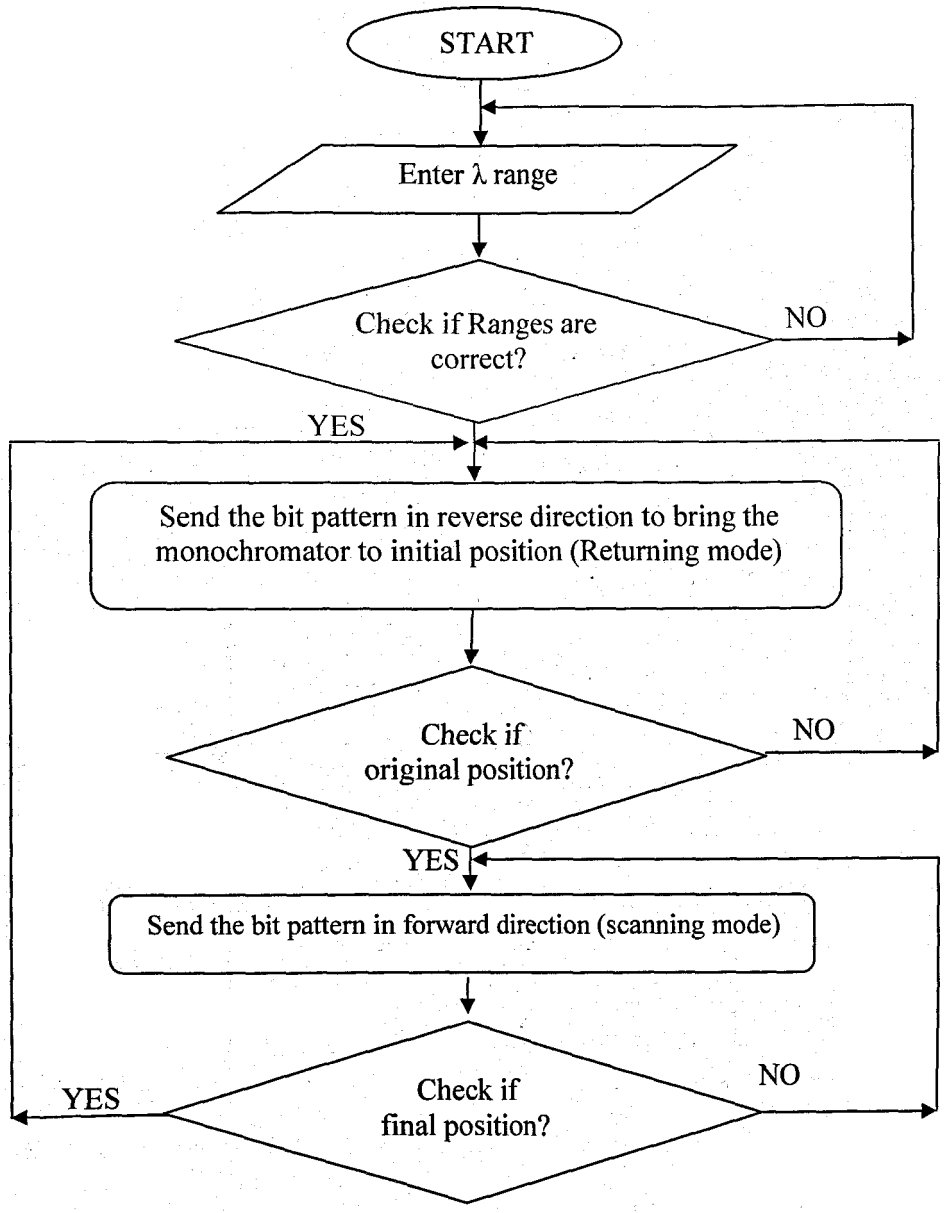

Figure 3.8: Flowchart of Altera soft-core controlled monochromator to select 2.0 μm - 2.5 μm

Initially we tried controlling the monochromator with ARM LPC 2138 processor. The C code for controlling is shown in ANNEXURE I. After successfully testing the ARM controlled monochromator, we then decided to control the monochromator by using Altera NIOS II soft-core since our ultimate aim is to design a Portable Glucometer and avoid using multiple devices. The designed NIOS II soft-core system using SOPC builder of Altera Quartus II software to control the monochromator is explained in chapter 4. The C code running on NIOS II soft-core to control the monochromator to select the spectral range 2.0 μm to 2.5 μm, is given in ANNEXURE II.

Calibration of Monochromator

The monochromator designed here is having the resolution of 1 nm. The Figure 3.9 shows the photo of the monochromator interfaced to CYCLONE II FPGA.

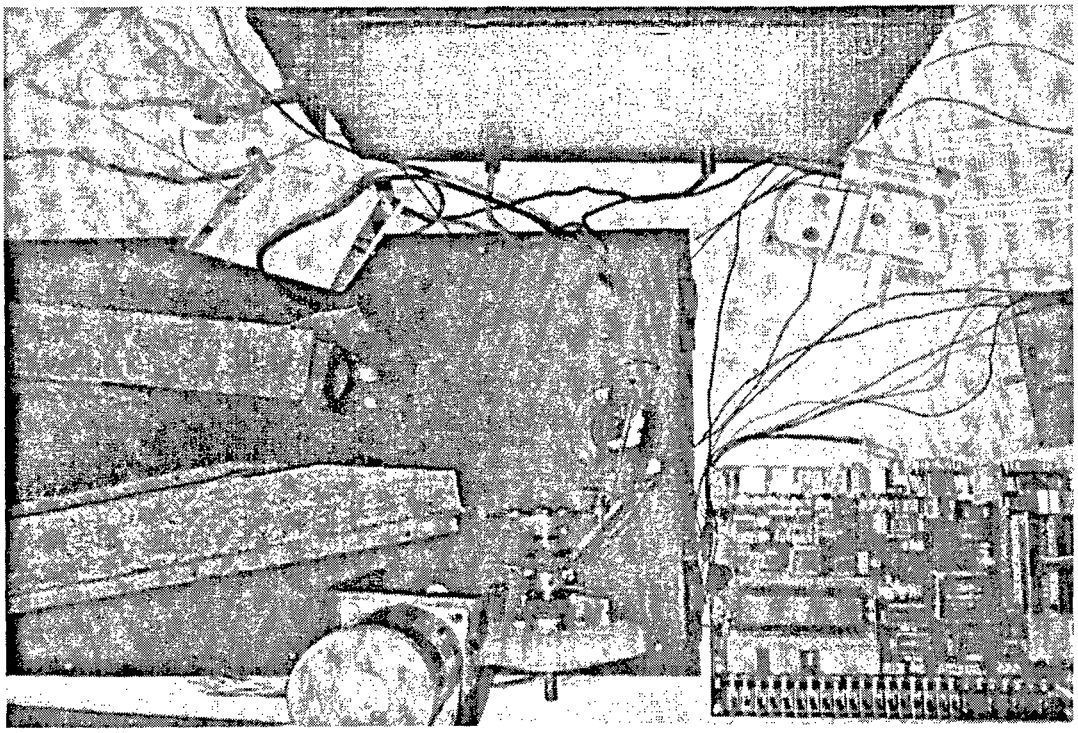

Figure 3.9: CYCLONE II FPGA controlled monochromator

Steps involved in calibration of monochromator

Figure 3.10 shows the ray diagram for calibration of monochromator. Here, two sources S1 of wavelength 660 nm (red laser) and S2 of wavelength 460 nm (blue laser) are used. First S1 is focused onto the reflection grating having 5000 lines / mm, thereby diffraction point is marked on plain paper as R. Then S2 is focused on the same spot on the grating and the diffraction point corresponding to the blue source is marked as B. Next the pulses are sent to the motor to rotate in the forward direction, thereby moving the grating till B reaches R. Once B reaches R, the motor is stopped and the number of pulses given to the motor is counted (in the present case the count is 200). The difference between red and blue wavelength is also 200 nm. The resolution of monochromator is the ratio of the no. of pulse given to the motor to the difference in the wavelength of the two sources used and is 1 nm in our case.

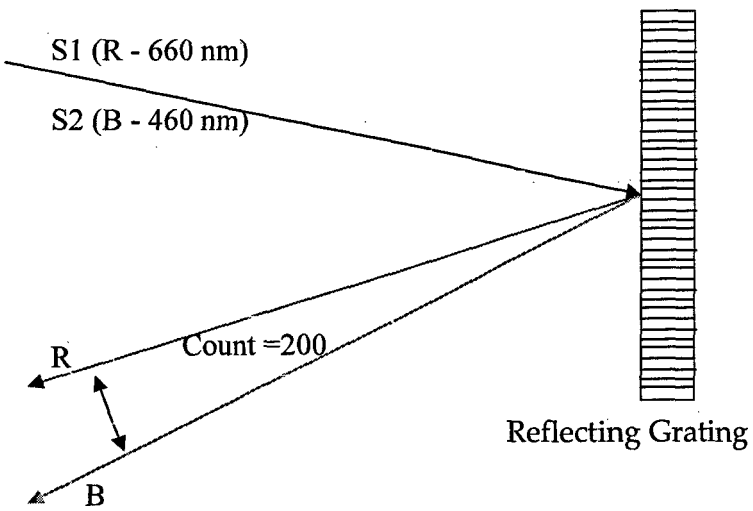

Figure 3.10: Ray diagram for calibration of monochromator

3.5.2 Spectral data acquisition using NIOS II Platform

Here we have developed an interface between Altera NIOS II platform and 12 bit ADC ADC7891 and also designed a signal conditioning circuit to interface NIR Detector to 12 bit ADC 7891. The block diagram of signal conditioning stage is shown in Figure 3.11. Here the InGaAs NIR detector is connected between inverting and non inverting terminal of first amplifying stage.

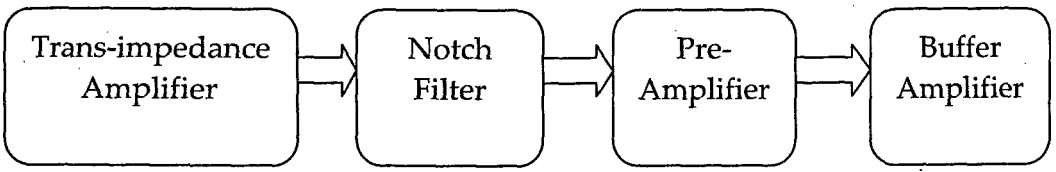

Figure 3.11: Signal conditioning Block

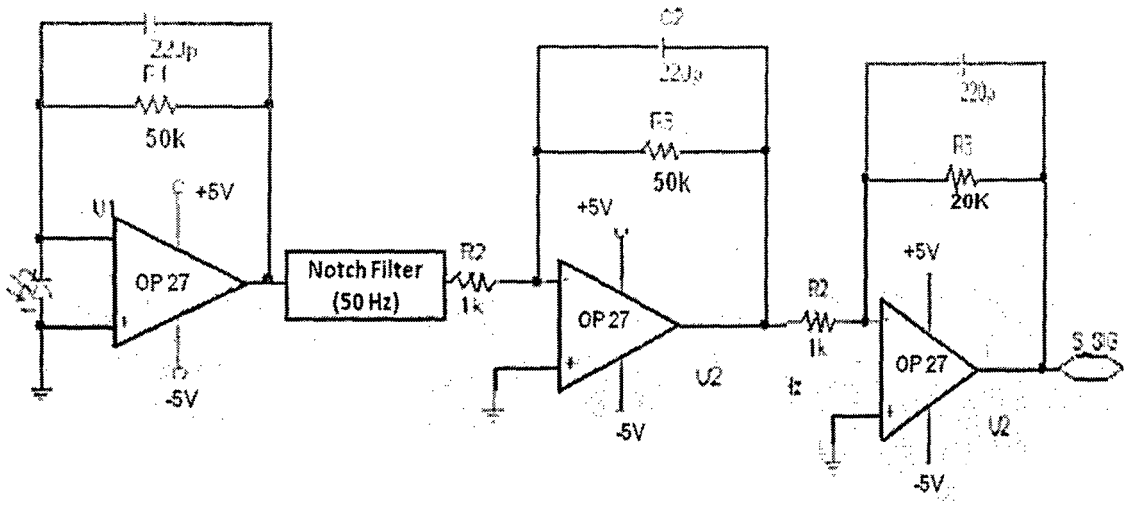

Figure 3.12: Signal conditioning circuit

The signal conditioning circuit is shown in Figure 3.12. The gain of first stage is 50. Notch filter is used between Trans-impedance amplifier and preamplifier stage to remove the mains pickup. The gain of second stage is 50 and gain of third stage is 20. All the 3 stages are in cascade, hence the total gain is 50,000. Here we have used OP-27 because of its low drift and low noise. The signal conditioned output is given to ADC 7891 which is configured in parallel mode. The ADC 7891 circuit connection is shown in Figure 3.13.

Here it may be noted that because of very high gain, there is a chance of instability in the amplifiers. Therefore, special care must be taken to shield these stages of amplifier and proper grounding rules should be followed.

The AD7891 is an eight-channel 12-bit data acquisition system with a choice of either parallel or serial interface structure. This contains an input multiplexer, an on-chip track / hold amplifier, a high speed 12-bit ADC, a 2.5 V reference and a high speed interface. It operates from a single 5 V supply and accepts a variety of analog input ranges. Output of ADC is configured in parallel mode by making mode = 1.

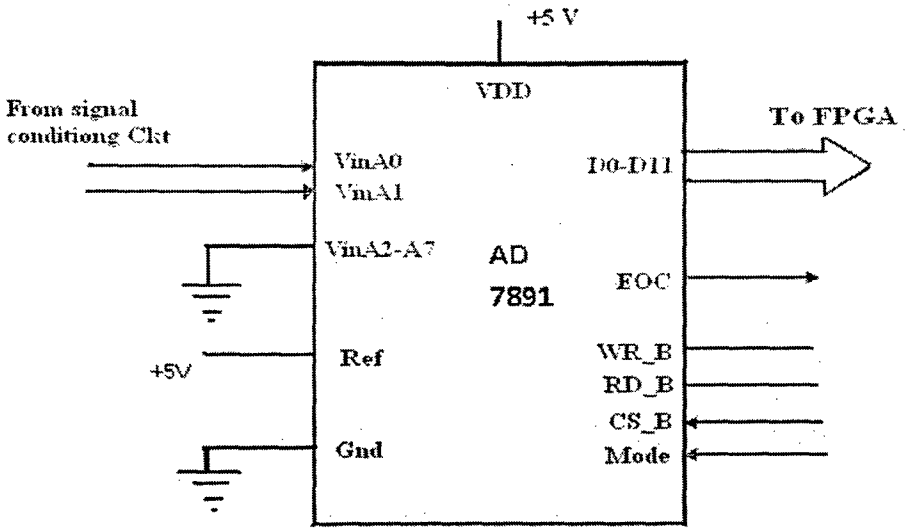

Figure 3.13: ADC 7891 circuit connection

Altera NIOS II core is developed to interact with ADC and it sets the mode of operation and accepts the digitized spectral information and stores it in the memory. The VHDL Code which interacts with ADC 7891 to configure and to accept data is given in ANNEXURE III. Detected spectra are passed through SIMPLS Partial least square regression C algorithms running on NIOS II processor to estimate the concentration of glucose (ANNEXURE IV).

CHAPTER 4

DESIGN OF FPGA SOFT-CORES FOR NON-INVASIVE GLUCOMETER

4.1 FPGA v/s Standard DSP Processors

Design Reliability and Maintenance

Digital Signal Processing (DSP) underpins modern wireless and wired communications, medical diagnostic equipment, military systems, audio and video equipment, and countless other products, becoming increasingly common in consumer lives. Due to advances in semiconductor technology, ever more complex DSP algorithms, protocols, and applications are now feasible, which in turn, increase the complexity of the systems and products. As the complexity increases, the system reliability is no longer solely defined by the hardware platform reliability but typically quantified in Mean Time Between Failure (MTBF) calculations. System reliability is increasingly determined by hardware and software architecture, development and verification processes, and the level of design maintainability. One fundamental architecture issue is the type of hardware platform. DSP functions are commonly implemented on two types of programmable platforms: DSP and Field Programmable Gate Arrays (FPGAs). DSPs are specialized forms of microprocessors, while FPGAs are forms of highly configurable hardware.

FPGA and Digital Signal Processor Development Process

All engineering project managers can readily quote the date of their next product software update or release. In most technological companies, there is usually a long internal list of software bugs or problem reports, along with the software releases that contain the associated patches or fixes. All software, including DSP code, contains some level of bugs and the best one can do, is to minimize it. By comparison, FPGA designs tend to be updated much less frequently and it is generally an unusual event for a manufacturer to issue a field upgrade of a FPGA configuration file. The reasons behind this are due to the differences in

the DSP and FPGA engineering development process. There is a fundamental challenge in developing complex software for any type of processor. In essence, the DSP is a specialized processing engine, which is constantly reconfigured for many different tasks, some DSP related, others more control or protocol oriented. Resources such as processor core registers, internal and external memory, DMA engines, and I/O peripherals are shared by all tasks, often referred to as "threads". These create many opportunities for the tasks to interact, often in unexpected or non-obvious ways. In addition, most DSP algorithms are required to run in "Real time", so that even unanticipated delays or latencies can cause system failures.

Managing Resources

Microprocessor, DSP and Operating System (OS) vendors have attempted to address these problems by creating different levels of protection or isolation between tasks or threads. The OS or kernel is used to manage access to the processor resources, such as allowable execution time, memory, or common peripheral resources. However, there is an inherent conflict between processing efficiency and the level of protection offered by the OS. In DSPs (Figure 4.1), where processing efficiency and deterministic latency are often critical, the result is usually minimal or zero OS isolation between tasks. Each task often requires unrestricted access to many processor resources in order to run efficiently. Compounding these development difficulties is incomplete verification coverage, during both initial development and regression testing for subsequent code releases. The near impossibility of testing all the possible and interactions between different tasks or threads that may occur during field operation makes it arguably the most challenging part of the software development process. Even with automated test scripts, it is not possible to test all possible scenarios.

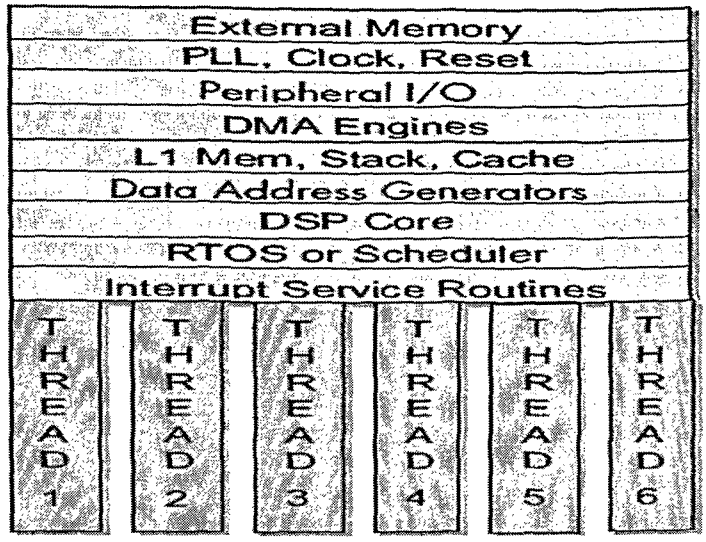

Figure 4.1: Digital Signal Processor block diagram

So how exactly does the FPGA development process improve on this unhappy state of affairs? The complexity of each task is more or less equivalent, no matter whether the design uses DSP or FPGA implementation. Both routes offer the option to use third-party implementations of common signal processing algorithms, interfaces and protocols. Each also offers the ability to reuse existing Intellectual Property (IP) on future designs, but that is where the similarity ends. FPGAs offer a more native implementation for most DSP algorithms. Each task is allocated its own resources and runs independently.

The FPGA resources assigned can be tailored to the task requirements, which can be broken up along logical partitions. This makes a well-defined interface between tasks and largely eliminates unexpected interaction between the same. As each task runs continuously, much less memory is required than in the DSP, which must buffer the data and process it in batches. As FPGAs distribute memory throughout the device, each task is permanently allocated the dedicated memory it needs. This provides a high degree of isolation between tasks and results in modification of one task being unlikely to cause unexpected behaviour in

another task. This, in turn, allows developers to easily isolate and fix bugs in a logical and predictable fashion.

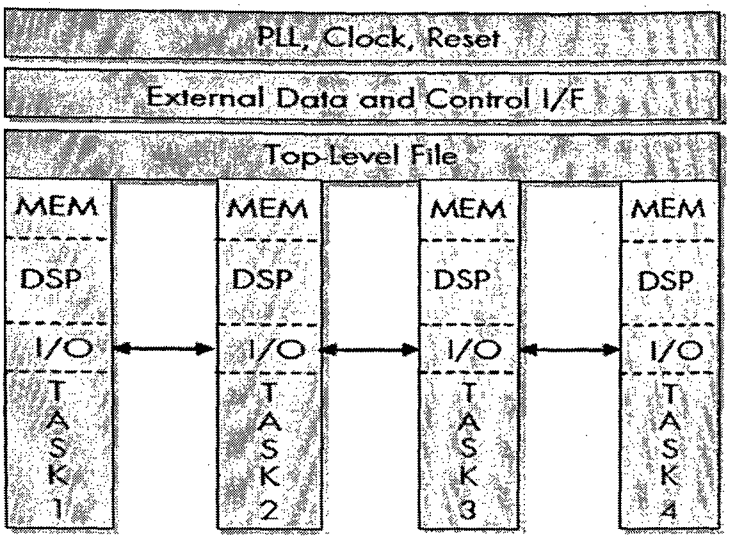

Figure 4.2: FPGA Block Diagram.

The following factors make FPGAs promising, particularly for high performance computing applications: (i) The potential for thousand-fold parallelism (ii) The embedding of control logic (iii) Presence of on-board memory in FPGA also has significant performance benefits. For one, having memory on-chip means that the processor's memory access bandwidth is not constrained by the number of I/O pins on device (iv) FPGA with greater capacity can occupy the same board footprint as an older device, allowing performance upgrades without board changes.[82] Diagram in the Figure 4.2 shows the how FPGA resources assigned can be tailored to the task requirements, which can be broken up along logical partitions. This makes a well-defined interface between tasks and largely eliminates unexpected interaction between tasks, because each task runs continuously, much less memory is required than in the DSP, which must buffer the data and process in batches. As FPGAs distribute memory throughout the device, each task is permanently allocated the dedicated memory it needs.

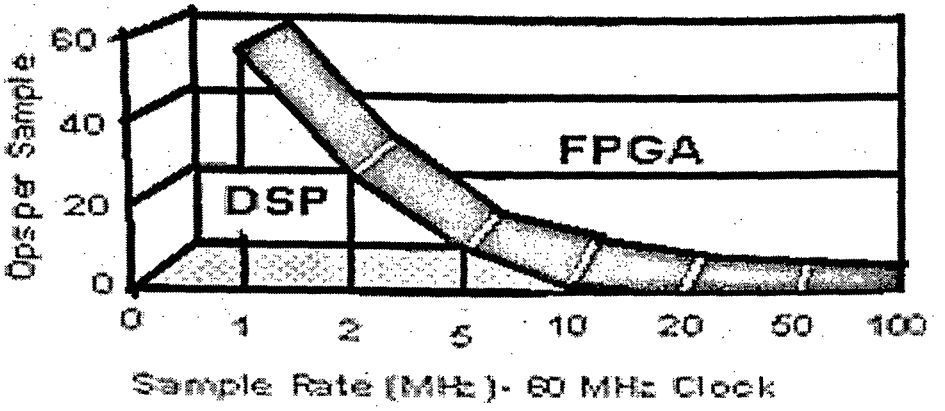

Figure 4.3: FPGAs are a better solution in the region above the curve.

In the past, the use of DSPs were nearly ubiquitous, but with the needs of many applications outstripping the processing capabilities of DSPs (measured in Million Instructions Per Second (MIPS)), the use of FPGA is growing rapidly (Figure 4.3). The primary reason nowadays most engineers prefer to use FPGAs over DSPs is because it is driven by the application's MIPS requirements. Thus the comparison between DSPs and FPGAs focuses on MIPS comparison, although certainly important, is not the only advantage of an FPGA. Equally important, and often overlooked, is the FPGA's inherent advantage in product reliability and maintainability. FPGAs have gained rapid acceptance and growth over the past decade because they can be applied to a very wide range of applications. Higher performance implementations of specific DSP algorithms are increasingly available through implementation within FPGAs. Ongoing architectural enhancements, advancement in development tools, speed increases and cost reductions are making FPGA implementations attractive for an increasing range of DSP dependent applications. FPGA technology advances have increased clock speeds and available logic resources, beyond the range required to implement many DSP algorithms effectively at an

attractive price. FPGA implementation provides the added benefits of reducing costs along with design flexibility and future design modification options.

The critical architectural transformation necessary to maximize an algorithm's performance within an FPGA is the process of translating every serial operation or group of operations into the most parallel implementation possible, up to the limits imposed by the resources available within the target FPGA device for implementing a specific function. Designs which require signal pre-processing can also benefit, since filtering and signal conditioning algorithms are generally straight-forward to implement within an FPGA architecture. When an algorithm is implemented in a structure which takes advantage of the flexibility of target FPGA architecture, the benefits can be tremendous. Algorithms can be customized to adjust to the system requirements on the fly. Filter coefficients, implementations, and architectures can be updated to reflect changing system conditions and user requirements.

The implementation of an algorithm within an FPGA also provides a range of implementation options. An FPGA device also provides a platform for integrating multiple design functions into a single package or a group of packages. Integration of functionality can result in higher performance, reduced real-estate requirements, and reduced power requirements. Further, design integration can be implemented by incorporating hard or soft processor cores within an FPGA to implement required control and processing functionality. The availability of pre-verified design functionality through IP availability can also be used to implement and incorporate common functionality. The ability to incorporate multiple system-level components and design functionality within a smaller quantity of components can potentially reduce risk, cost, and schedule.

4.2 Selection of FPGA for Developing DSP architecture for Non Invasive Glucose Analysis

DSP is one of the most powerful technology that shapes science and engineering. Applying DSP tools has revolutionized various fields: communications, medical imaging, radar & sonar, high fidelity music reproduction, oil prospecting, etc. Each of these areas have developed an indepth DSP technology, with its own algorithms, mathematics, and specialized techniques. DSP education involves two tasks: learning general concepts that apply to the field as a whole, and learning specialized techniques for a particular area of interest.

In this chapter DSP tools are applied to the multivariate analysis using state of art technology with IP cores and FPGA. Altera & Xilinx are major players in FPGA device. Both company Electronics Design Automation (EDA) tools were explored for DSP implementation, wherein Altera soft-core processor based approach was found more suitable for the model implementation for the reasons explained in later sections.

4.2.1 DSP Implementation on programmable embedded system

To select the best embedded platform for Novel DSP architecture, we have implemented DSP algorithms on Xilinx and Altera platforms and also done the comparison of soft-core processors and found that Altera platform is the best one in terms of speed and resource utilization.

4.2.1.1 DSP algorithm on Xilinx Spartan board

We have designed a Xilinx Spartan III based embedded platform for implementing the DSP algorithms. The photo of designed board is shown in Figure 4.4. The block diagram of the system is shown in Figure 4.5.

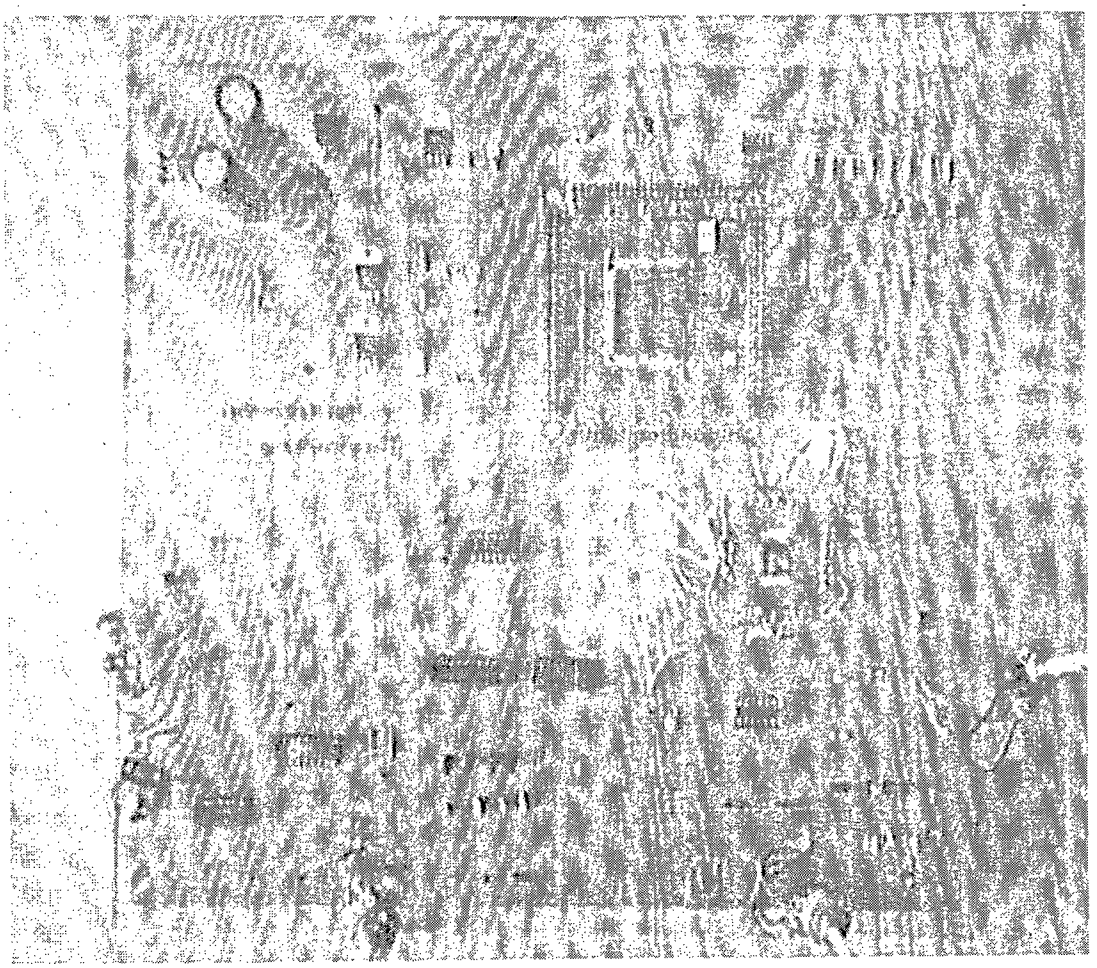

Figure 4.4: Xilinx Spartan III board

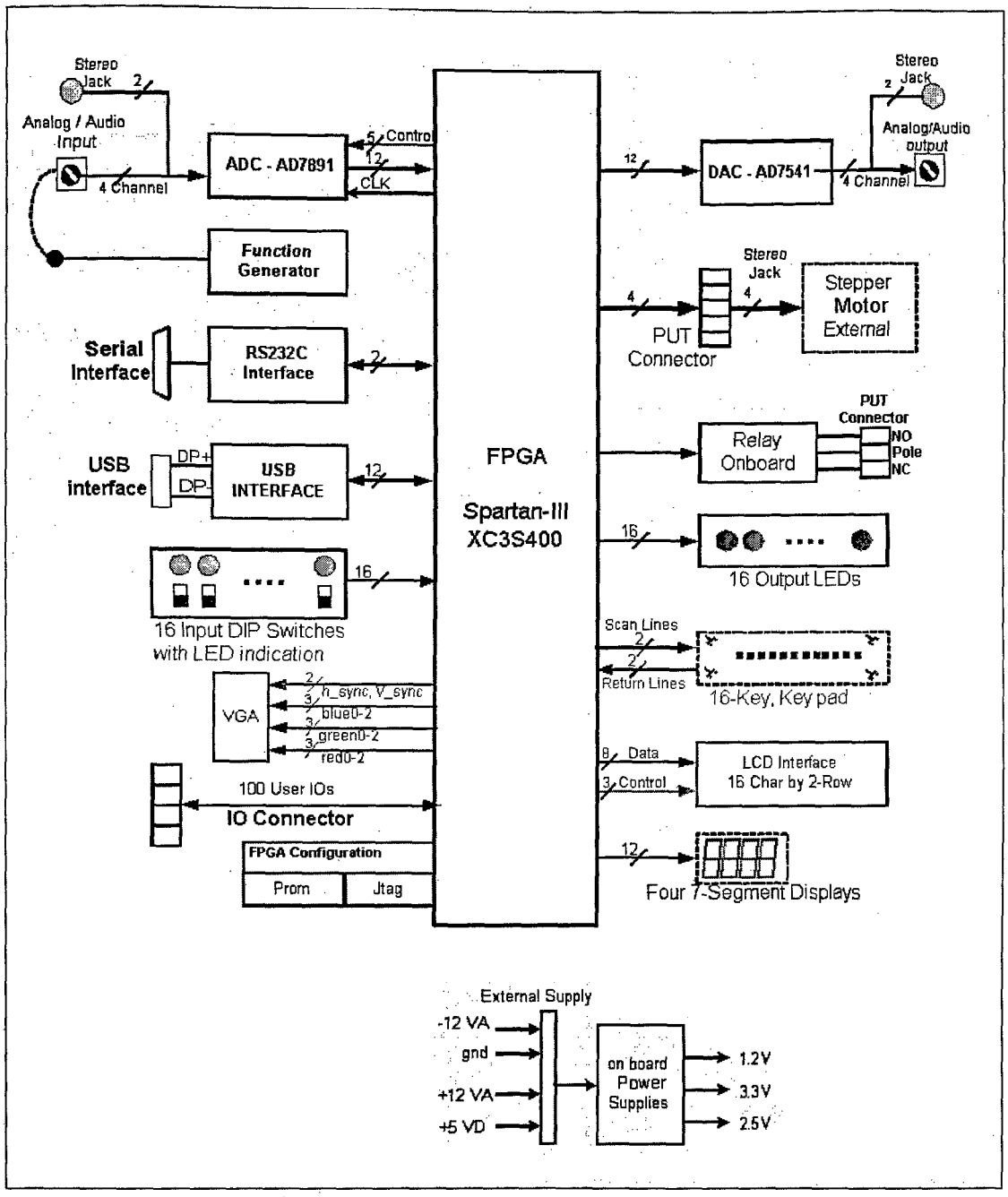

Figure 4.5: Block diagram of the Spartan III DSP boards.

The diagram in Figure 4.6 shows the detailed implementation of the embedded platform using Spartan III XC 3S 400 FPGA. A digital signal is applied as an input to the operational amplifier LM324 which acts as a buffer and is then given to the 12- bit ADC AD7891module.

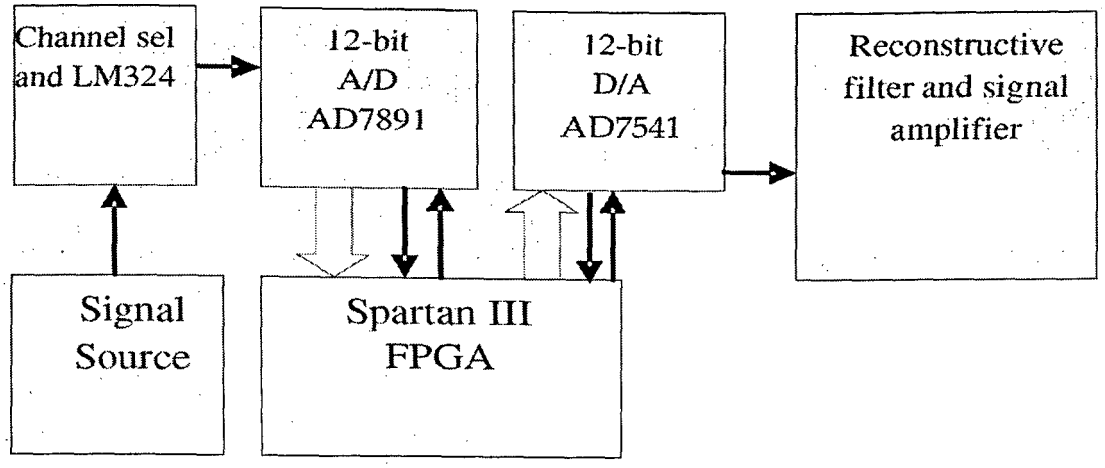

Figure 4.6: Block diagram of Spartan III based embedded Platform.

This ADC converts the analog signal into the digital domain. The digitized data is then fed to the FPGA XC3S400 Spartan-III for further processing. The FPGA is programmed using Xilinx ISE Webpack over JTAG interface. The FPGA is programmed through IDE Xilinx ISE Webpack 6.3i. The processed data from FPGA is then converted back to analog form using a 12-bit DAC AD7541. The reconstructed analog signal is then given to LM324 for amplification. The design hardware has several handshake signals as shown in the Figure 4.7 for external onboard ADC and DAC interface. The data from the ADC after conversion is routed over a 12-bit data bus known as 'db'. The processed data over a user's logic is then given to DAC over 'dac_out' (12-bit). The DAC output is reconstructed back to analog form for representation and display for end user. Any computation in digital signal domain can be manually written using HDL which later can be ported on to FPGA. With increasing complexities of systems and varied levels of expertise of embedded designers, there is an increasing need for tools that provide a higher level of abstraction. This is to empowering the domain experts to use DSPs in building embedded systems rather than spending precious time at the prototyping stage.

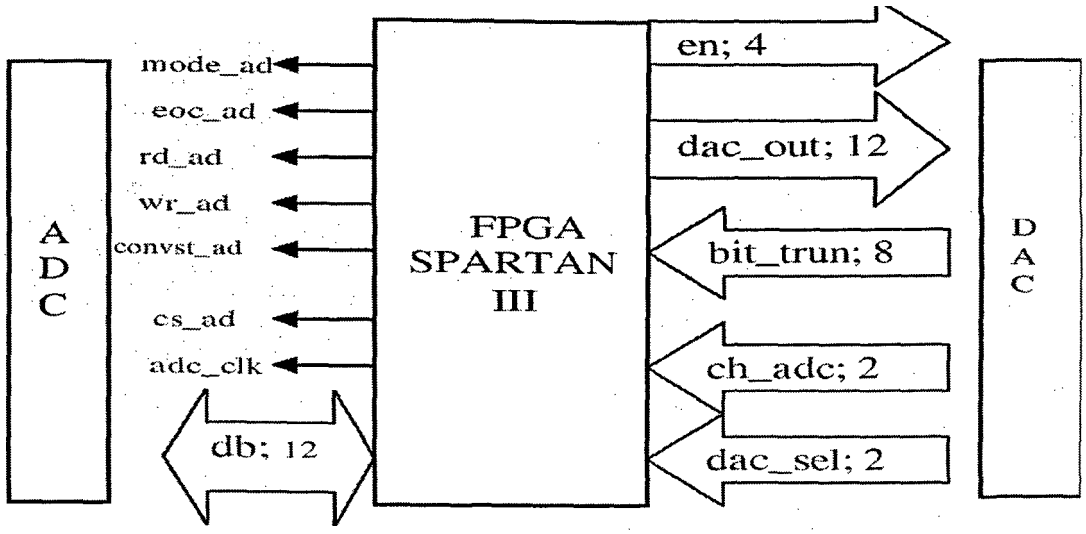

Figure 4.7: Higher level schematic.

The proper EDA interface of the automatic code generator is shown in Figure 4.8. Here, the required logic code of the user is generated by a system generator. The system generator compiles the intermediate code in the form of HDL and the same is available as a component of HDL. The component is then mapped with the entity of HDL code of the ADC and DAC interface as shown in Figure 4.7. The 'bit' file after compilation is programmed over FPGA for required performance. The VHDL architecture of the above described mapping, requires four major processes, which will monitor the overall handshake that is the conversion of data over ADC, reading from ADC, writing ADC data to DAC, selection of DAC channel.

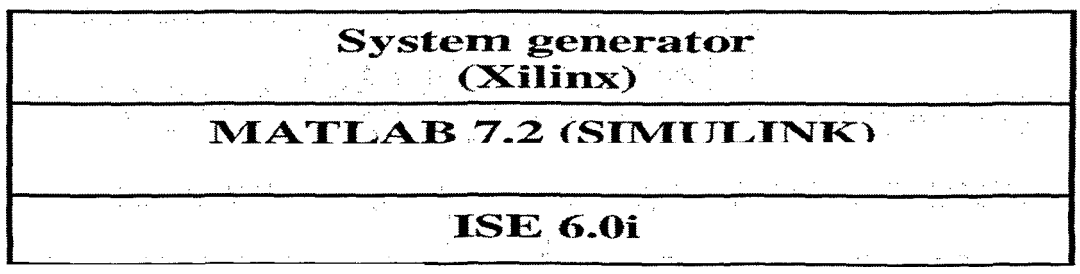

Figure 4.8: Xilinx EDA interface for DSP application.

Audio Synthesis Case Study

The system has been demonstrated to process the audio signal. We have selected audio signal since the electrical equivalent of transmitted optical radiation through human tissue has signal level and bandwidth similar to that of a audio signal. Various effects like echo, chorus, reverberation, flanging, fading and equalization can be implemented to test the system reliability. Echo effect (If the delay is more than 50 - 70 ms, is perceptible to human ear as an echo.) was tested for satisfactory performance and the effect of change in 50 -70 ms delay over superimposed ensemble of signal was studied.

Echo effect

Echo is the repetition of a sound by reflection of sound waves from a surface. It arises in communication systems, when signals encounter a mismatch in impedance.[83] The same has been modeled using Simulink Signal generator as shown in Figure 4.9.

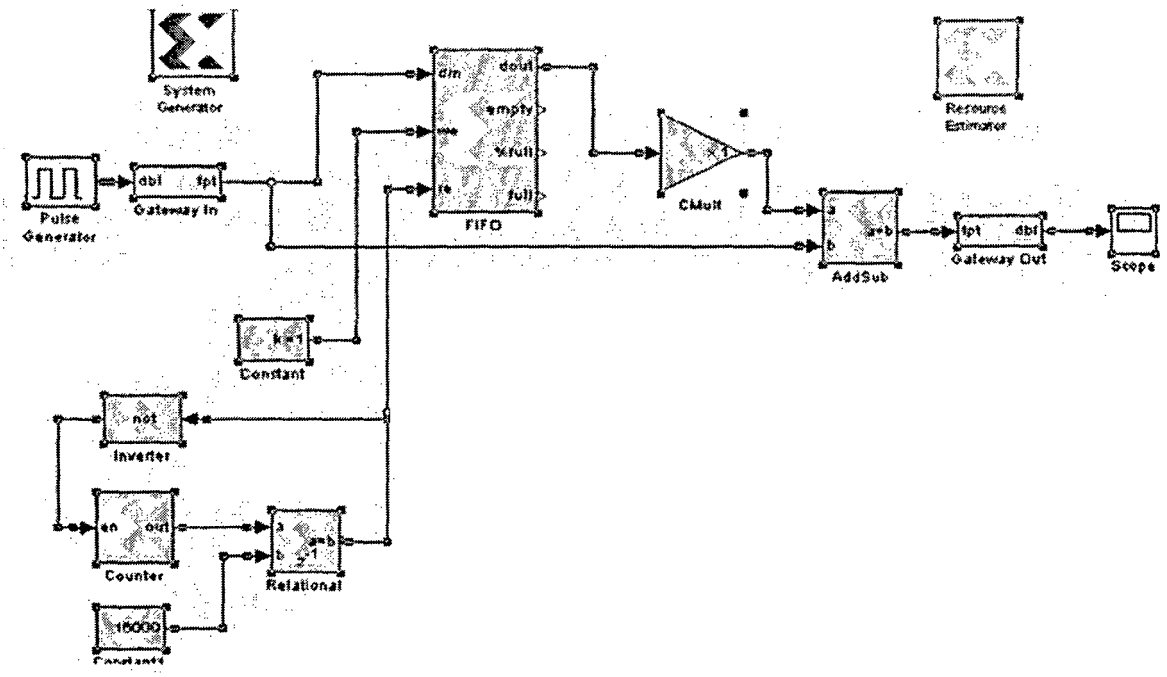

Figure 4.9: Block diagram of the Echo in the DSP generator of Xilinx IDE.

Chorus effect

The chorus effect is often produced when an instrument sounds as if multiple instruments are playing. Multiple voices or instruments are perceived since there is always an imprecise synchronization and a slight pitch variation when they are playing at the same time. The block diagram of the chorus effect is shown in Figure 4.10.

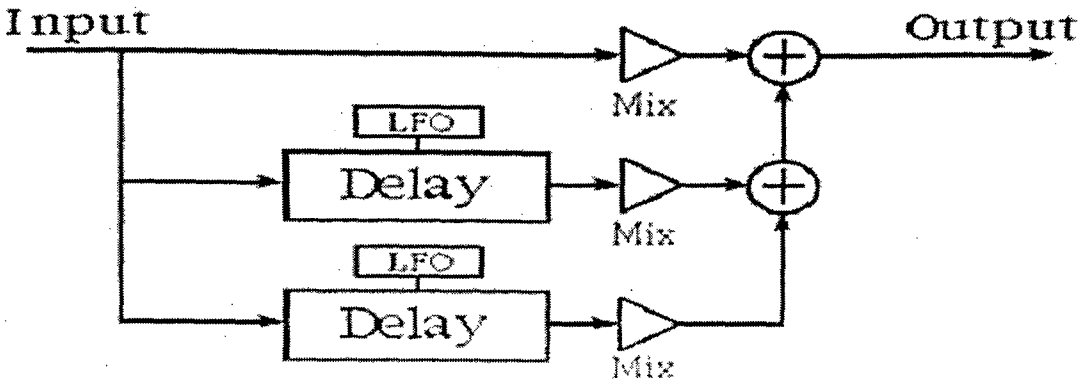

Figure 4.10: Block diagram of the chorus effect.

4.2.1.2 DSP algorithm on Altera Cyclone II platform

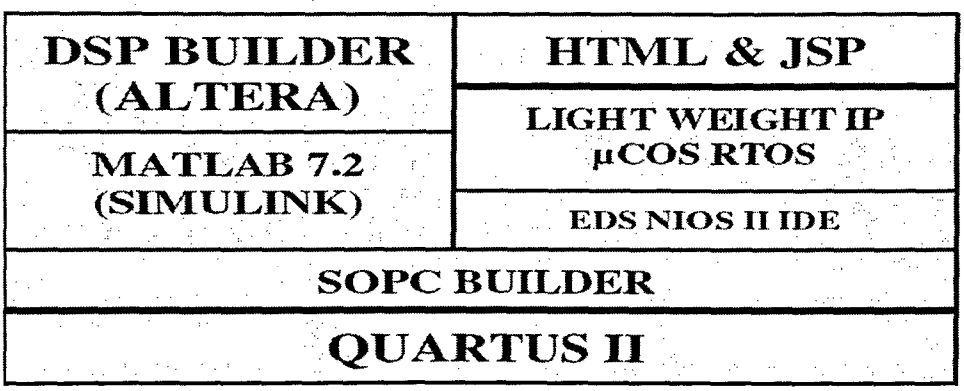

Figure 4.11: ALTERA EDA interface.

The Altera EDA interface of the automatic code generator for DSP application is shown in Figure 4.11. Altera DSP generator is more user-friendly, as the input and output port ADC/ DAC are available in the block form compared to Xilinx HDL code to interact

with ADC. The audio signal is given to 12 - bit ADC ADS55001, the digitized data is then passed through the different audio synthesis blocks like Echo, Reverberation, Flanging etc. These effects are selected based on the logic at DIP switches. The synthesized output is then passed through a 12 - bit D/A converter AD 9706. The analog output of a D/A converter is connected to speakers, to hear the desired audio effect. The photo of Altera cyclone II development is shown in Figure 4.12.

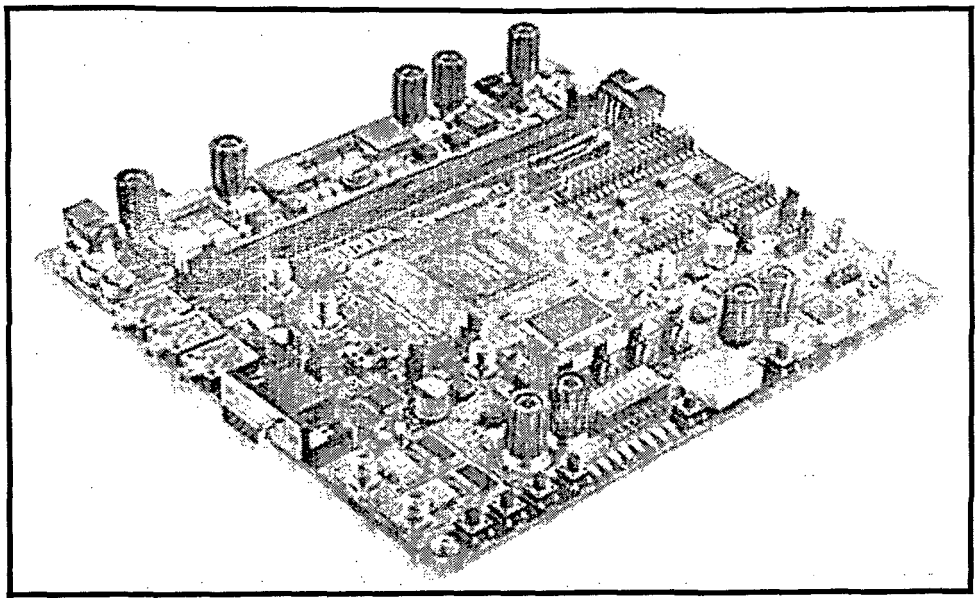

Figure 4.12: ALTERA Cyclone II development board

Audio synthesis case study on cyclone II Platform

Here we have tested Echo, Reverberation, Flanging etc. algorithm on Cyclone II platform. The block of Echo effect is shown in Figure 4.13.

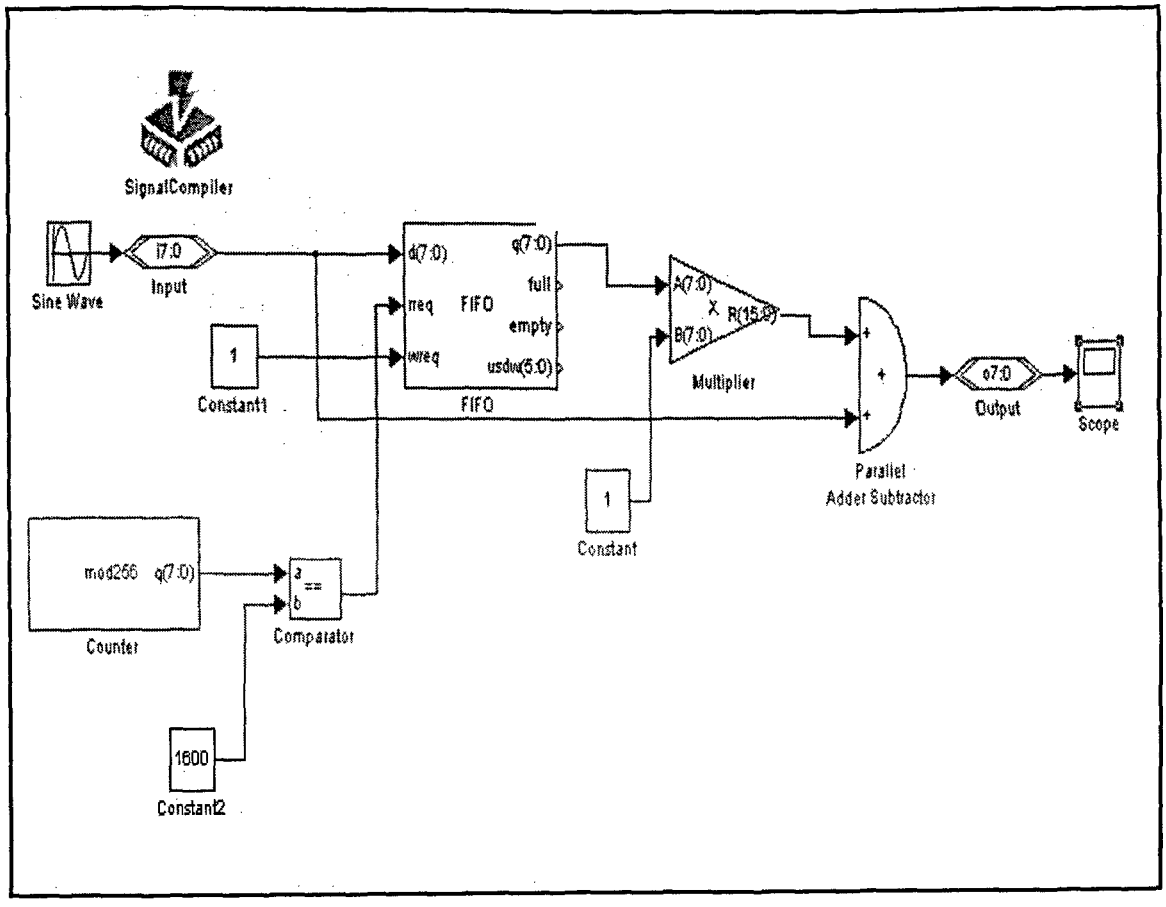

Figure 4.13: DSP design for ECHO generator.

4.3 Resources Used By Altera and Xilinx Platform to Implement Audio Synthesis Algorithms

The compared resources used by Altera and Xilinx platform to implement audio synthesis algorithms are given in Table 4.1. After analyzing the compilation report of both the platforms, it was found that Altera platform is more versatile and their designs are more optimized than Xilinx for said application.

Table 4.1: Comparison between Altera & Xilinx for Echo generation

a)Altera

Resource	Available	Used
Logic elements	68416	2374 (3%)
Registers	1183	0
Pins	422	35 (1%)
Total memory bits	1,152,000	5,780 (1%)
Embedded multiplier 9-bit elements	300	1
PLL	4	0

b)Xilinx

Resource	Available	Used
System gate	200 k	25 K
Logic cells	4320	3135
Dedicated multipliers	12	4
User I/O	173	35
Block RAM	216K	30K

The execution speed of audio signal algorithms on Altera platform is 100μs and Xilinx platform is 140μs.

4.4 Soft-Core Processors for Embedded Systems

Embedded Systems are combination of hardware and software components working together to perform a specific application. They exist in abundance in our modern society and play a vital role in our everyday lives. They can be found in places such as our automobiles, in the medical field, in industrial control systems, and in entertainment electronics etc.[84] The hardware platform of the embedded system often consists of a microprocessor/microcontroller, an on-board memory, an output display, an input device for a user to enter data and application software. The design of embedded systems is now becoming increasingly difficult due to the tight constraints on area usage, size, power consumption and performance. In addition to these constraints, many embedded system developers are faced with tight time to market deadlines.[85] Hence, the hardware/software co-design methodology is often used to design embedded systems in order to help reduce the amount of time spent on development and debugging.[86]

As the complexity of embedded systems designs increased over time, designing each and every hardware component of the system from scratch soon became far too impractical and expensive for most designers. Therefore, the idea of using pre-designed and pre-tested IP cores in designs became an attractive alternative. Soft-core processors are microprocessors whose architecture and behaviour are fully described using a synthesizable subset of a HDL. They can be synthesized for any ASIC or FPGA technology; therefore they provide designers with a substantial amount of flexibility. The use of soft-core processors holds many advantages for the designer of an embedded system. First, soft-core processors are flexible and can be customized for a specific application with relative ease. Second, since soft-core processors are technology independent and can be synthesized for any given target ASIC or FPGA technology, they are therefore more immune to becoming

obsolete when compared with circuit or logic level descriptions of a processor. Finally, since a soft-core processor's architecture and behaviour are described at a higher abstraction level using an HDL, it becomes much easier to understand the overall design.

4.5 A Survey of Soft-Core Processors

In this section we will survey the available soft-core processors provided by commercial vendors and open source communities.

4.5.1 Commercial Cores and Tools

NIOS II, MicroBlaze and PicoBlaze are the leading soft-core processors provided by Altera and Xilinx respectively. In this section, we will discuss the important features of each soft-core processor.

NIOS II by Altera Corporation:

Altera Corporation is one of the leading vendors of CPLDs and FPGAs.[87] They offer the Stratix, Stratix II and Cyclone families of FPGAs that are widely used in the design of embedded systems and DSP applications. They also provide associated CAD tools such as Quartus II and System-on-Programmable-Chip (SOPC) Builder that allow designers to synthesize, program, debug their designs and build embedded systems on Altera's FPGAs. The NIOS II Processor is their flagship IP soft-core processor and can be instantiated with any embedded system design.[88] The NIOS II Soft-Core Processor is a general purpose Reduced Instruction Set Computer (RISC) processor core and features a Harvard memory architecture. This processor features a full 32-bit Instruction Set Architecture (ISA), 32 general-purpose registers, single-instruction 32x32 multiply and divide operations, and dedicated instructions for 64-bit and 128-bit products of multiplication. The NIOS II also has a performance of more than 150 Dhrystone MIPS (DMIPS) on the Stratix family of

FPGAs. This soft-core processor comes in three versions: economy, standard and fast core. Each core version modifies the number of pipeline stages, instructions, data cache memories and hardware components for multiply / divide operations. In addition, each core varies in size and performance depending on the features that are selected. Adding peripherals with the NIOS II Processors is done through the Avalon Interface Bus which contains the necessary logic to interface the processor with off-the-shelf IP cores or custom made peripherals.

Micro Blaze and Pico Blaze by Xilinx Incorporated:

Xilinx Incorporated are the makers of the Spartan and Virtex families of FPGAs. In addition, they also offer soft IP cores that target their FPGAs. MicroBlaze soft-core is a 32-bit processor that is optimized for embedded applications. It can operate at up to 200 MHz on a Virtex-4 FPGA, and it features a Harvard RISC architecture, 32-bit instructions, a 3-stage pipeline, a 32 register wide register file, a shift unit and two levels of interrupt. Memory can reside on-chip or as an external peripheral. A general purpose interface known as the On-chip Peripheral Bus (OPB) can be used to interface MicroBlaze with both on-chip and off-chip memories as well as other peripherals.

The MicroBlaze soft-core processor is targeted for the Virtex and Spartan families of FPGAs only.[89] Xilinx also offers the Embedded Development Kit (EDK) which includes Xilinx Platform studio and a set of IP cores that are required for developing embedded systems using MicroBlaze. Xilinx also supplies the PicoBlaze soft-core processor, a compact 8-bit Microcontroller that is optimized for the Spartan-3, Virtex-II and Virtex-II Pro families of FPGAs.[90] The PicoBlaze processor is a small, cost-effective soft-core processor that is useful for simple data processing applications.

Other FPGA Vendors

Tensilica Inc. offers a number of soft IP processing cores for embedded systems design. Their Diamond Standard Series of synthesizable processors offer a set of six preconfigured off-the-shelf processors with a variety of features.[91] They range in size and feature set from small, power-optimized controllers such as the 108MiniRISC Controller, to large, high-performance cores such as the 545CK, which has been optimized for DSP applications.[92]

Tensilica's flagship product is the Xtensa Series of "configurable and extensible" processors.[93] They are configurable, in that they offer the designer a set of predefined parameters which they can configure in order to tailor the processor to the intended application. They are also extensible, in that designers can also invent custom instructions and execution units and integrate them directly into the processor core.

Open-source Cores

Open-source cores are IP components that are freely available in the open-source community.[94] Usually these types of cores are used in academia for research as well in the development of embedded systems. UT NIOS is an example of an open-core processor used in academia.[95] Sun Microsystems provides its own soft-core processor, OpenSPARC, which is widely used in the development of ASICs, but it can also be synthesized for FPGAs as well.[96] In this section, we will review the LEON and OpenRISC 1200 soft-core processors that are available in the open-source community.

LEON by Gaisler Research

Gaisler Research is a provider of IP cores and supporting development tools for embedded processors based on the SPARC architecture.[97] Their main product is the LEON line of synthesizable soft-core processors and associated library of IP cores, called the GRLIB IP Library. Several successive versions of the LEON processor have been

developed, and currently Gaisler Research maintains and supplies the LEON2 and the LEON3 processors.

OpenRISC 1200

OpenRISC 1200 is one of the popular open core processors available at OpenCores.org.[98] This soft-core processor features a 32-bit and 64-bit RISC architecture suitable for numerous applications including networking and telecomm devices, home entertainment, consumer products and automotive applications. This processor is optimized for high performance, low power consumption, and versatility in a wide range of applications. The processor features a Harvard architecture containing separate data and instruction caches, each 8 KB in size. It has a 32-bit ISA containing the OpenRISC Basic Instruction Set, a scalar, single-issue 5-stage pipeline delivering sustained throughput and single-cycle instruction execution on most instructions. This processor can be synthesized and downloaded onto Altera and Xilinx FPGAs and supports embedded Real Time Operating Systems (RTOS) such as Linux, μLinux and OAR RTEMS RTOS. For software development, tools are available that allow developers to compile programs written in C/C++, Java and Fortran to run on the OpenRISC processor.

4.6 Comparison of Soft-Core Processors

Table 4.2 below shows a comparison of the features and characteristics of several processors that we have surveyed.

The first column presents the features across which the processors are being compared. The subsequent columns show the available features inside of each soft-core processor. As shown in the Table 4.2, The NIOS II and MicroBlaze soft-core processors

have the highest operating frequency for FPGA implementation. NIOS II also has the capability of expanding its instruction set by adding up to 256 custom instructions. MicroBlaze does not have this kind of feature. NIOS II and MicroBlaze soft-core processors are targeted and optimized mainly for FPGA implementation. In contrast, the other three cores are not optimized for any specific target technology. Each core surveyed has different performance characteristics and features that are suitable for specific applications. Embedded system designers should choose a processor core based on the requirements and performance constraints of their particular application.

Table 4.2: Comparison of Soft-Core Processors

Category	**NIOS II (Fast Core)**	**MicroBlaze**	**Xtensa**	**OpenRISC 1200**	**LEON3**
Maximum MHz	200 (FPGA)	200 (FPGA)	350 (ASIC)	300 (ASIC)	400/125 (ASIC/FPGA)
ISA	32-bit RISC	32-Bit RISC	32-Bit RISC	32-bit RISC	32 or 64-bit RISC
Custom Instructions	Up to 256 Instructions	None	Unlimited	Unspecified limit	None
Pipeline	6 Stages	3 Stages	5 Stages	5 Stages	7 Stages
Register File Size	32	32	32 or 64	32	2 to 32
Area	700-1800 LEs	1269 LUTs	0.26 mm^2	N/A	N/A

We have designed an embedded DSP architecture for blood glucose non-invasively around the Altera NIOS II soft-core processor.

4.7Altera NIOS II soft-core for Non-Invasive Glucometer

System-on-a-Programmable-Chip (SOPC) for Glucose analysis:

SOPC Builder is a powerful system development tool. SOPC Builder enables you to define and generate a complete SOPC in much less time than using traditional, manual integration methods.[99] SOPC Builder is included as part of the Quartus II software. SOPC builder is used to create systems based on the NIOS II processor. NIOS II system builder is a general-purpose tool for creating systems that may or may not contain a processor and may include a soft processor other than the NIOS II processor. SOPC Builder automates the task of integrating hardware components. Using traditional design methods, one must manually write HDL modules to wire together the pieces of the system. Using SOPC Builder, one specifies the system components in a GUI and SOPC Builder generates the interconnect logic automatically. SOPC Builder generates HDL files that define all components of the system, and a top-level HDL file that connects all the components together. SOPC Builder generates either Verilog HDL or VHDL equally. Figure 4.14 shows an FPGA design that includes an SOPC Builder system and custom logic modules. One can integrate custom logic inside or outside the SOPC Builder system. In this example, the custom component inside the SOPC Builder system communicates with other modules through an Avalon-MM master interface. The custom logic outside of the SOPC Builder system is connected to the SOPC Builder system through a PIO interface. The SOPC Builder system includes two SOPC Builder components with Avalon-ST source and sink interfaces. The system interconnect fabric connects all of the SOPC Builder components using the Avalon-MM or Avalon-ST system interconnect as appropriate.

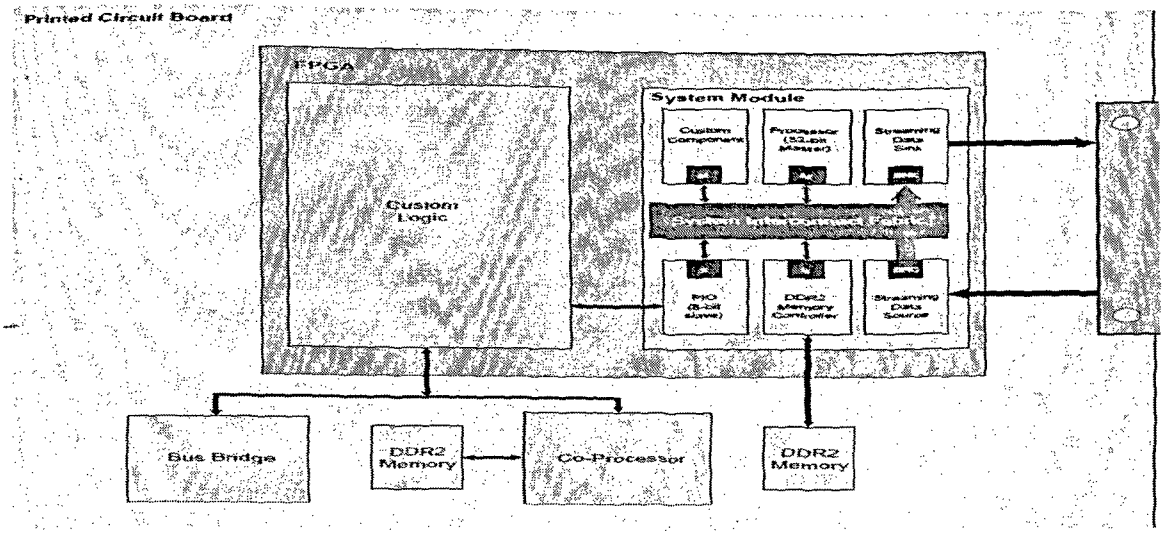

Figure 4.14. SOPC Builder system and custom logic modules

Altera NIOS II Soft-Core for Non-Invasive Glucometer

As the complexities of systems increase in embedded designing, there is an increasing need for tools that provide a higher level of abstraction. It was found that the utility of the said approach is limited due to non-availability of the soft IP core from the manufacturers for PLS regression techniques. Therefore the total design was shifted to ALTERA domain. The ALTERA boards like DE2 & DSP development boards having Cyclone II target which support the 32 bit NIOS – II soft-core processor. The NIOS-II has its own small entities like ROM, TIMER, SDRAM, SRAM, FLASH support as shown in Figure 4.15.

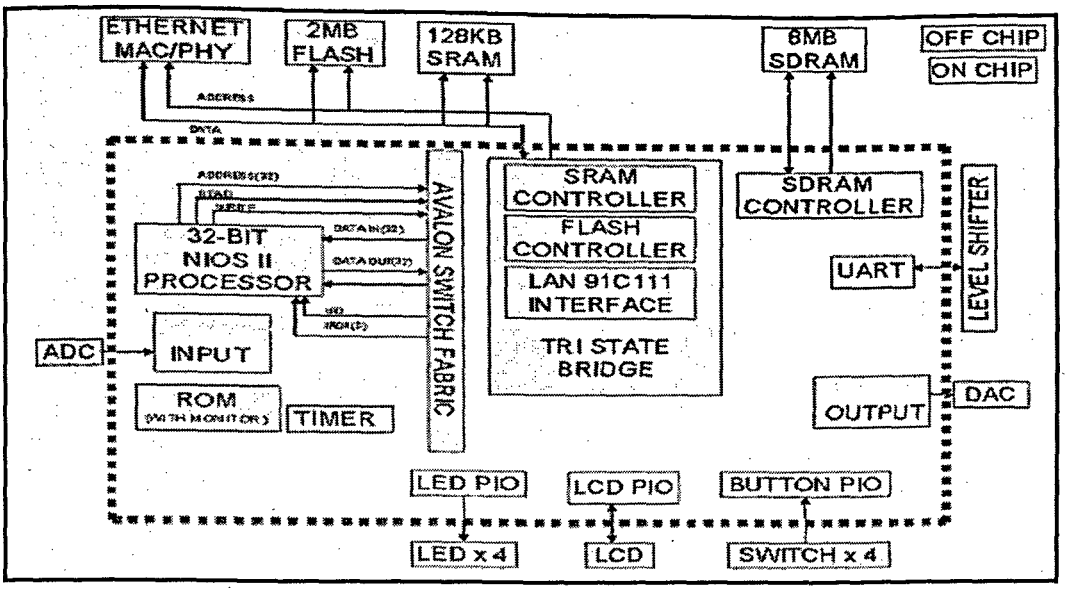

Figure 4.15: NIOS II soft-core processor architecture for glucose signal processing.

The System On Chip (SOC) building implementation of the resources required is shown in Figure 4.16. The multivariate program can be easily programmed on to the programmable device Cyclone II with the help of NIOS-IDE wherein the C algorithm is running.

Use	Module Name	Description	Input Clock	Base	End	IRQ
☑	⊟ cpu_0	Nios II Processor - Altera Corporation	clk			
	instruction_master	Master port				
	data_master	Master port		IRQ 0	IRQ 31	
	jtag_debug_module	Slave port		0x00480000	0x004807FF	
☑	⊞ tri_state_bridge_0	Avalon Tristate Bridge	clk			
☑	⊞ cfi_flash_0	Flash Memory (Common Flash Interface)		0x00000000	0x003FFFFF	
☑	⊞ sdram_0	SDRAM Controller	clk	0x00800000	0x00FFFFFF	
☑	⊞ epcs_controller	EPCS Serial Flash Controller	clk	0x00480800	0x00480FFF	8
☑	⊞ jtag_uart_0	JTAG UART	clk	0x004810B0	0x004810B7	1
☑	⊞ uart_0	UART (RS-232 serial port)	clk	0x00481000	0x0048101F	2
☑	⊞ timer_0	Interval timer	clk	0x00481020	0x0048103F	3
☑	⊞ timer_1	Interval timer	clk	0x00481040	0x0048105F	4
☑	⊞ lcd_16207_0	Character LCD (16x2, Optrex 16207)	clk	0x00481060	0x0048106F	
☑	⊞ led_red	PIO (Parallel I/O)	clk	0x00481070	0x0048107F	
☑	⊞ led_green	PIO (Parallel I/O)	clk	0x00481080	0x0048108F	
☑	⊞ button_pio	PIO (Parallel I/O)	clk	0x00481090	0x0048109F	5
☑	⊞ switch_pio	PIO (Parallel I/O)	clk	0x004810A0	0x004810AF	
☑	⊞ SEG7_Display	SEG7_LUT_8	clk	0x004810C0	0x004810C3	
☑	⊞ DM9000A	DM9000A	clk	0x004810B8	0x004810BF	6
☑	⊞ sram_0	SRAM_16Bits_512K	clk	0x00400000	0x0047FFFF	

Figure 4.16: Selected SOPC components to built system.

The acquired data can be processed using PLS algorithm in 'C language' for computing the unknown concentration of the variants. We have tested the designed system for multivariate analysis by running SIMPLS algorithm in C to estimate the level of blood glucose .To make sure that system works efficiently, we have also tested the designed system for various Matrix manipulation for application involving curve fitting, finding square root of numbers, mean of numbers, sorting numbers, finding the solutions of quadratic equations, matrix transpose, finding determinant, multiplication and interpolation before actual implementation of SIMPLS algorithm.

NIOS II Interaction with NEWPORT Optical power meter:

The interface between Altera NIOS II and Newport power meter was successfully developed, and the system design using NIOS II soft-core with all the interfacing signals is shown in Figure 4.17. Here the NIOS II core is interfaced to the on board memories (Flash and SRAM) to store the code and the data received from power meter and the core is operating at 50MHz. NIOS II interacts with Newport power meter using the RS232 interface(RxD,TxD).It may be noted that the NIOS II core is designed on Altera CYCLONE II.It is estimated that the said interface would utilize 14 % of available resource, leaving other resource open for the development of other application.

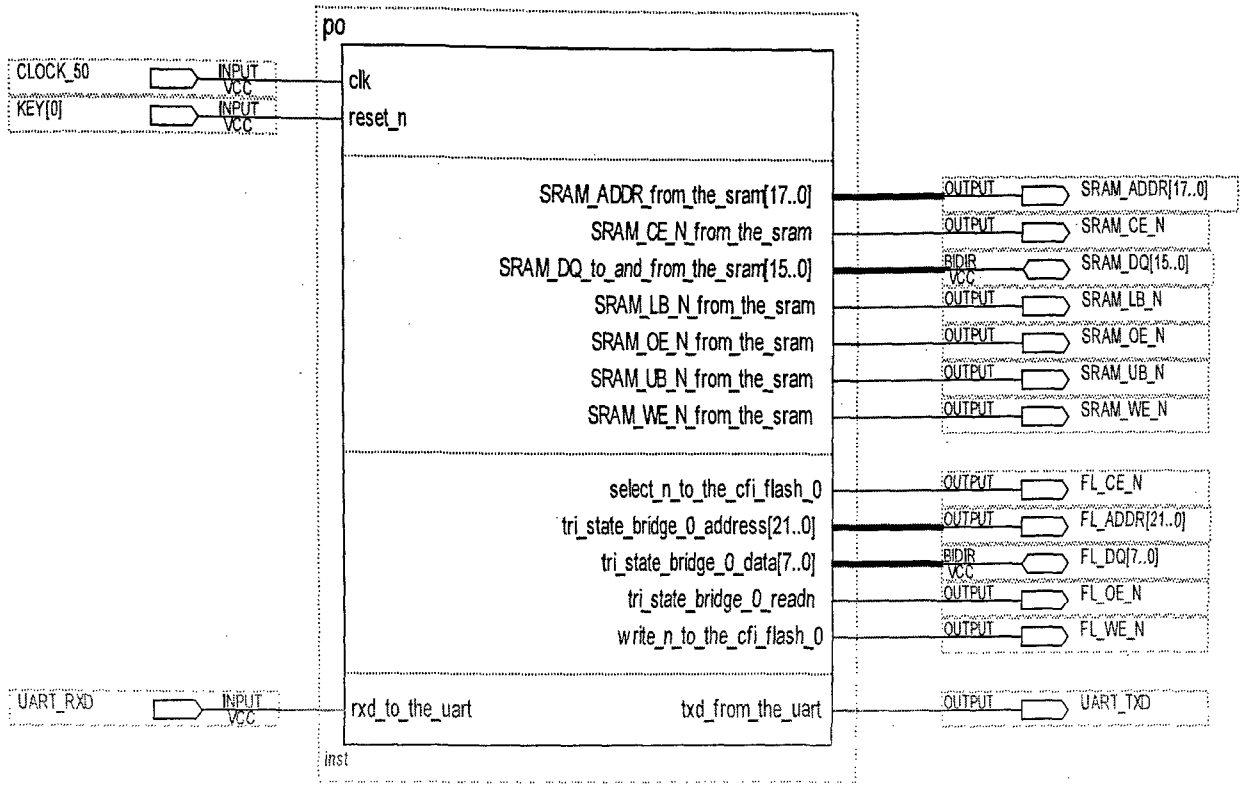

Figure 4.17: Altera NIOS II soft-core system for controlling optical power meter

Figure 4.18 shows the photo of Interface diagram of CYCLONE II FPGA and Newport power meter. The C code running on NIOS II system to select the wavelength in the range 2.0 μm to 2.5 μm and receiving the data corresponding to respective wavelength is given in ANNEXURE V. The data received is then stored in the SRAM and can be access very easily in order to perform the required processing algorithms. Here the thermally cooled NIR detectors are used to minimize the noise .one of the common problems found in IR detector is the noise due to thermal excitation at room temeprature.Most of the time the signal gets deeply buried in the noise. This is more prominent in germenium (Ge) based detectors. Whereas, InGaAs detector have comparatively less noise and further reduced by cooling techniques.

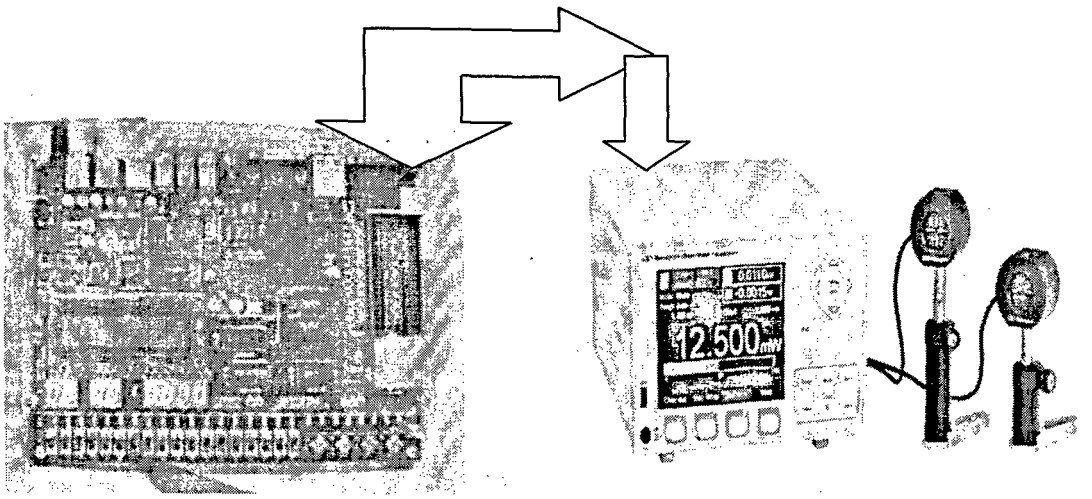

Figure 4.18: Interface diagram of CYCLONE II FPGA and Newport power meter

NIOS II Soft-core system to control Monochromator

The designed NIOS II soft-core system to control monocromator is shown in Figure 4.19. Here the 4 line interface is connected to motor through motor driving stage. Two sense inputs to sense the initial and final position. Apart from this 4x4 matrix key pad is interfaced to enter the respective scan range and resolution.In this stage NIOS II cotrol forward and backward motion of stepper motor and this takes care of grating position of the monochromator to a great degree of precision.Though the highend FPGA configured as processor is not required for such application. Since FPGA gives flexibility to integrate the various modules we have used FPGA for our purpose rather than using the Hard core Micontrollers.

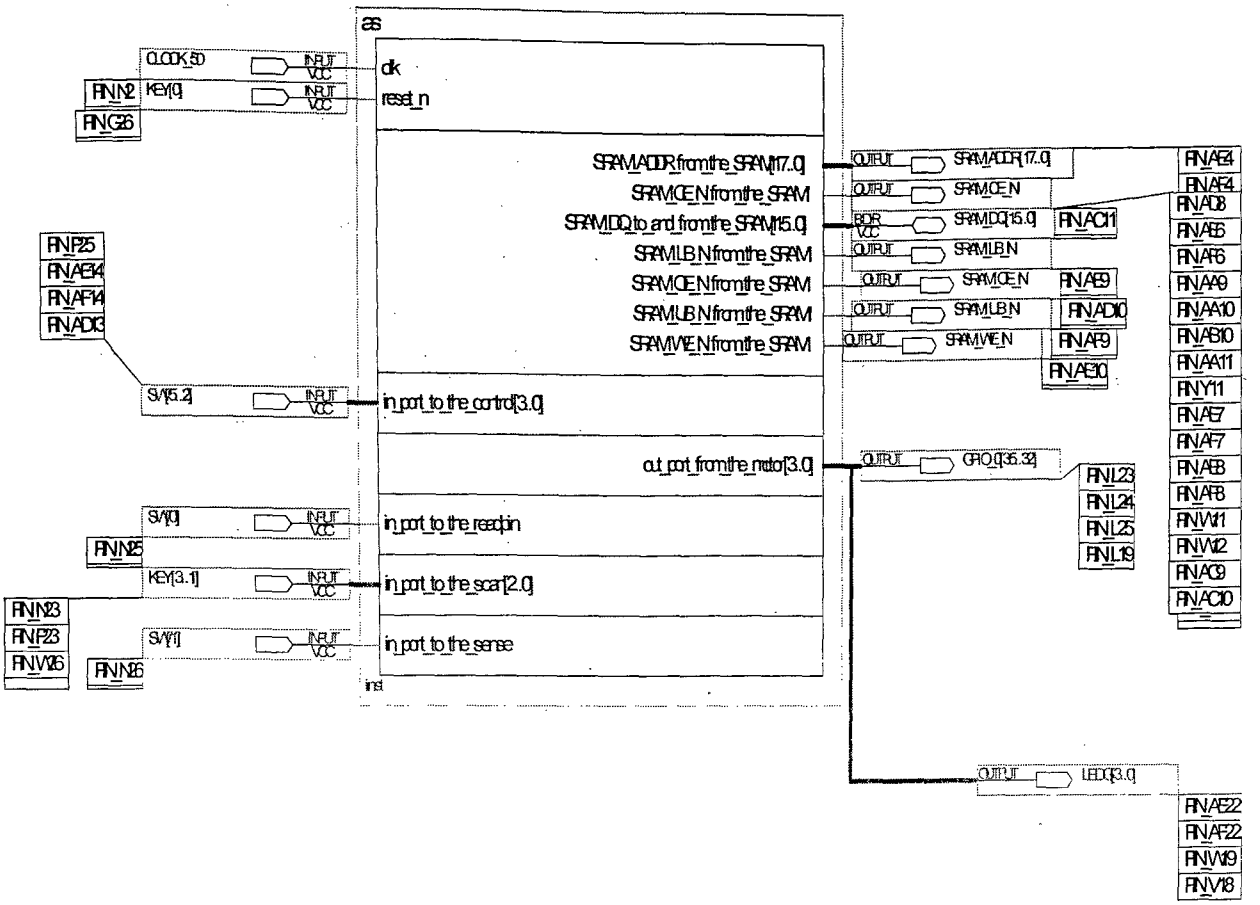

Figure 4.19: Altera NIOS II soft-core system for monochromator control

The SOPC builder components required to build the system which control monochromator is shown in Figure 4.20. The selected componets are 32 bit NIOS II CPU, SRAM, FLASH, System clock, Timer, PIO's for output and input etc. After selecting all the required SOPC components, the total system is generated and then the final pin mapping is done.

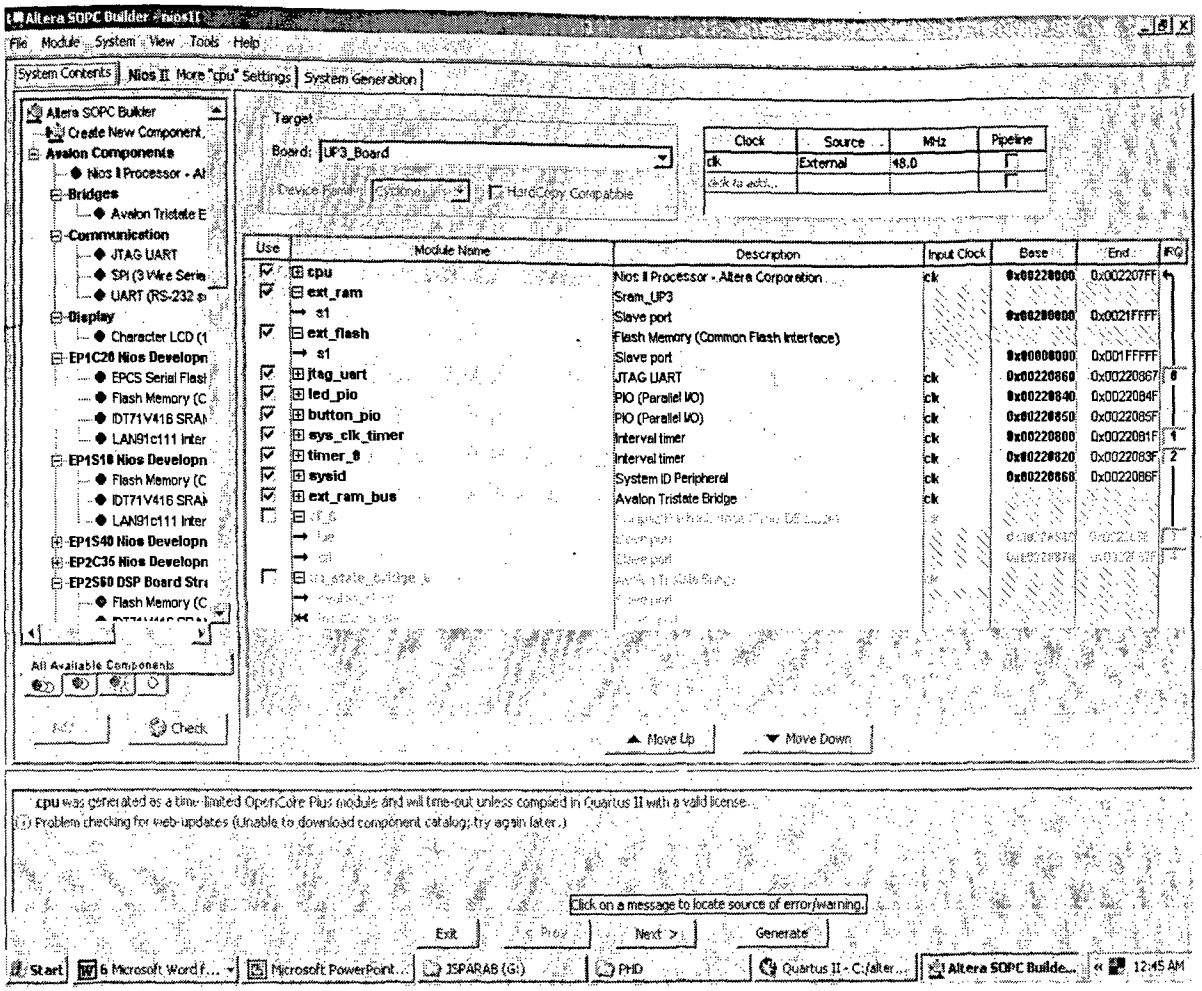

Figure 4.20: SOPC blocks selected to build the system

The C code running on NIOS II soft-core to control the monochromator to select the spectral range 2.0 μm to 2.5 μm is given in ANEXURE II. It is estimated that the said interface would utilize 24 % of available resource, leaving other resource open for the development of other application.

NIOS II soft-core Platform Spectral data acquisition

Here we have Altera NIOS II core developed to interact with ADC 7891 and DAC is shown in Figure 4.20. Here NIOS II interacts with ADC to configure the ADC and accept the digitized spectral information and stores it in the memory. Various interfacing signals

used to interact are eoc_ad7891 to see if the conversion is complete, convstst_ad7891 to start the conversion process.acd_out is 12 bit interface to acquire the converted data .After processing the data is passed on to dac_out (12 bit) to interface the signal to external world.mode_7891 to set the ADC in parallel mode and wr_ad7891/rd_7891 is used to write and read data from ADC buffer etc. It is estimated that the Altera NIOS II soft-core system and ADC 7891 interface would utilize 8% of available resource, leaving other resource open for the development of other application.

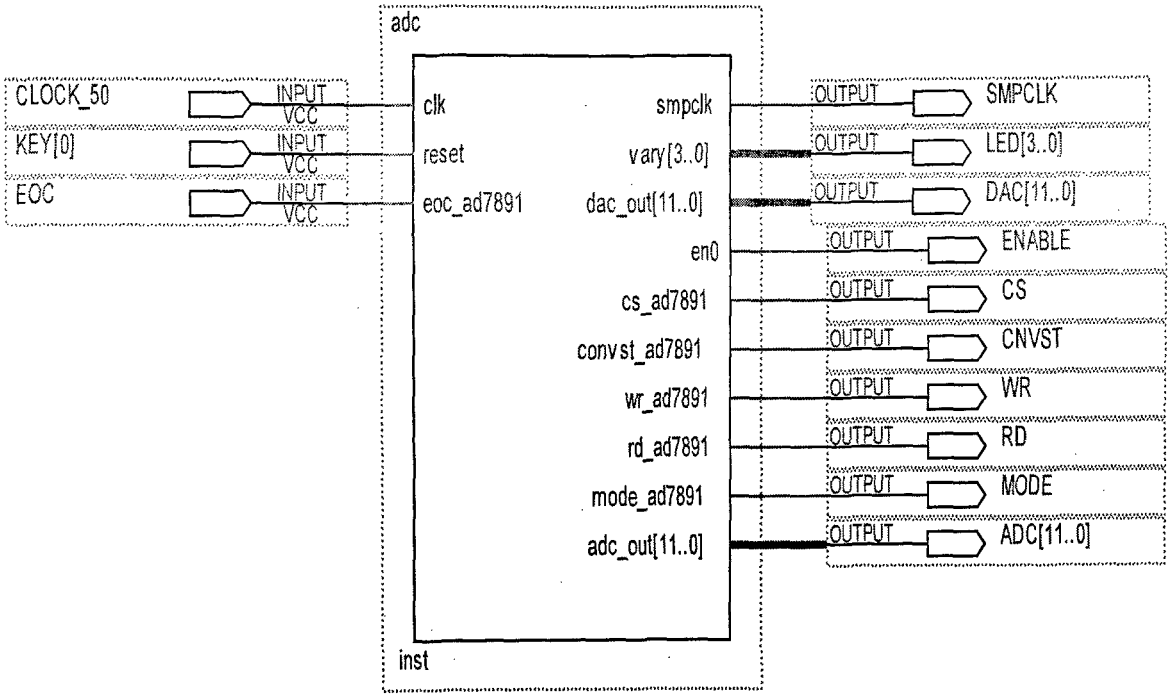

Figure 4.21: Altera NIOS II soft-core system and ADC 7891 interface

Full-fledged Altera NIOS II based DSP architecture for glucose estimation:

The designed DSP architecture for glucose estimation is shown in Figure 4.22. Here we have built an full-fledged Altera NIOS II system consisting of controlling monochromator to select the respective wavelength range (2.0μm-2.5μm) with resolution of 1nm, Interacting with 12-bit ADC AD7891 which collects data from detector connected to channel 1 of AD7891 (InGaAs) .The block also selects 2nd channel of ADC, where ordinary detector is connected for stabilization purpose. The SIMPLS algorithm developed in C on the acquired spectral data. The result of the estimated concentration of glucose in whole blood is displayed on LCD display. It is estimated that the Full-fledged DSP system for Glucose estimation would utilize 45% of available resource, leaving other resource open for the development of other application. Figure 4.23 shows the photo of full fledged sytem for glucose estimation

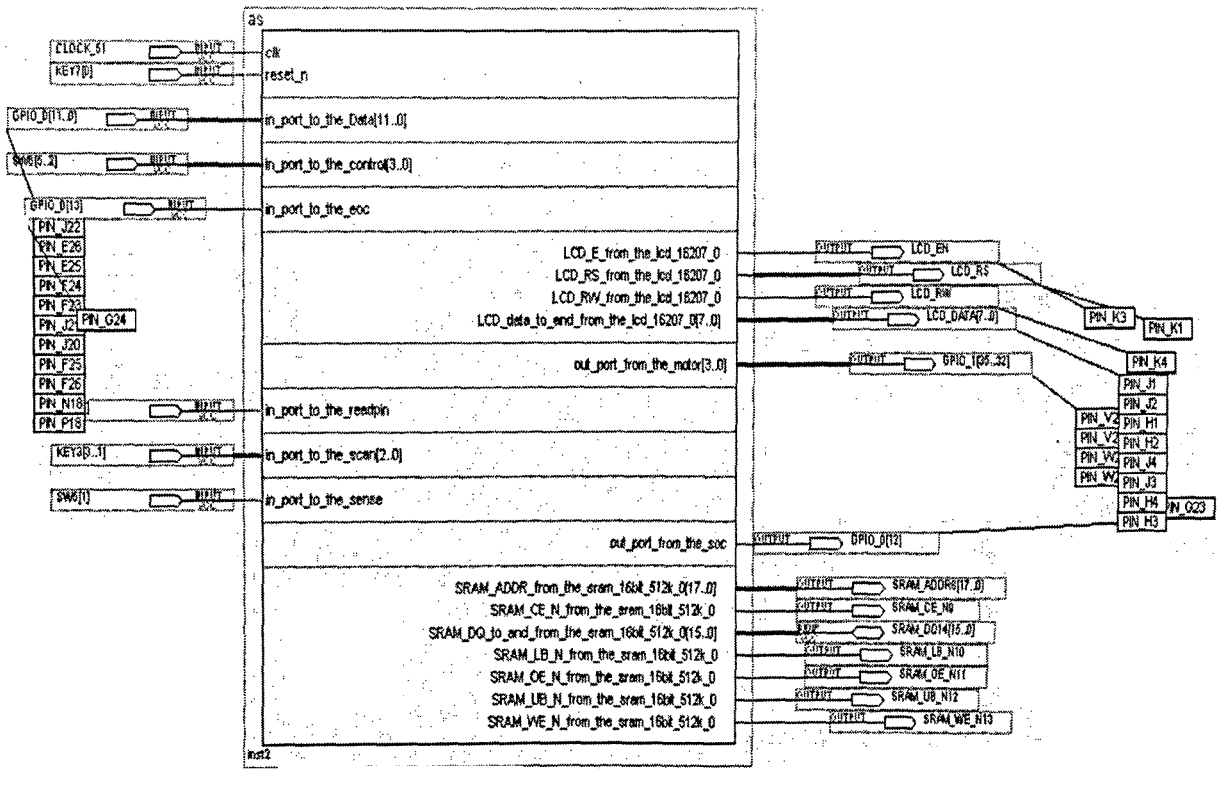

Figure 4.22: Full-fledged DSP system for Glucose estimation.

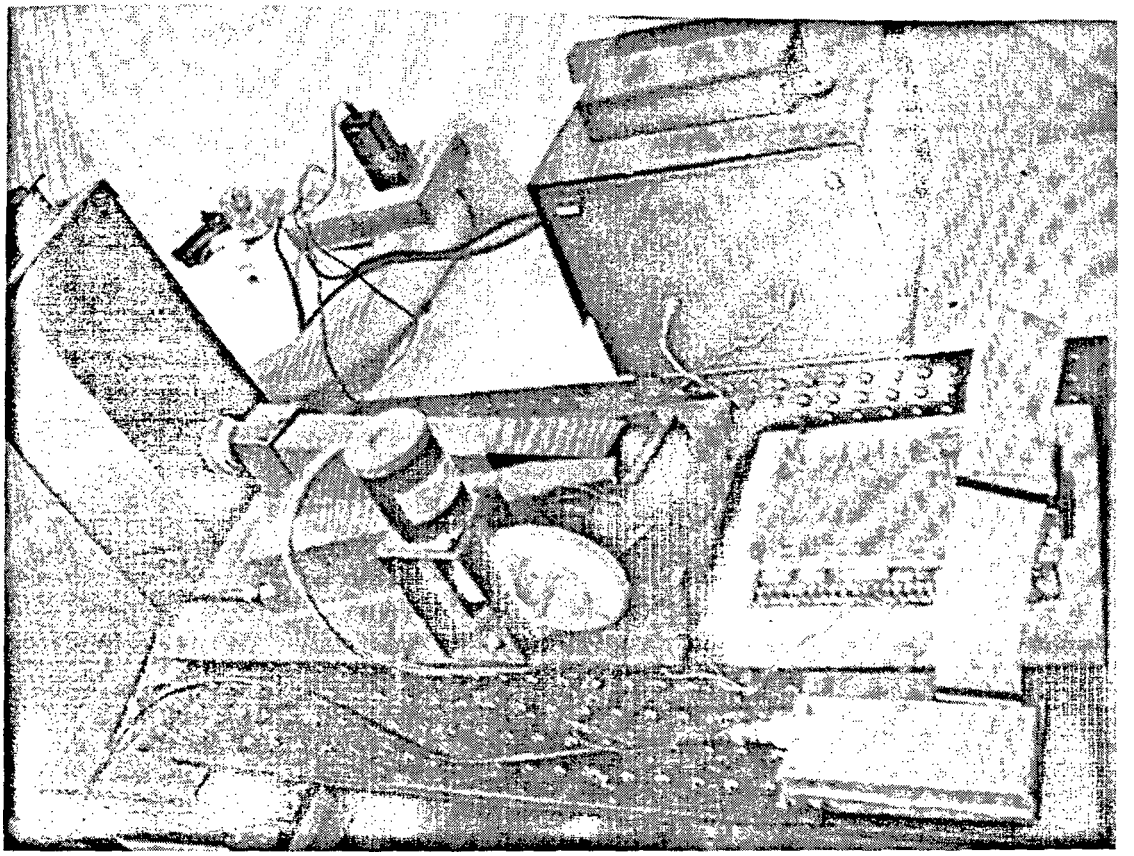

Figure 4.23: Photo of full fledged sytem for Glucose estimation.

CHAPTER 5

MULTIVARIATE DATA ANALYSIS

5.1 Multivariate Analysis:

Recent advances in computer technology and instrumentation techniques have enabled us to collect precise and varieties of data from chemical and biological processes. With the increased data dimensionality, Multivariate Statistical Process Control (MVSPC) has become very important and essential tool to extract the useful information from the measured data for improving process performance and product quality. During the last decade, this has been successfully applied for monitoring and modelling chemical / biological processes.[100][101][102][103][104]

One of the most popular MVSPC techniques is Partial Least Squares (PLS). PLS is a multivariate process identification method that projects the input-output data down into a latent space, extracting a number of principal factors with an orthogonal structure, while capturing most of the variance in the original data.[105][106]

5.1.1: Partial Regression Analysis - Basic Idea

Partial least squares regression is an extension of the multiple linear regression models. In its simplest form, a linear model specifies the relationship between a dependent (response) variable 'Y', and a set of predictor variables, the 'X's', as given in Equation 5.1.

$$Y = b_0 + \sum_{i=1}^{p} b_i X_i \qquad 5.1$$

In this equation 'b_0' is the intercept and the 'b_i' values are the regression coefficients (for variables 'X_1' to 'Xp') computed from the data sets with known constant concentrations (for example, one could estimate (i.e. predict) a person's weight as a function of the person's height and gender. You could use linear regression to estimate the respective regression coefficients from a sample of data to measure height, weight and gender). For data analysis

problems, relationships between response for a given set of variables are adequate to describe the observed data, and to make reasonable predictions for unknown observations (Multiple Regression or General Stepwise Regression).

Types of Regression

The multiple linear regression models have been extended in a number of ways to address more sophisticated data analysis problems. There are 4 important types of regression methods to solve multivariate problems involving voluminous data as listed below. It also serves as the basis for a number of multivariate methods such as *discriminant analysis* (i.e., the prediction of group membership from the levels of continuous predictor variables), *principal components regression (PCR)* (i.e., the prediction of responses on the dependent variables from factors underlying the levels of the predictor variables) and *canonical correlation* (i.e., the prediction of factors contributing responses of the dependent variables from factors underlying the levels of the predictor variables). These multivariate methods all have two important properties in common. These methods impose restrictions such that (1) factors underlying the X and Y variables are extracted from the $X'X$ and $Y'Y$ matrices, respectively (where **X'** is a transpose of **X** and **Y'** is a transpose of **Y**), and never from cross-product matrices involving both the X and Y variables, and (2) the number of prediction functions can never exceed the minimum of the number of X and Y variables.[107]

PLS regression (PLSR) extends multiple linear regressions without imposing the restrictions imposes by *discriminant analysis, PCR* and *canonical correlation.* In PLSR, prediction functions are represented by factors extracted from the $Y'XX'Y$ matrix. In short, partial PLSR is probably the least restrictive of the various multivariate extensions of the multiple linear regression models. This flexibility allows it to be used in situations where the use of traditional multivariate methods is severely limited, when there are fewer

observations than predictor variables. Furthermore, PLSR can be used as an exploratory analysis tool to select suitable predictor variables and to identify outliers before classical linear regression. PLSR has been used in various disciplines such as chemistry, economics, medicine, psychology, pharmaceutical, medical science where predictive linear modeling, especially with a large number of predictors, is necessary. In chemometrics, PLSR has become a standard tool for modeling linear relations between the multivariate measurements.

5.1.2: PLSR Computational Basic Model

As in multiple linear regression, the main purpose of PLSR is to build a linear model, givern in Equation 5.2.

$$Y = XB + E, \qquad 5.2$$

Where Y is n cases by m variables response matrix, X is n cases by p variables predictor matrix, B is a p by m regression coefficient matrix, and E is a noise term for the model. Usually, the variables in X and Y are normalized by subtracting their means and scaled by dividing with their standard deviations.

Both PCR and PLSR produce factor scores as linear combinations of the original predictor variables, so that there is no correlation between the factors score used in the predictive regression model. Let us assume we have a data set with response variables Y (in matrix form) and a large number of predictor variables X (in matrix form), and some of which are highly correlated. A regression using factor extraction method for this type of data generates the factor score matrix T as given in Equation 5.3.

$$\mathbf{T} = \mathbf{XW} \qquad 5.3$$

Where **W** is a weight matrix with p *by* c weight.

For regression technique it can be proved that B has the form as shown in Equation 5.4

$$\mathbf{B} = \mathbf{WQ} \qquad 5.4$$

Where **Q** is a matrix of regression coefficient for **T** of dimension n x c.

Substituting equation 5.4 & 5.3 in 5.2, we get Equation 5.5

$$\mathbf{Y} = \mathbf{TQ} + \mathbf{E} \qquad 5.5$$

PCR and PLSR differ in the methods used in extracting factor scores. In short, PCR produces the weight matrix W reflecting the covariance structure between the predictor variables, while PLSR produces the weight matrix W, reflecting the covariance structure between the predictor and response variables. One additional matrix which is necessary for a complete description of PLSR procedures is the p by c factor loading matrix P, which gives a factor model as given in Equation 5.6

$$\mathbf{X} = \mathbf{TP} + \mathbf{F}, \qquad 5.6$$

Where F is the unexplained part of the X scores.

We can now describe the algorithms for PLSR as given below.

5.1.3: SIMPLS Algorithm

A novel algorithm for partial least squares (PLS) regression, Statistical Inspired Modification of PLS (SIMPLS) is proposed which calculates the PLS factors directly as linear combinations of the original variables. The PLS factors are determined such as to maximize a covariance criterion, while obeying certain orthogonality and normalization restrictions. The flowchart for SIMPLS is given in Figure 5.1. We have used the SIMPLS algorithm for the purpose of Multivariate analysis. We have written SIMPLS algorithms in C and ported it on the NIOS II system discussed in Chapter 4.

For each h=1,…,c, where $A_0=X'Y$, $M_0=X'X$, $C_0=I$ and c given,

1. Compute q_h, the dominant eigenvector of $A_h'A_h$
2. $w_h=A_hq_h$, $c_h=w_h'M_hw_h$, $w_h=w_h/sqrt(c_h)$, and store w_h into W as a column
3. $p_h=M_hw_h$, and store p_h into P as a column
4. $q_h=A_h'w_h$, and store q_h into Q as a column
5. $v_h=C_hp_h$, and $v_h=v_h/||v_h||$
6. $C_{h+1}=C_h - v_hv_h'$ and $M_{h+1}=M_h - p_hp_h'$
7. $A_{h+1}=C_hA_h$

Where **Q'** is transpose of **Q**.

An alternative estimation method for PLSR components is the Nonlinear Iterative PLS (NIPALS) algorithm, which can be described as follows.

1. For each h=1,…,c, where $A_0=X'Y$, $M_0=X'X$, $C_0=I$, and c given,
2. Compute q_h, the dominant eigenvector of $A_h'A_h$
3. $w_h=G_hA_hq_h$, $w_h=w_h/||w_h||$, and store w_h into W as a column
4. $p_h=M_hw_h$, $c_h=w_h'M_hw_h$, $p_h=p_h/c_h$, and store p_h into P as a column
5. $q_h=A_h'w_h/c_h$, and store q_h into Q as a column
6. $A_{h+1}=A_h - c_hp_hq_h'$ and $B_{h+1}=M_h - c_hp_hp_h'$
7. $C_{h+1}=C_h - w_hp_h'$

NIPALS and SIMPLS algorithms are the most commonly used algorithms for partial least squares analysis. When the number of objects, N, is much larger than the number of explanatory, K, and/or response variables, M, the NIPALS algorithm can be time consuming. Even though the SIMPLS is not as time consuming as the NIPALS and can be preferred over the NIPALS, there are kernel algorithms developed especially for the cases where N is much larger than number of variables. In practice the SIMPLS algorithm appears to be fast and easy to interpret as it does not involve a breakdown of the data sets.[108]

Since SIMPLS is more popular technique for the reasons explained above, the present research is based on this technique.

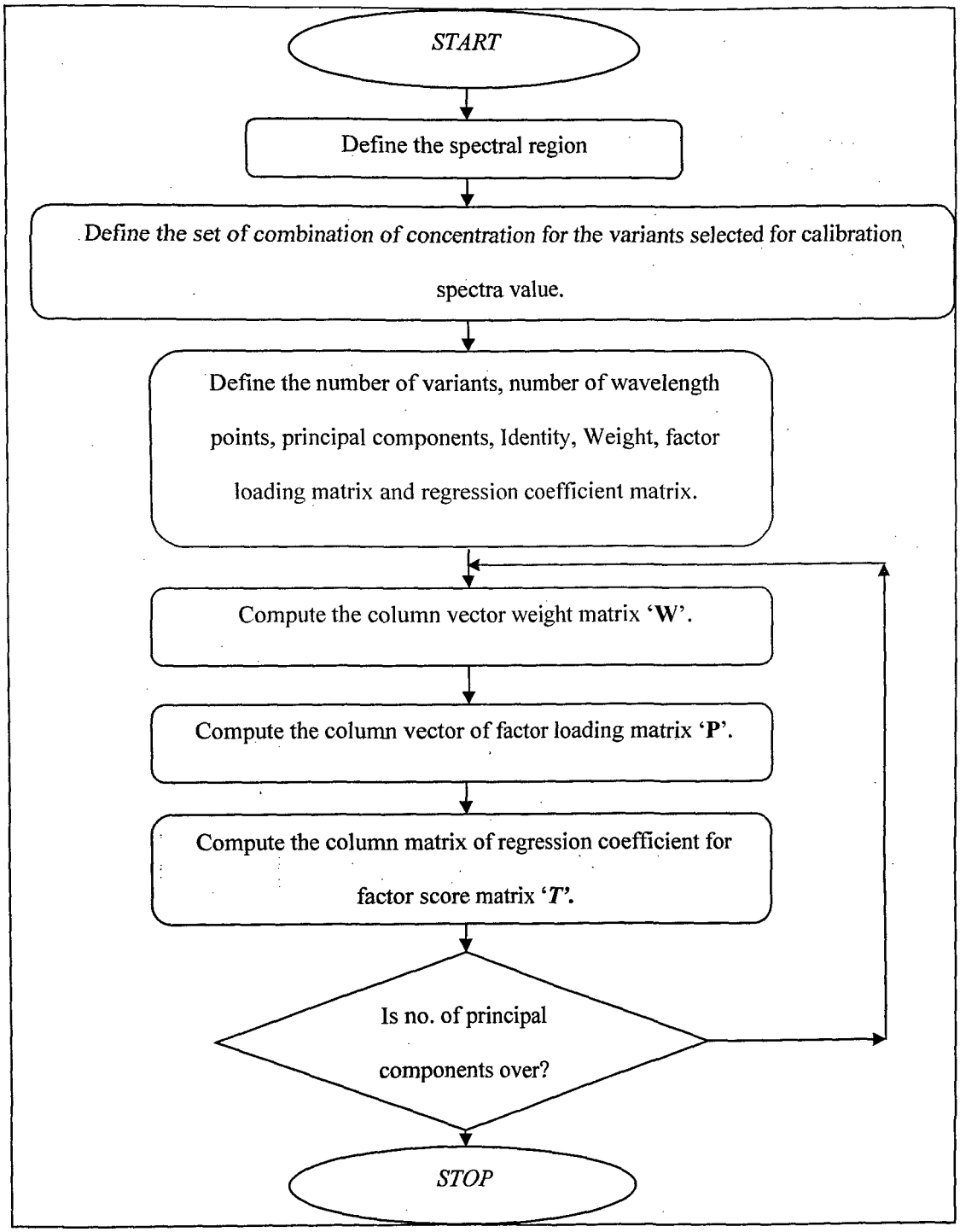

Figure 5.1: Flowchart of the SIMPLS algorithm.

5.2. Spectra Preprocessing

As already seen, blood is a complex fluid consisting of many compounds with spectra overlapping in a wide range of measurements. In this case there are a large number of variables, which make it difficult to find a model that relates all of them. Baseline preprocessing can eliminate undesired substances overlapping as well as minimize the errors caused by instrumentation and temperature instabilities.[109] After the choice of one or more correction techniques, attention must be given to the data treatment, which is explained in this chapter. The derivation of a model to recover quantitative information of complex mixtures spectra requires calibration procedures, which are able to predict analyte specific information without knowing the relationship between the variables.[110] Dimension reduction can be achieved by treating spectral data in a PLS system.

Preprocessing

In chemometrics it is recommended to preprocess any data in order to remove noise from the original spectrum, caused by instrumentation instability, overlapping bands, and environment influence. This procedure is useful especially when comparing curves or measuring peak intensities and can be implemented by either physical or mathematical means.. Manual estimation, polynomial fitting, frequency filtering and derivative processing can be classified as preprocessing methods for noise removal.[111]

Visual inspection

The baseline can be manually estimated by visual inspection, which has been done extensively in many fields and requires the choice of explicit points in the graphics. The technique is based on drawing a line through 2 points and turns it into the horizontal axis.

Drawbacks from this treatment are that the process is very slow, as each spectrum must be carefully inspected and the quality of the correction will be greatly dependent on the experience of the user.[112]

Polynomial fitting

Polynomial fitting is the estimation of the baseline as a mathematical equation, in order to subtract it from the original spectrum. The baseline can be assumed to be a sloping line, or a function resulting from the selection of many points. It is also possible to assume that the baseline would have an exponential, logarithmic or power dependence.[113]

The simplest polynomial fitting is an offset, where a constant is subtracted from each channel. When many spectra are collected, the elimination of offsets in the reference improves the quantification of data through a more accurate and stable measurement.[114]

Filtering

Digital filtering is one component in a signal processing method used to alter specific frequency components from recorded spectra. Low frequency errors in signal spectrum are mostly due to temperature and instrument drifts, while high frequency noises are produced by substances overlapping and by measurement problems.[115]

5.3 Multivariate Calibration Model for Non Invasive Blood Glucose Analysis

PLSR Model described in Section 5.1.1 finds good use in the multivariate spectroscopic data. PLSR is an extension of the multiple linear regression models. Therefore PLSR is mostly used as an exploratory analysis tool to select suitable predictor variables and to identify outliers.

We have developed PLSR model based on SIMPLS algorithm in C language and ported on NIOS II platform to estimate the glucose concentration. The C code of the model is given in ANNEXURE IV.

We have validated the PLSR model for 4 different cases, **1)** Multivariate model for Human Whole Blood Tissue for Glucose where data sets are generated using Lorentz oscillator by considering only 5 constituents Adding their respective amplitudes we get spectra shown in Figure 5.2; **2)** Multivariate model for Human Whole Blood Tissue for Glucose where spectra are generated using Lorentz oscillator for blood by considering skin colour and temperature along with five blood constituents; **3)** Multivariate model for Human Whole Blood Tissue for Glucose where the data is obtained by mixing the various blood constituents like Glucose, Alanine, Ascorbate, Lactate and Urea (The spectra were recorded on Schimatzu FTIR 8400); **4)** Actual blood spectra provided by Y.C.Shen.[116]

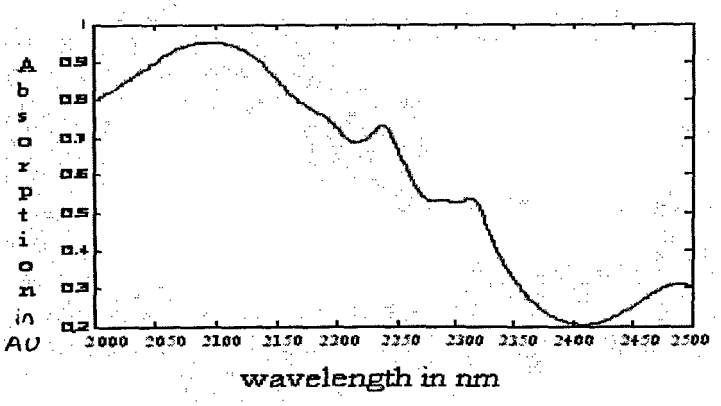

Figure 5.2: Normalized spectra of various components simulated using Lorentz Oscillator.

5.3.1 Case 1: Multivariate model for Human Whole Blood Tissue for Glucose (Lorentz oscillator)

Methods of non-invasive optical diagnosis involve various issues which have been described above. The absorption spectrum depends on the type of predominant absorption center and water content of tissue. Absolute value of absorption coefficients for typical tissue lies in the range of 10^{-2} to 10^{14} cm^{-1}.[117][118][119][120] The role of glucose and its signature in the spectral range are already described in Section 2.3. The five major constituents interfering with glucose in the region of 2000 – 2500 nm are serum Alanine, serum urea, HDL Lactate, Glucose, Ascorbate generates a complex signature in the spectrum region.[121] From the literature it is also found that tissue temperature and skin complexion due to pigment variation over the globe population has influence on the transmission characteristics. There are many other factors influencing the signature of a spectrum, but the analysis becomes complex as the physiology of the body is very sensitive and dynamic over the catabolic processes involved. It has been decided to model this complex ensemble over various concentrations of five chemical constituents and two physical components namely skin complexion and the body temperature. [122][123][124][125][126][127][128][129][130]

Generalized Multivariate Model of the System

We have generated the required generalized response and predictor matrix using Lorentz Oscillator Equation 5.7, with respective oscillator strength, width and central frequency. The flowchart for spectra generation in region of interest is given in Figure 5.3

$$(n+i.k)=\left(\varepsilon_{\infty}+\sum_{j}\frac{S_j\nu^2{}_j}{\nu^2{}_j-\nu^2-i\nu\Gamma_j}\right)^{1/2} \qquad 5.7$$

Where 'n' →response of spectrum

'i.k' → imaginary components of the frequency response

'Sj' → strengths of the oscillators

'νj' → central frequency

'Γj' → width of oscillator

'ε_∞'→ represents the electronic contribution to the complex dielectric constant.

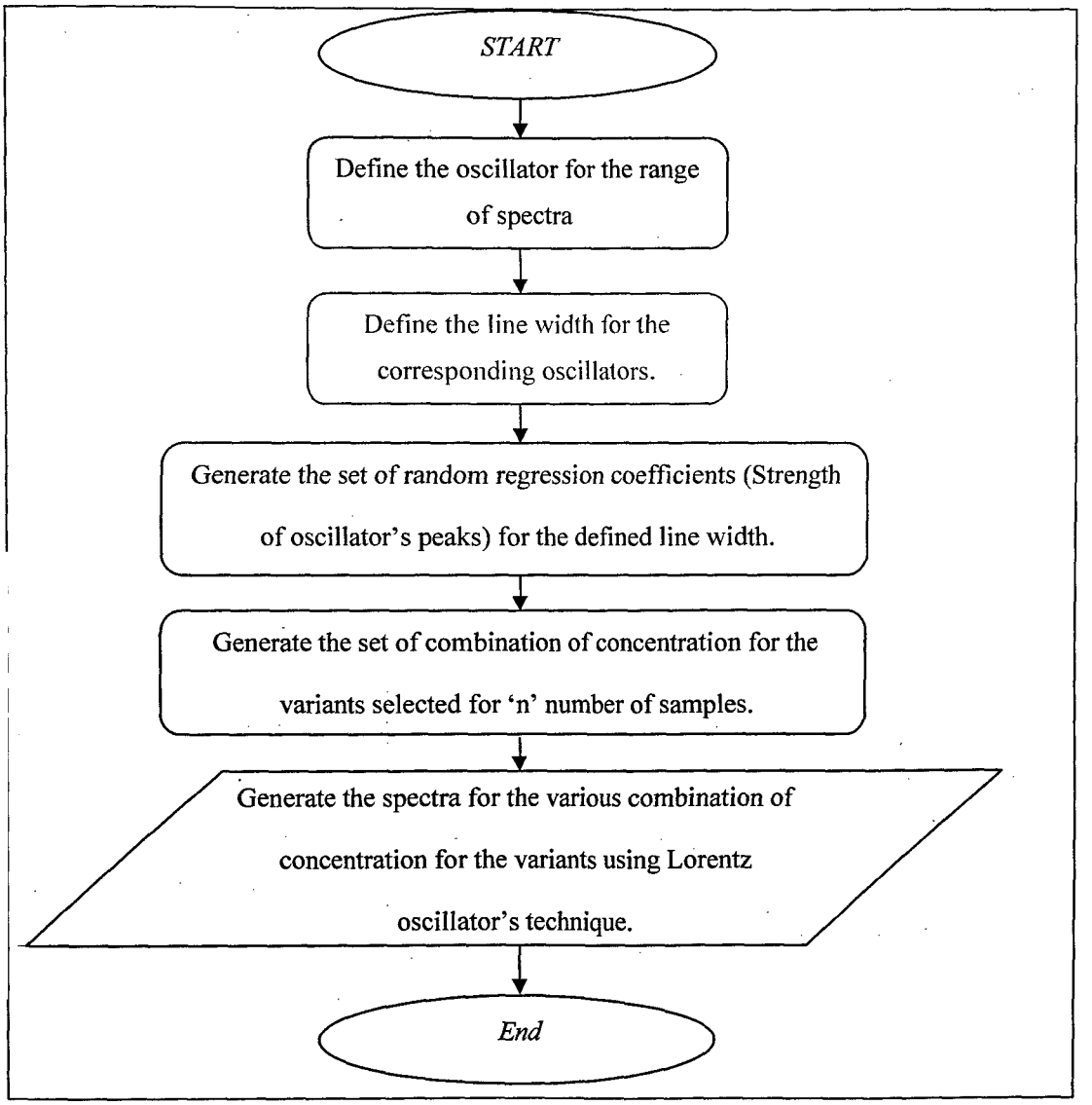

Figure 5.3: Flowchart for the implementation Lorentz oscillator model for simulated spectra generation.

Table 5.1: Various oscillators' parameters used in the Lorentz expression.

Variants	Oscillator number	1	2	3	4	5
Alanine	CF	2130	2242	2295	2320	2530
	OW	150	25	30	30	50
	OS	230	30	20	51	40
Urea	CF	2080	2150	2200	2240	2550
	OW	40	50	50	140	250
	OS	1	3	10	16	12
HDL Lactate	CF	2050	2150	2198	2258	2350
	OW	150	100	80	40	80
	OS	1.5	10	10	10	12
Glucose	CF	2100	2150	2250	2320	2480
	OW	100	100	60	60	100
	OS	1.4	0.6	0.5	0.5	0.6
Ascorbate	CF	2125	2160	2280	2340	2490
	OW	70	100	60	100	50
	OS	48	90	30	40	40

CF: Centre Frequency; OW Oscillator Width; OS Oscillator Strength

The whole blood spectrum model for various concentrations of the five variants were generated using the parameters given in the above table. The model considered the following values of concentration for the human blood chemometrics system well within the pathological range. The concentrations of the five constituents were: C1 = Alanine (1 - 21 mg / dl), C2 = Serum Urea (7 - 18 mg / dl), C3 = HDL Lactate (4.5 - 14.4 mg / dl), C4 =

Glucose (70 - 110 mg / dl), C5 = Ascorbate (0.4 - 1.5 mg / dl). Oscillators' parameters as shown in Table 5.1 were used to generate the signature of the five chromospheres as shown in Figure 5.4.

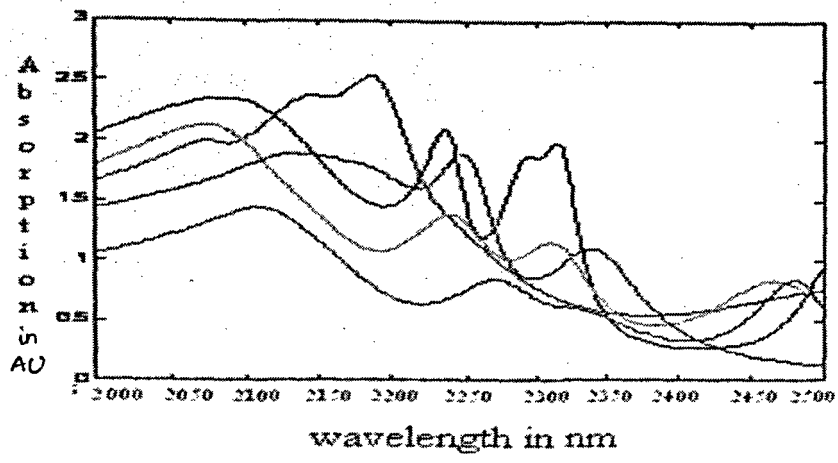

Figure 5.4: Signature of five major components simulated using Lorentz Oscillators.

The Lorentz model is so flexible that just by varying the strength, line width and natural frequency any practical spectrum can be generated with highly non-linear behaviour. The unknown spectrum within the confidence interval of the calibrated spectra can be generated by adopting the same principle as that of calibration spectra as shown in flowchart (Figure 5.3). ANNEXURE VI illustrates the MATLAB code for the Oscillator system spectra using Equation 5.7. Model was validated with the PLSR software (ParLes software). The predicted concentration for glucose and RMSE analysis is given in Table 5.2. The average RMSE analysis was performed over the prediction of the glucose concentrations as shown in Table 5.3.

The resultant spectra of all blood constituents in the range 2000 nm to 2500 nm will have the form shown in Figure 5.2. Samples template were generated for different combinations of blood constituents as shown in Figure 5.5. Figure 5.6 shows the graphical representation of RMSE for the designed model.

Table 5.2: Predicted concentration of glucose and RMSE analysis

Sr.no	Glucose concentration mg/dL	Predicted mg/dL	RMSE mg/dL
1	70	71.235	1.235
2	75	78.03	3.03
3	80	80.598	0.598
4	85	84.26	0.74
5	90	92.55	2.55
6	95	96.116	1.116
7	100	101.088	1.088
8	105	105.969	0.969
9	110	112.291	2.291
10	120	121.543	1.543
11	130	132.831	2.831
12	150	154.88	4.88
13	200	205.99	5.99

Table 5.3: Average RMSE analysis for Glucose.

Sample	RMSE mg/dL
Theoretical (15 sample)	2.459

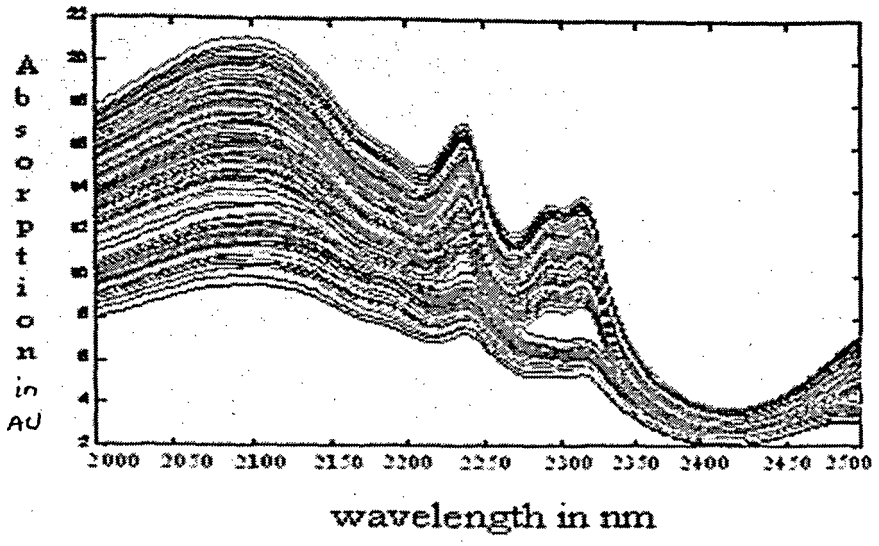

Figure 5.5: 1024 samples Template for the PLSR model.

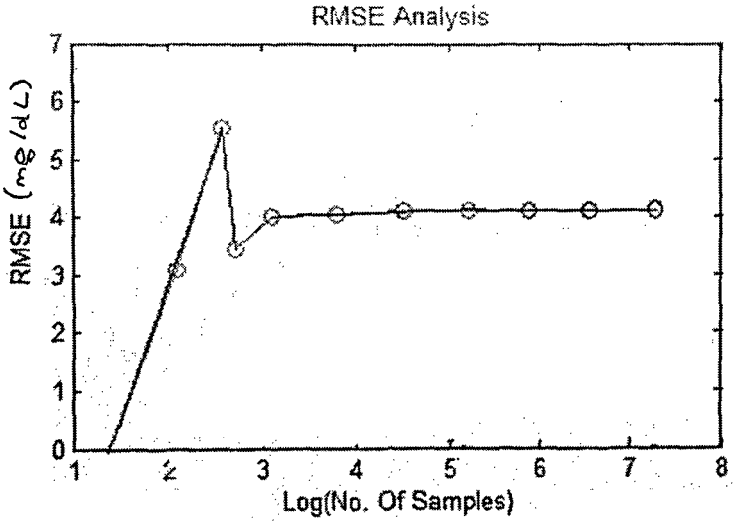

Figure 5.6: RMSE analysis for glucose

5.3.2 Case 2: Multivariate model for Human Whole Blood Tissue for Glucose where spectra are generated using Lorentz oscillator for blood by considering skin colour and temperature along with 5 blood constituents

Spectra generation

We have generated the approximate simulated spectra of human tissues having the nature shown in Figure 5.7 using Lorentz oscillator and concentration of the variants of values as follows: C1 = Alanine (1 - 21 mg / dl), C2 = Serum Urea (7 - 18 mg / dl), C3 = HDL Lactate (4.5 - 14.4 mg / dl), C4 = Glucose (70 - 110 mg / dl), C5 = Ascorbate (0.4 - 1.5 mg / dl) and lambda = 2.0 to 2.5, Temperature t = 25 - 40 degrees, Skin complexion s = 0.2 0.4.

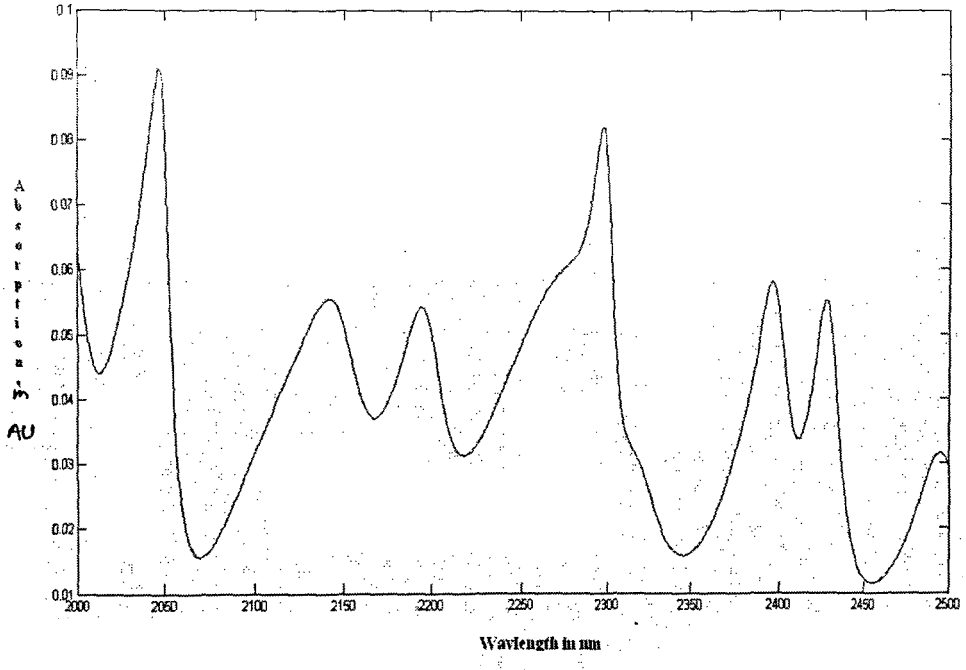

Figure 5.7: Spectrum generated using Lorentz technique.

The model considered the following values of concentration for the chemomet system which are in normal pathological ranges. The concentrations of the 5 constitue were as follows: C1 = Glucose (70 - 110 mg / dl); C2 = Serum Cholesterol (130 - 220 mg /

dl); C3 = Serum Urea (10 - 45 mg / dl), C4 = serum triglycerides (65 - 160 mg / dl), C5 = HDL cholesterol (35 - 60 mg / dl), C6 = LDL Cholesterol (130 - 150), C7 = LDL (130 – 150 mg / dl) and lambda = 2000 to 2500 nm, Temperature t = 25 - 40 degrees, Skin complexion s = 0.2 - 0.4 cm^{-1}

Various spectra were generated using the different combinations of variants concentration. The spectra generated are shown in Figure 5.8.

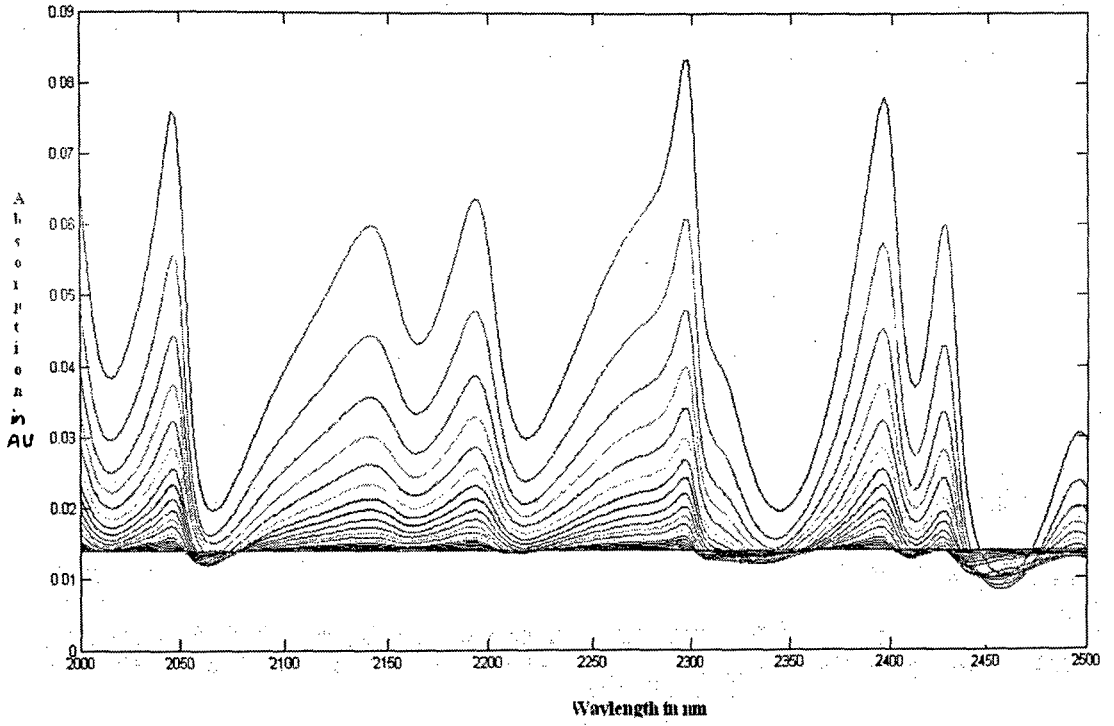

Figure 5.8: Spectra generated using Lorentz oscillator model (a non linear behavior).

Prediction

To test the prediction capability of designed PLS model we have passed the unknown spectrum having the concentrations. Further to validate this simulation model it was compared with ParLes-V2.1.9.vi software obtained from Sydney University, Australia. The results were encouraging and confirmed the simulated multivariate human whole blood

tissue model. The value of R^2=0.99 indicates that the regression model is good. The predicted concentration for glucose and RMSE is given in Table 5.4. The average RMSE analysis was performed over the prediction of the glucose concentrations as shown in Table 5.5.

Table 5.4: Predicted concentration of glucose and RMSE analysis

Sr.no	Glucose concentration mg/dL	Predicted mg/dL	RMSE mg/dL
1	70	73.124	3.124
2	75	77.12	2.12
3	80	78.678	1.322
4	85	86.189	1.189
5	90	92.78	2.78
6	95	96.342	1.342
7	100	101.638	1.638
8	105	104.569	0.431
9	110	111.749	1.749
10	120	123.452	3.452
11	130	134.257	4.257
12	150	156.34	6.34
13	200	207.48	7.48

Table 5.5: Average RMSE Analysis for glucose

Sample	RMSE mg/dL
(13 sample)	2.86

5.3.3 Case 3: Multivariate model for Human Whole Blood by mixing the 5 blood constituents (Glucose, urea, lactate, Ascorbate, Alanine) using standard solutions.

Spectra Generation: Spectra were collected with a Schimatzu Fourier transform infrared spectrometer. The spectrometer was equipped with a 20-watt tungsten-halogen light source and a silicon detector.

Reagents: Glucose, sodium lactate, sodium ascorbate, alanine and urea were obtained from Loba Chemical Co., Inc.

Procedure: 13 samples were prepared by carefully weighing quantities of standard material and mixing them in different proportion as shown in Table 5.6. Error propagation indicates a relative concentration uncertainty of nearly 0.2% for these mixtures, which corresponds to a maximum uncertainty of 0.07 mM (mili Mole). This level of uncertainty ultimately limits the analytical performance of all PLS calibration models. 13 spectra recorded with the help of Schimatzu FTIR are shown in Figure 5.9 in the range 2000 nm to 2500 nm. This recorded 13 sample spectra having 1000 points per spectra were used for calibrating the model. In the predicted model one sample spectrum is considered as 'unknown' and the prediction of each analyte is donefor this spectra. The prediction result obtained using the model which we have designed is verified with the ParLes Model for over the same sets of samples and were found to compare satisfactorily. To verify the model over a range of concentration of various constituents, we have passed all the samples one by one as unknown for the prediction of constituent concentration. The comparison chart of predicted and actual concentration is shown in Table 5.7. Figure 5.10 shows the graphical representation of RMSE. Figure 5.11 shows the prediction result of glucose for all concentartions. The average RMSE analysis was performed over the prediction of the glucose concentrations as shown in Table 5.8.

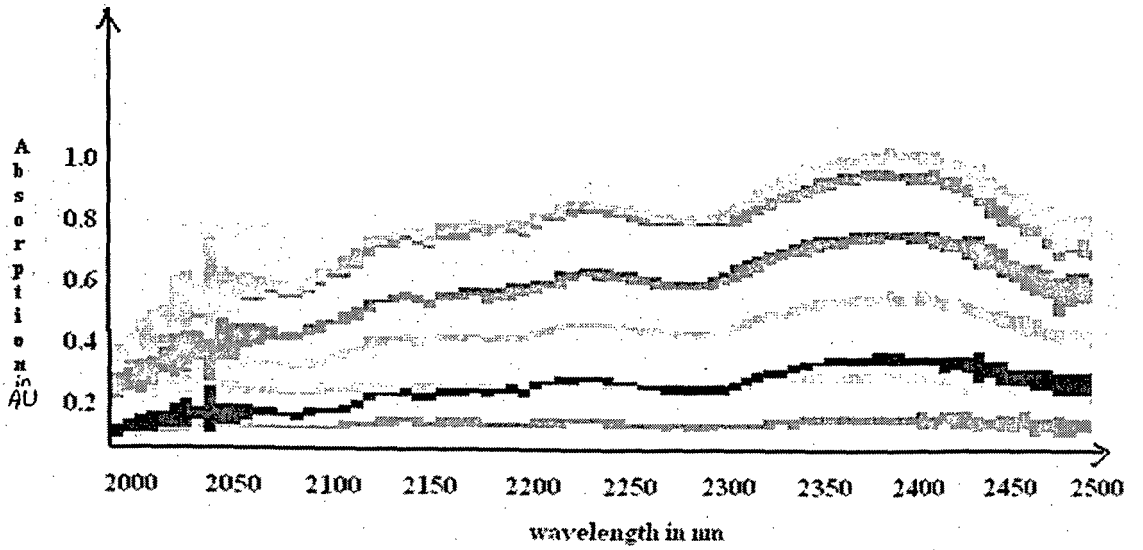

Figure 5.9: 13 spectra of mixture of blood constituents (1000 points per sample)

Table 5.6: Different proportion of Mixture

Sr.no	Actual concentration in (mg/dL)				
	Glucose	Urea	Alanine	Ascorbate	Lactate
1	70	20	20	2	15
2	70	10	10	1	10
3	70	15	20	2	15
4	95	20	20	2	15
5	95	10	20	2	15
6	95	15	30	2	15
7	95	15	10	2	15
8	95	15	20	3	15
9	95	15	20	1	15
10	95	15	20	2	20
11	95	15	20	2	10
12	120	10	20	2	15
13	120	15	20	2	15

Table 5.7: Predicted concentration of glucose and RMSE analysis

sr.no	Actual concentration in mg/dL					Predicted Glucose (mg/dL)	RMSE (mg/dL)
	Glucose	Urea	Alanine	Ascorbate	Lactate	Glucose	
1	70	20	20	2	15	72.04	2.04
2	70	10	10	1	10	73.26	3.26
3	120	15	20	2	15	121.84	1.84
4	70	15	20	2	15	68.11	1.89
5	95	20	20	2	15	92.42	1.58
6	95	10	20	2	15	79.30	5.70
7	95	15	30	2	15	99.60	4.60
8	95	15	10	2	15	99.62	4.62
9	95	15	20	3	15	92.87	2.13
10	95	15	20	1	15	93.84	1.16
11	95	15	20	2	20	97.00	2.00
12	95	15	20	2	10	98.43	3.43
13	120	10	20	2	15	117.65	2.35

Table 5.8: Average RMSE Analysis for glucose

Sample	RMSE mg/dL
Experimental (13 sample)	4.143

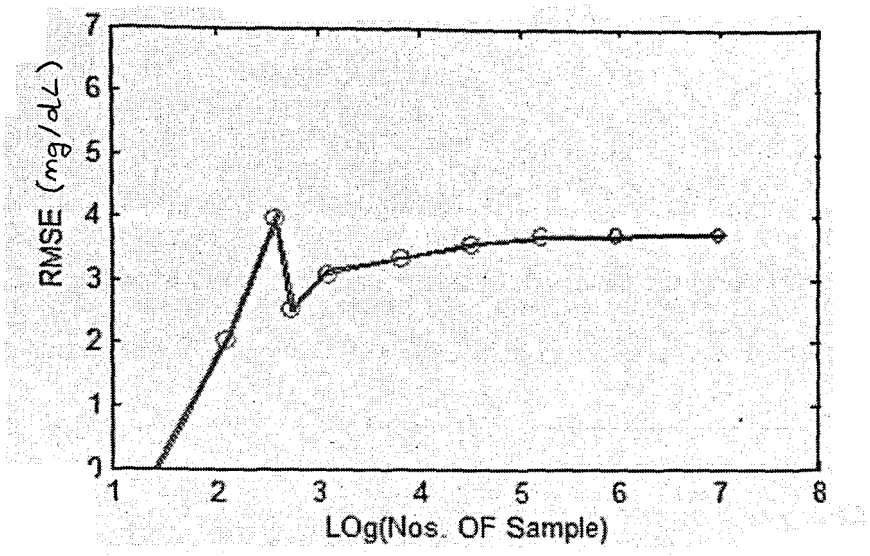

Figure 5.10: RMSE analysis of glucose

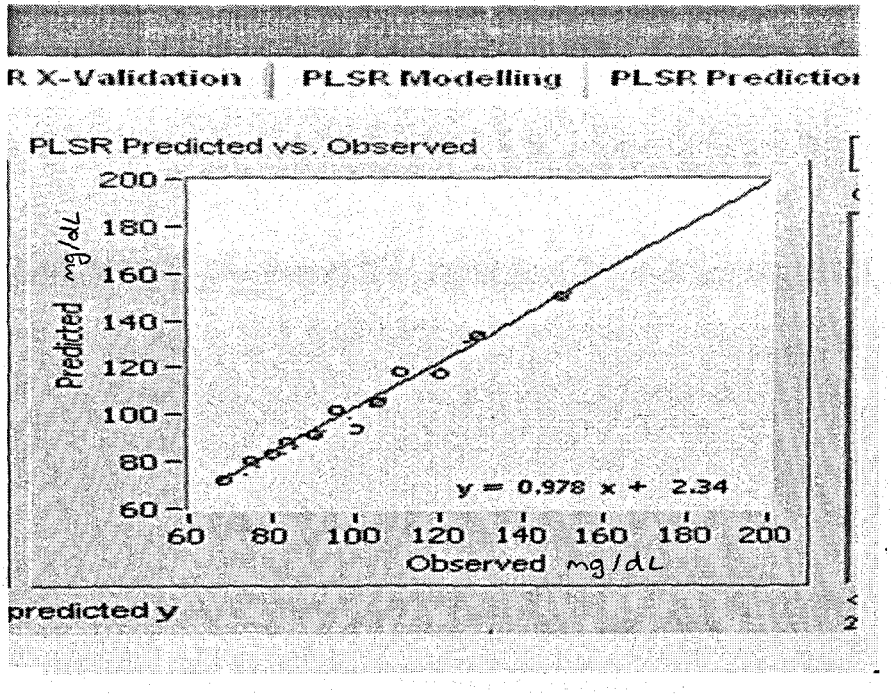

Figure 5.11: Predicted result for glucose

Testing Model for Reduced sample points

Here we have taken the same 13 samples spectra and we have generated resultant spectra consisting of 150 sample points per spectra which contains the information pertaining to glucose. The reduced sample point spectra are shown in Figure 5.12. Figure 5.13 shows the graphical representation of RMSE. The comparison chart of predicted and actual concentration is shown in Table 5.9. RMSE analysis was performed over the prediction of the variants concentrations as shown in Table 5.10.

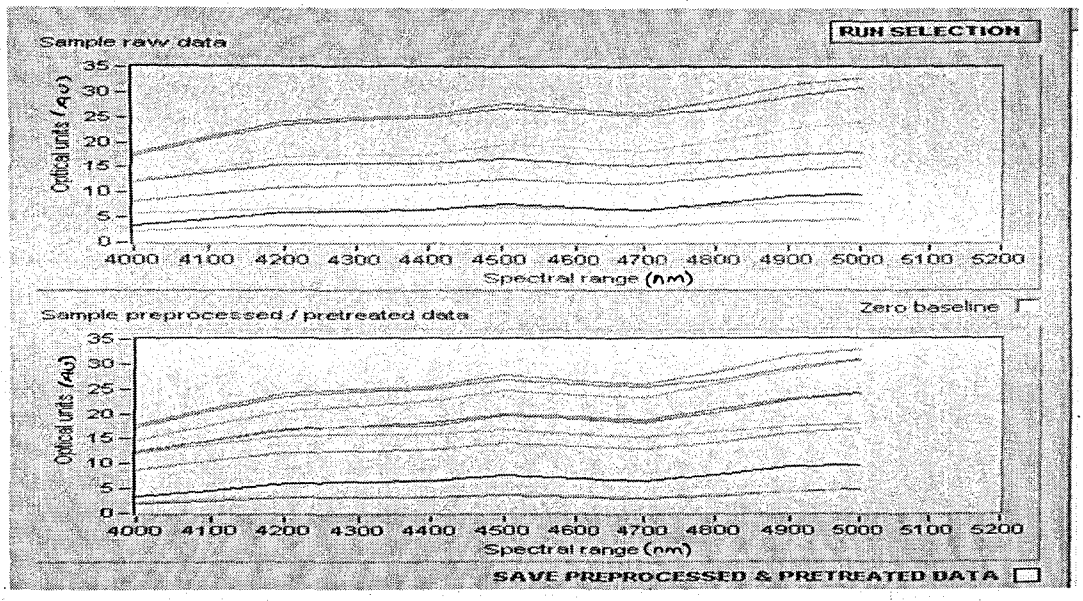

Figure 5.12: Spectra of mixture with 150 sample points

Table 5.9: Predicted result with 150 points

Sr.no	Actual concentration in mg/dL					Predicted Concentration	RMSE (mg/dL)
	Glucose	Urea	Alanine	Ascorbate	Lactate	Glucose (mg/dL)	Glucose
1	70	20	20	2	15	76.12	6.12
2	70	10	10	1	10	72.81	2.81
3	95	15	30	2	15	88.99	6.01

Table 5.10: Average RMSE Analysis for glucose with 150 sample points

Sample	RMSE mg/dL
Experimental (13 sample)	5.326

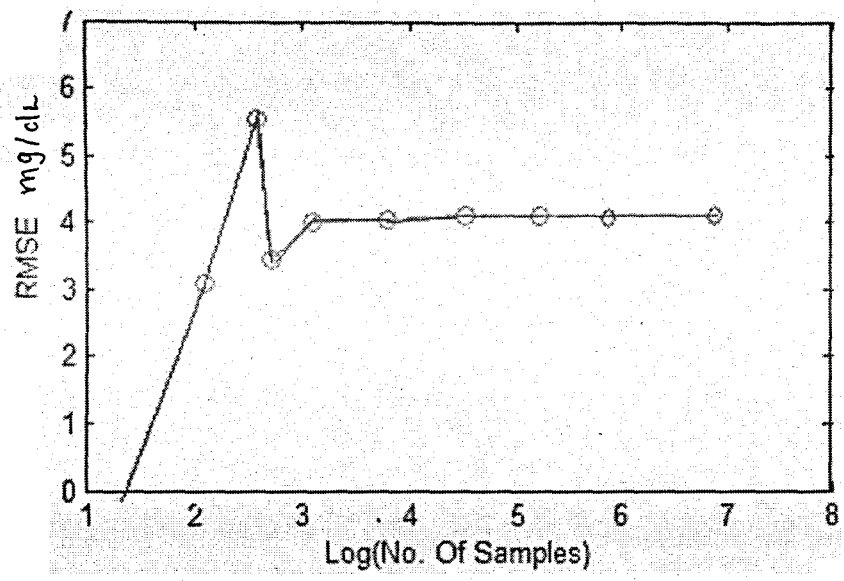

Figure 5.13: RMSE analysis of glucose.

5.3.4 Case 4: Multivariate model for actual Human Whole Blood spectra

To test our model for actual human blood spectra, we had taken the whole blood spectra recorded by Y. C. Shen using a Nicolet FTIR for his research work as shown in Figure 5.14.There are 15 spectra in the said figure each of which has a different contituent concentration as given in Table 5.11.

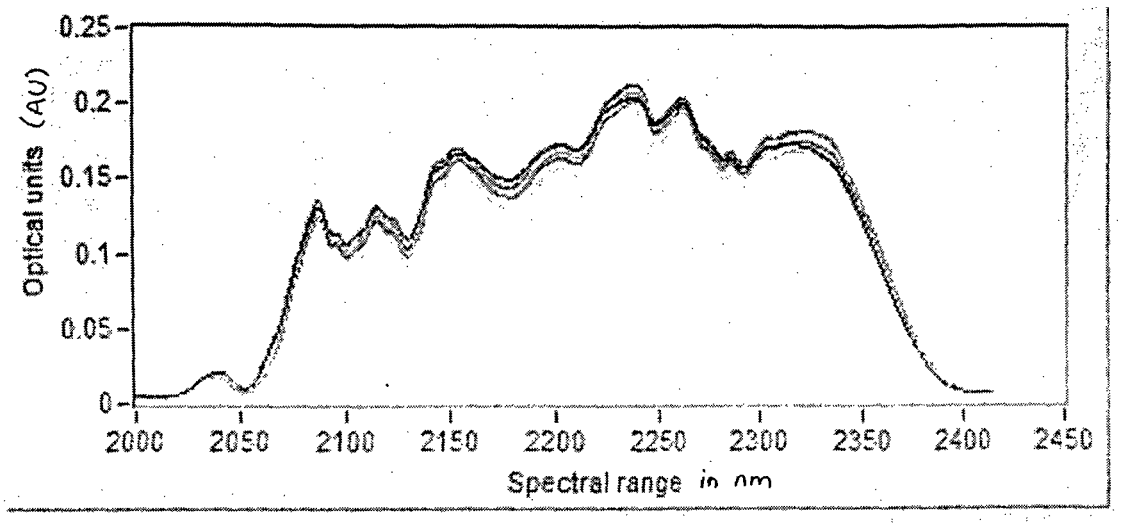

Figure 5.14: Human whole blood spectra

We have passed all these 15 samples of whole blood as calibration set to the ParLes software model. Before recording the spectra, all the blood samples were analyzed in pathological labs to measure the concentration of important blood variants. Here we have taken skin complexion as 2 which is a constant since we measured the blood over the same region and all the spectra are recorded at 25 °C temperature.

Table 5.11: Actual concentration of different constituents in mg / dl

Samples	Temperature (°C)	Skin Complexion (cm^{-1})	Glucose (mg/dL)	Urea (mg/dL)	Alanine (mg/dL)	Ascorbate (mg/dL)	Lactate (mg/dL)	Triglyceride (mg/dL)	Cholesterol (mg/dL)
1	25	0·2	70	20	20	2	15	100	130
2	25	0·2	70	10	10	1	10	100	140
3	25	0·2	120	15	20	2	15	125	130
4	25	0·2	70	15	20	2	15	125	130
5	25	0·2	95	20	20	2	15	125	130
6	25	0·2	95	10	20	2	15	150	130
7	25	0·2	95	15	30	2	15	150	130
8	25	0·2	95	15	10	2	15	150	135
9	25	0·2	95	15	20	3	15	125	140
10	25	0·2	95	15	20	1	15	125	140
11	25	0·2	95	15	20	2	20	100	140
12	25	0·2	95	15	20	2	10	125	140
13	25	0·2	95	15	20	2	15	130	130
14	25	0·2	95	15	20	2	10	130	130
15	25	0·2	120	10	20	2	20	130	130

Prediction Study with the ParLes PLS Software

Details steps involved in prediction using ParLes software for 9 variable and 10 factors are given below:

The modeling and predicting data is imported into the software, the screen shot of which is shown in Figure 5.15. There are nine variable i.e. Seven constituents and two physical parameters (temperature, skin complexion). Figure 5.16 shows the technique to

apply pre processing such as transforming data, baseline correction, noise filtering, differentiation and pretreatment. The screen shot of PCA generation is shown in Figure 5.17.

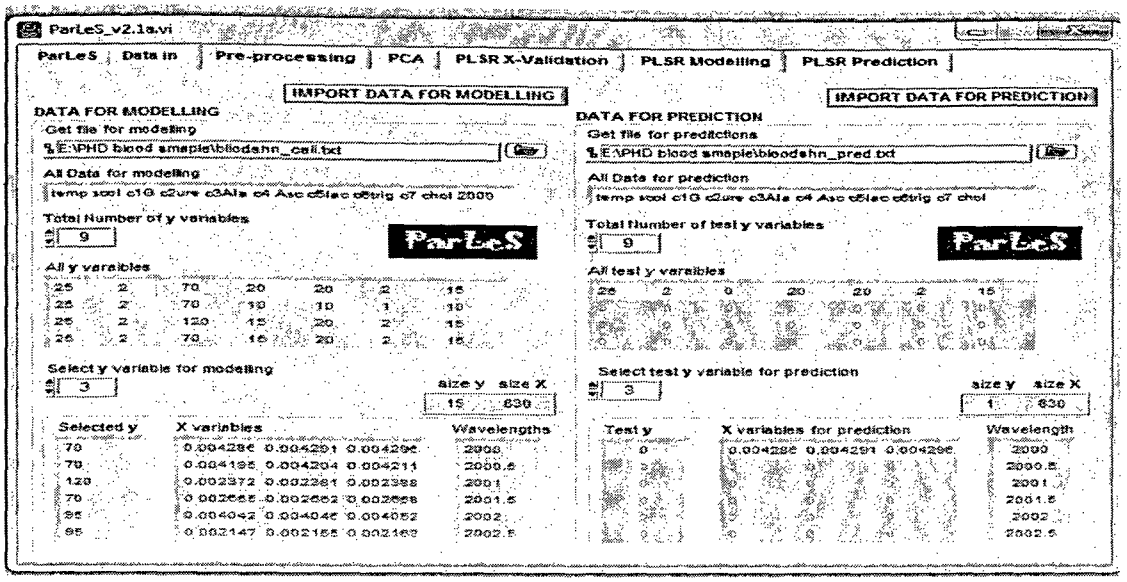

Figure 5.15: Importing of data files into the Parlessoftware

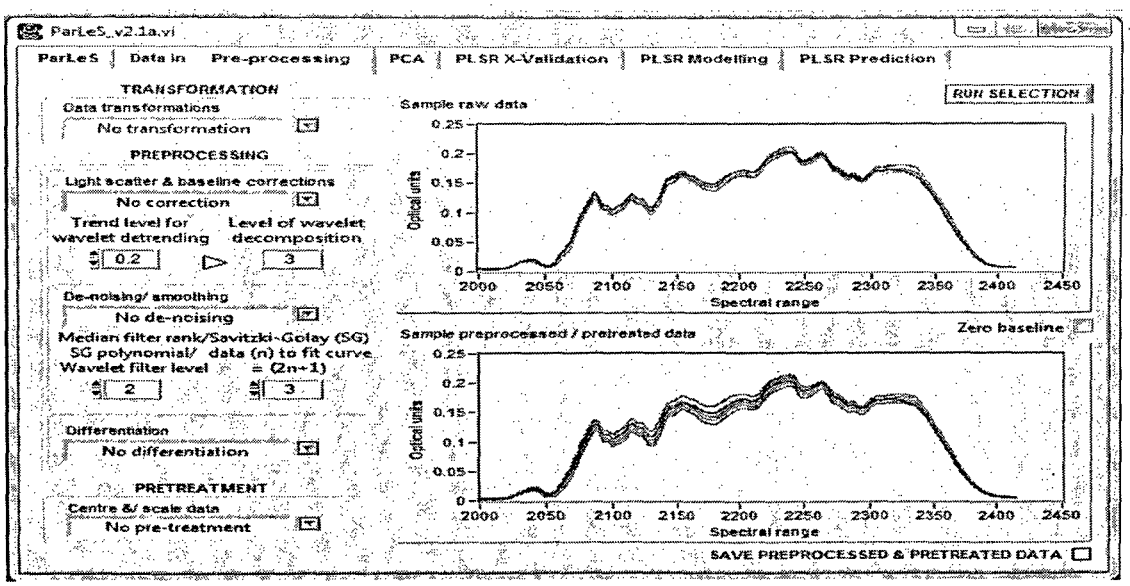

Figure 5.16: Preprocessing the datasets for calibration

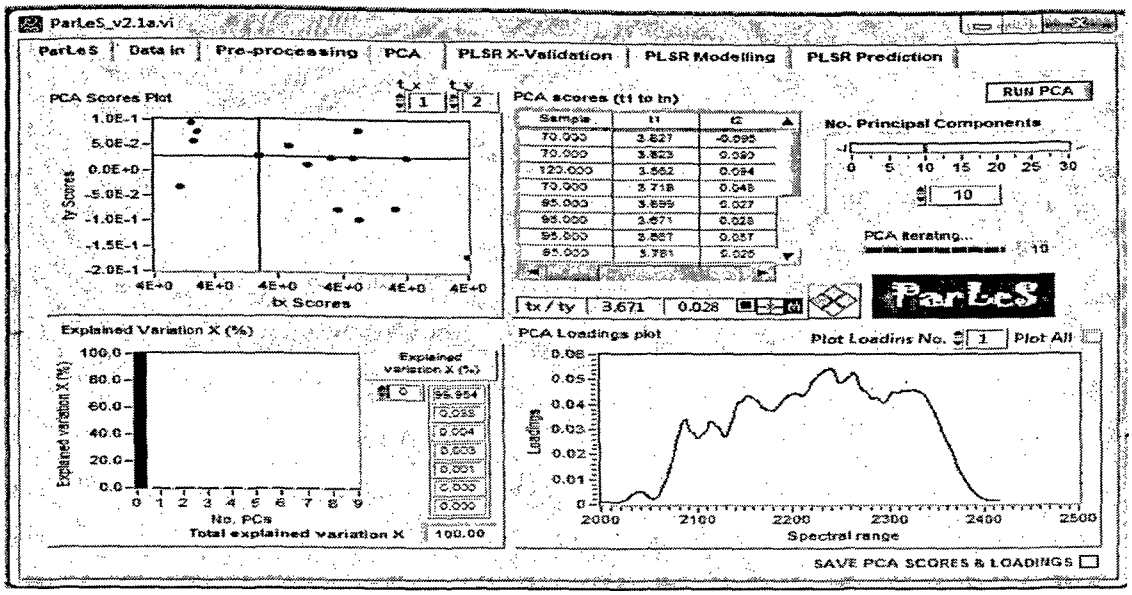

Figure 5.17: Generating PCA score for the multivariate analysis

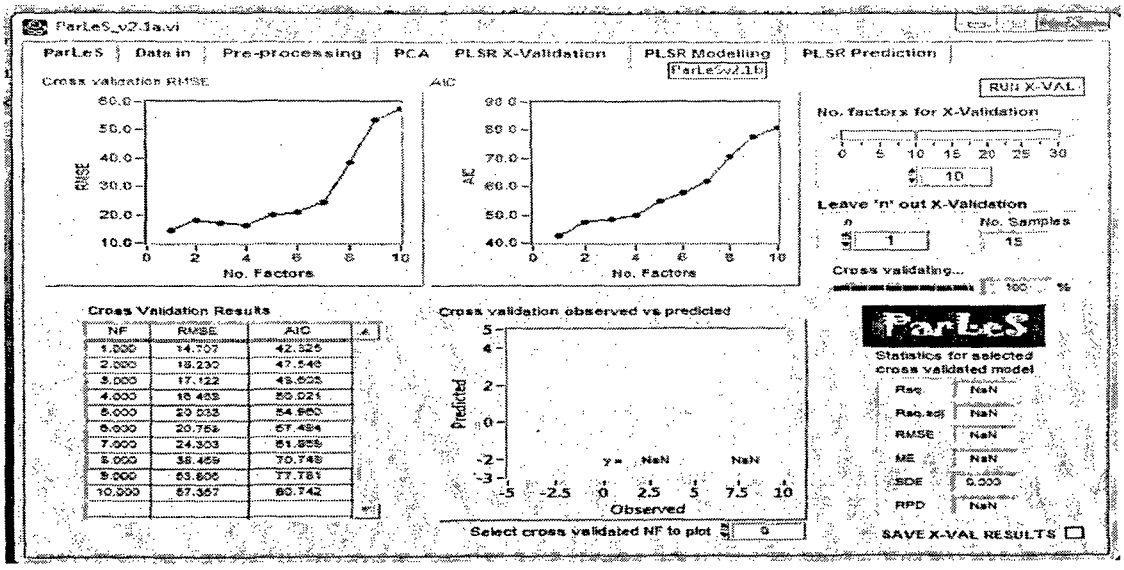

Figure 5.18: PLSR X validation

Figure 5.18 shows the screen shot of PLSR X validation. The screen shot of PLSR modeling with 10 PLS factors is depicted in Figure 5.19. Figure 5.20 shows the screen shot which shows the final concentration for the selected i.e. Glucose. The computed value is 72.74 mg / dl and is very close to the observed value of 70 mg/dl.

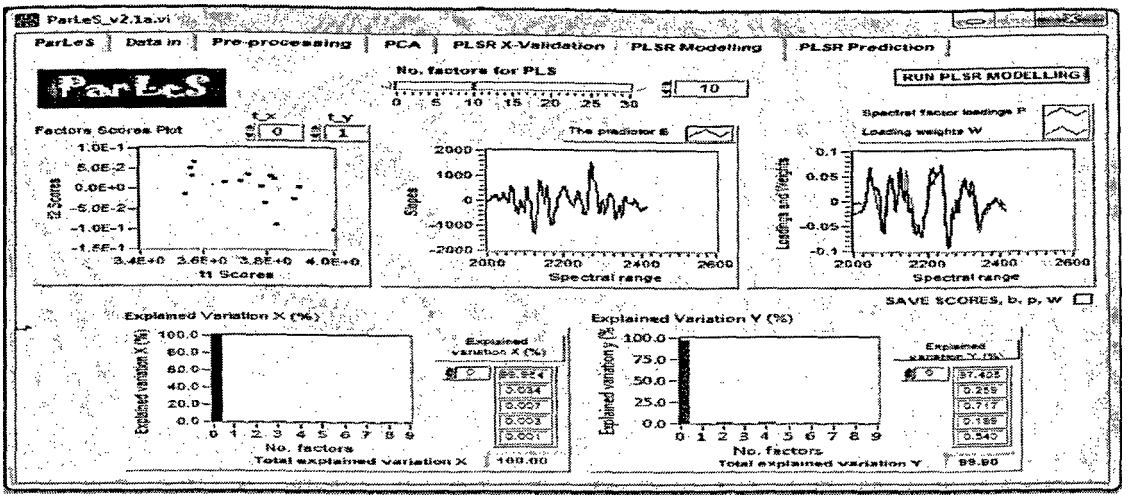

Figure 5.19: PLSR modeling with 10 PLS factors:

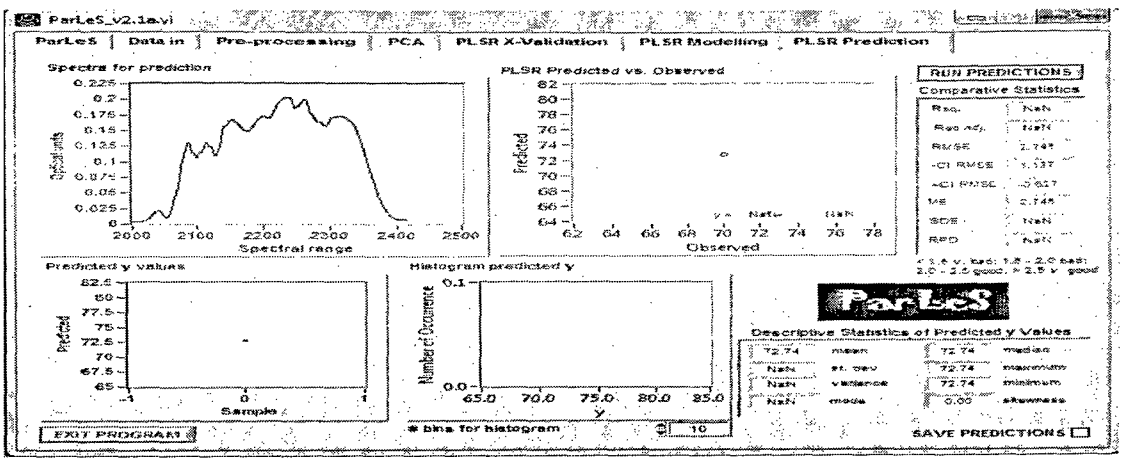

Figure 5.20: PLSR prediction for glucose (70 mg / dl):

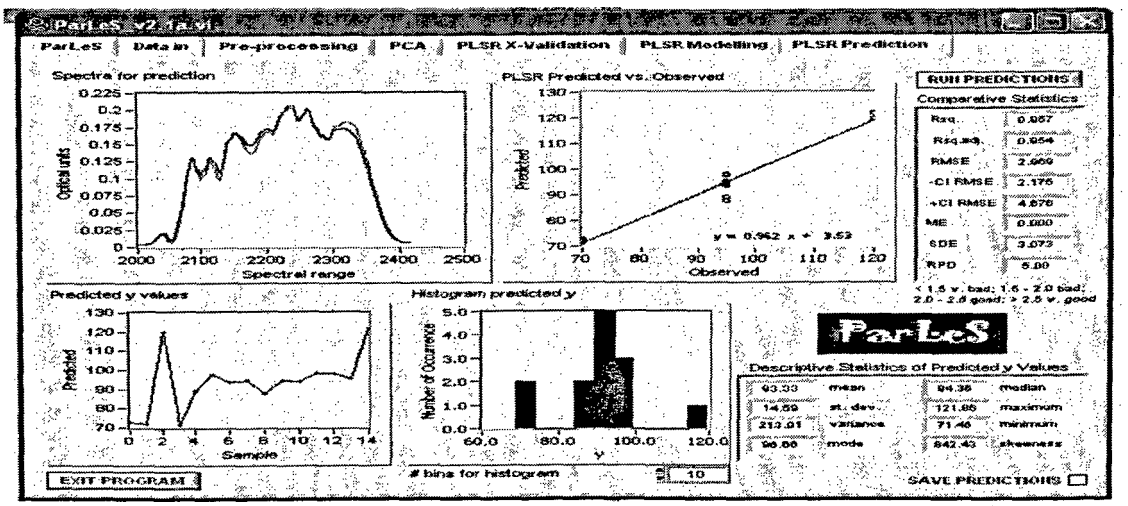

Figure 5.21: PLSR prediction for all the glucose concenetrations.

The RMSE, prediction result of Glucose and other variants and also the result of the same after applying preprocessing techniques as MSC and pretreatment as Mean centre are shown in Table 5.12. Figure 5.21 shows the PLSR prediction for all the glucose concenetrations. The predicted values of all the analytes are found to be very close to the actual concentration measured in pathological lab. RMSE analysis before and after preprocessing was performed over the prediction of all variants concentrations as shown in Table 5.13.

Table 5.12: Predicted concentration of glucose and RMSE analysis

Samples	Actual Glucose mg/dL	Predicted glucose mg/dL	Predicted glucose (Preprocessing=MSC & pretreatment=mean centered (mg/dL)	RMSE mg/dL	RMSE(After preprocessing and pretreatment) (mg/dL)
1	70	72.74	71.91	2.74	1.91
2	70	71.23	71.00	1.23	1.00
3	120	123.55	123.11	3.55	3.11
4	70	73	72.09	3	2.09
5	95	96.25	95.88	1.25	0.88
6	95	97.48	96.55	2.48	1.55
7	95	94.26	95.12	0.74	0.12
8	95	93.44	94.00	1.56	1.00
9	95	92.88	93.88	2.12	1.12
10	95	97.55	96.45	2.55	1.45
11	95	95.45	95.34	0.45	0.34
12	95	97.95	97.10	2.95	2.10
13	95	92.56	93.11	2.44	1.89
14	95	93.47	93.68	1.53	1.32
15	120	118.23	119	1.77	1.00

Table 5.13: Average RMSE for all the variants before and after preprocessing

Experimental (15blood sample)	Glucose mg/dL
RMSE	2.971
RMSE after preprocessing and pretreatment	2.155

5.4 Testing Accuracy of PLSR Model

One of the common methods used for testing the accuracy of prediction model is by using Clark Error Grid Analysis (EGA). Matlab code to generate the grid analysis plot to test the acceptability of PLSR model is given in ANNEXURE VII.

5.4.1 Clark Error Grid Analysis (EGA)

EGA was developed in 1987 to quantify clinical accuracy of the blood glucose value obtained in a glucometer as compared to the actual glucose content for a given patient.[131] Eventually in the same year a proper definition, description, methodology, etc were standardized.[132] The EGA became accepted as one of the "gold standards" for determining the accuracy of blood glucose meters. The grid breaks down a scatter plot of a reference glucose meter and an evaluated glucose meter, into five regions as shown in Figure 5.22.

The method uses a Cartesian diagram, in which the values predicted by the technique under test are displayed on the y-axis, whereas the actual glucose content values are displayed on the x-axis. The diagonal represents the perfect agreement between the two, whereas the points below and above the line indicate overestimation and underestimation of the predicted values respectively.

- Region A are those values within 20 % of the reference,

- Region B contains points that are outside of 20 % are not so accurate but would not lead to inappropriate treatment,
- Region C are those points leading to chances of wrong treatment,
- Region D are those points indicating a potentially dangerous failure to detect hypoglycemia or hyperglycemia, and
- Region E are those points that would confuse treatment of hypoglycemia for hyperglycemia and vice-versa.

The values that fall within zones A and B are clinically acceptable, whereas the values included in areas C-E are potentially dangerous and there is a possibility of making clinically significant mistakes.[133][134]

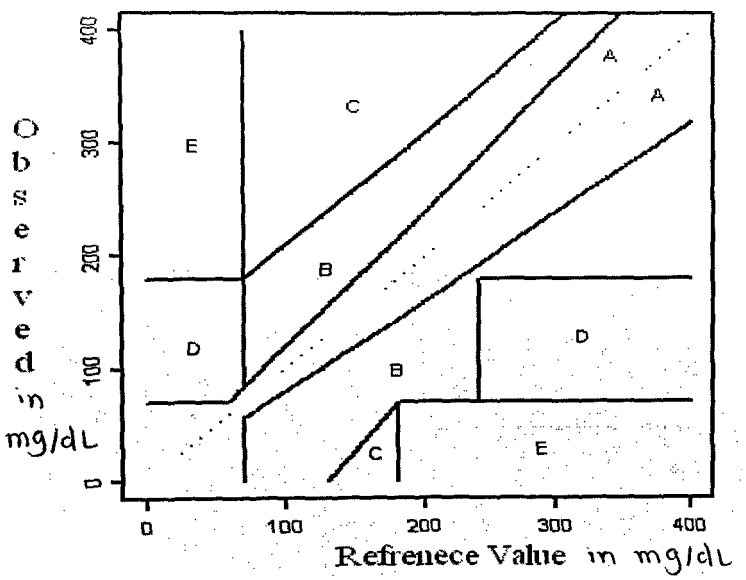

Figure 5.22: The general Clark Error Grid plot

For instance, if the patient's blood glucose is low, and the device being used to test says that it is high, the patient might take more insulin, lose consciousness and place his life in danger. On the other hand, if the true glucose value is high, and the device reads low, the patient might eat some food or drink fruit juice, but it is not likely that immediate harm will

result. The goal of a traditional meter would be to have 98 % of the values in the A and B regions, with less than 0.1 % in E. For non-invasive devices, generally there are no accepted standards, and each group tries to define what they think will be found "acceptable" by the FDA. EGA is computed for all the 4 multivariate cases discussed in 5.3 and the results are discussed in Chapter 6.

5.5 Correlation

It is a quantitative measure of the strength of the relationship that may exist among certain variables. The Pearson formula to calculate the correlation between X and Y is given below. In order to compute the correlation between the variables X and Y , we begin by finding mean error i.e. by computing the mean for X and subtracting this mean from all values of X. The new variable is called "x." and corresponding "y" variable. The variables x and y are said to be deviation scores because each score is a deviation from the mean. Next we compute product of x and y and also the square of x and y. All the computed variables are put in a Equation 5.8 to calculate correlation.

$$r = \frac{\sum xy}{\sqrt{\sum x^2 \sum y^2}} \qquad 5.8$$

One of the most widely used statistics is the **coefficient of correlation** 'r' which measures the degree of association between the two values of related variables given in the data set. It takes values from + 1 to 0. If two sets or data have r = +1, they are said to be perfectly **correlated positively.**

Here the correlation plot is plotted as reference v/s predicted level. When this value is squared (r^2), it is a measure of the amount of agreement between the points (If r^2= 1.0, there is perfect agreement and if r^2 = 0, there is no agreement whatsoever). Generally

speaking, the value of r^2 is 0.9 for a non-invasive test. We have computed the correlation for the all above 4 multivariate cases and results are discussed in Chapter 6.

5.6: Cross-validation of Model

Cross-validation is a technique for assessing how the results of a statistical analysis will generalize to an independent data set. It is mainly used in settings when the goal is prediction and one wants to estimate how accurately a predictive model will perform in practice. One round of cross-validation involves partitioning a sample of data into complementary subsets, performing the analysis on one subset (called the training set) and validating the analysis on the other subset (called the validation set). To reduce variability, multiple rounds of cross-validation are performed using different partitions and the validation results are averaged over the rounds Model performance was judged by comparing standard error values for each type of data set. The standard error of calibration (SEC) and standard error of prediction (SEP) were computed by the following Equations 5.9 & 5.10.[135]

$$SEP = [1/n_p(\sum_{i}^{n_p}(c_a - c_p)^2)]^{1/2} \qquad 5.9$$

$$SEC = [1/(n_c - f - 1)(\sum^{n_c}(c_a - c_p)^2)]^{1/2} \qquad 5.10$$

Where n_c → number of spectra in the calibration,

n_p → number of spectra in the prediction sets,

f → the number of PLS factors used to build the model,

c_a → assigned glucose concentration,

c_p → glucose concentration predicted by the model.

The SEP and SEC for the different multivariate cases discussed in section 5.3 are computed and explained in result section i.e. Chapter 6.

CHAPTER 6

RESULTS AND CONCLUSIONS

6.1 Results

Non-invasive blood glucose sensing by NIR spectroscopy requires the transmitted light through the body tissue in the NIR range and glucose absorption signatures. Clearly, the amount of light absorbed by glucose must be significantly greater than the absorption due to other constituents of blood and also intensity fluctuations caused by measurement noise; Both sensitivity and accuracy demand high SNR, where high signals correspond to large absorbance values originating from glucose and low noise corresponds to performance of the instrumentation. Selection of the tissue for probing must consider the physical and chemical characteristics as they pertain to the overall SNR.

In this Thesis "Novel Embedded DSP architecture" is developed using Altera NIOS II soft-core platform designed using Altera DE2 board having target as CYCLONE II (EP2C6) to estimate the level of blood glucose in the human body, Non-Invasively. The technique uses the NIR radiation in the range 2.0 um to 2.5 um. PLSR model based on SIMPLS algorithm is also developed in C language and ported on NIOS II platform to estimate the glucose concentration.

As NIR spectroscopy continues to be developed for blood glucose measurement, it is critical to assess model accuracy, precision and validation on the basis of clinically acceptable criteria. To test the accuracy of the PLSR model which we have developed, EGA method is used. To confirm the validation of model, we have calculated the SEP, SEC, RMSE and correlation coefficient(r).

6.1.1 Testing the accuracy of the model:

We have developed the EGA plot for all the 4 cases of sample spectra discussed in Section 5.3. By analyzing the EGA plot for the four cases we have found out that, the developed PLSR model is very accurate and its accuracy is within the satisfactory limit of well established guidelines given in Section 5.4.1. It is interesting to know that popular glucometer available in the drug house are not certified by WHO due to the accuracy and repeatability. However, our technique has consistently predicted glucose content with acceptable limits of medical fraternity and high degree of repeatability. We are therefore confident that this technique will be able to get certification from the WHO.

Case 1: Multivariate model for Human Whole Blood Tissue for Glucose (Lorentz oscillator)

Here spectra in the NIR range is generated with the help of Lorentz Oscillator algorithm designed in Matlab 7.0. EGA for glucose in simulated whole blood is shown in Figure 6.1. Almost 100 % of the predicted result lies in 'A' region .

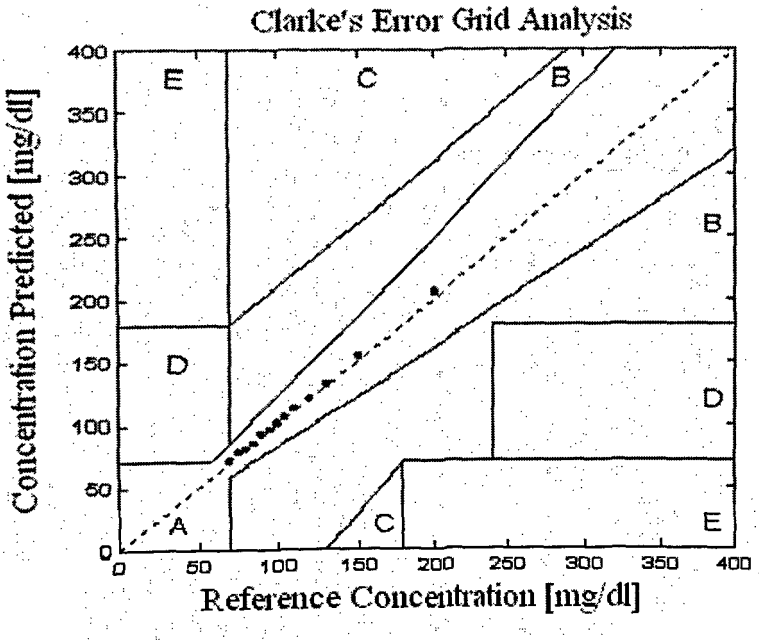

Figure 6.1: Clark Error Grid plot for glucose in simulated whole blood spectra

Case 2: Multivariate model for Human Whole Blood Tissue for Glucose where spectra are generated using Lorentz oscillator *for blood by considering skin colour and* temperature along with 5 blood contituents.

Here simulated spectra of human tissue in the NIR range is generated with the help of Lorentz Oscillator algorithm designed in Matlab 7.0. EGA for glucose in simulated whole blood is shown in Figure 6.2. The results show 100% of predicted values lie in 'A' region which is around the reference line in 'A' region.

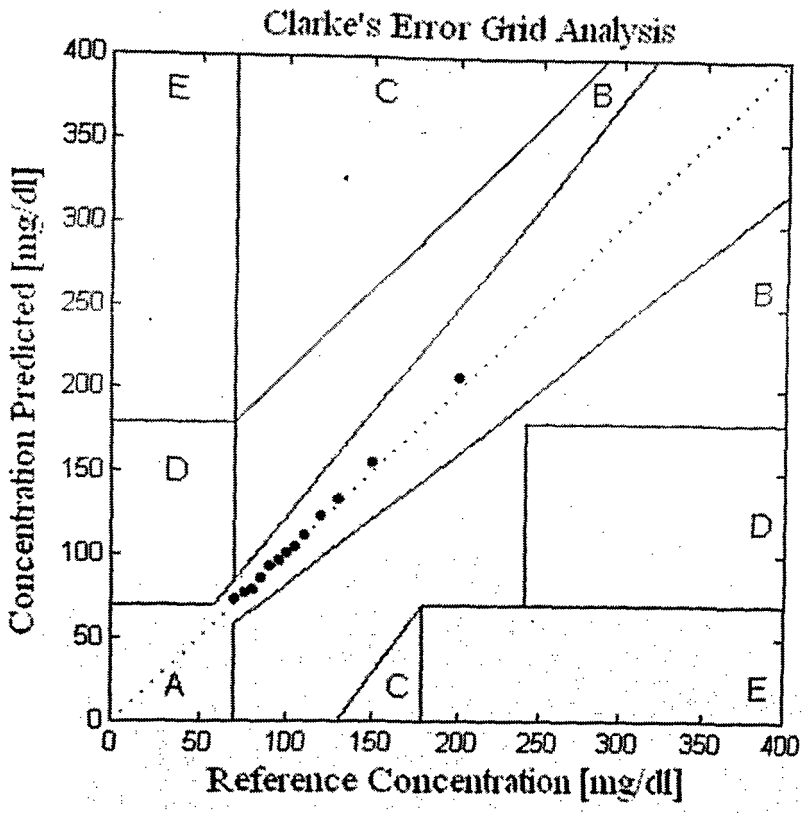

Figure 6.2: Clark Error Grid plot for glucose in simulated human tissue

Case 3: Multivariate model for Human Whole Blood by mixing the 5 blood *constituents* (Glucose, Urea, Lactate, Ascorbate, Alanine) using standard solutions.

Thirteen spectra were recorded with the help of Schimatzu FTIR in the range 2000 nm to 2500 nm. Samples were prepared by carefully weighing masses of standard materials and mixing them in different proportion as shown in Table 5.6 of Chapter 5. EGA for glucose is shown in Figure 6.3. From the plot it is clear that 99.5 % of the predicted result lies in the 'A' region and 0.5 % lies on the boundary of 'A' and 'B'.

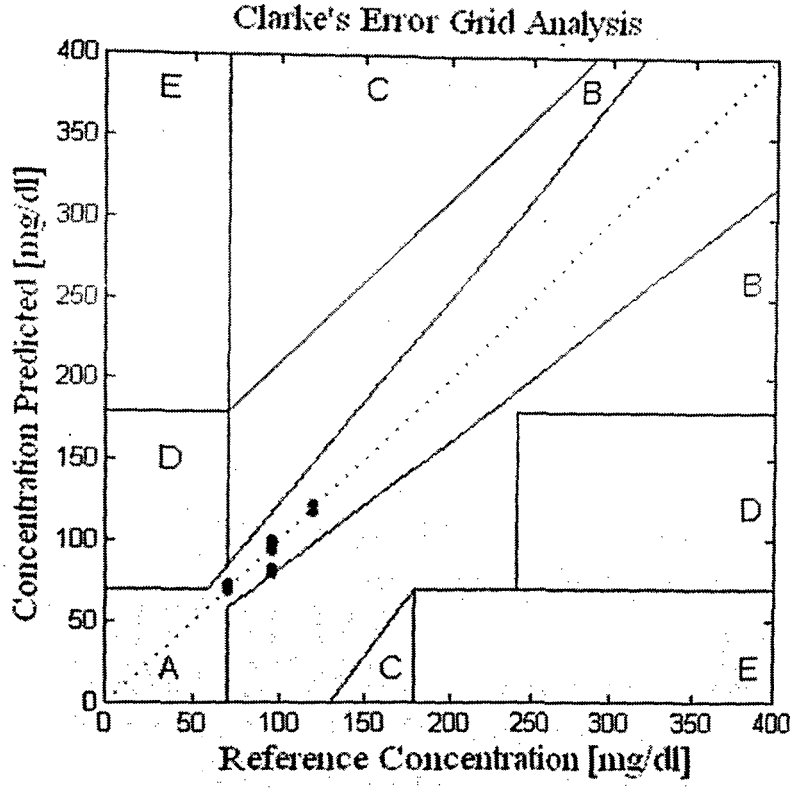

igure 6.3: Clark Error Grid plot for glucose in Human Whole Blood by mixing the 5 blood constituents

Case 4: Multivariate model for actual Human Whole Blood Spectra

Blood spectra in the range 2000 nm to 2500 nm were provided by Y.C. Shen. The same spectra we have used in our PLSR model with the 10 PLS factors. The Figure 6.4 shows the EGA for glucose in whole blood. It is found from the EGA plot that all the predicted readings fell into the 'A' region, which is clinically accurate.

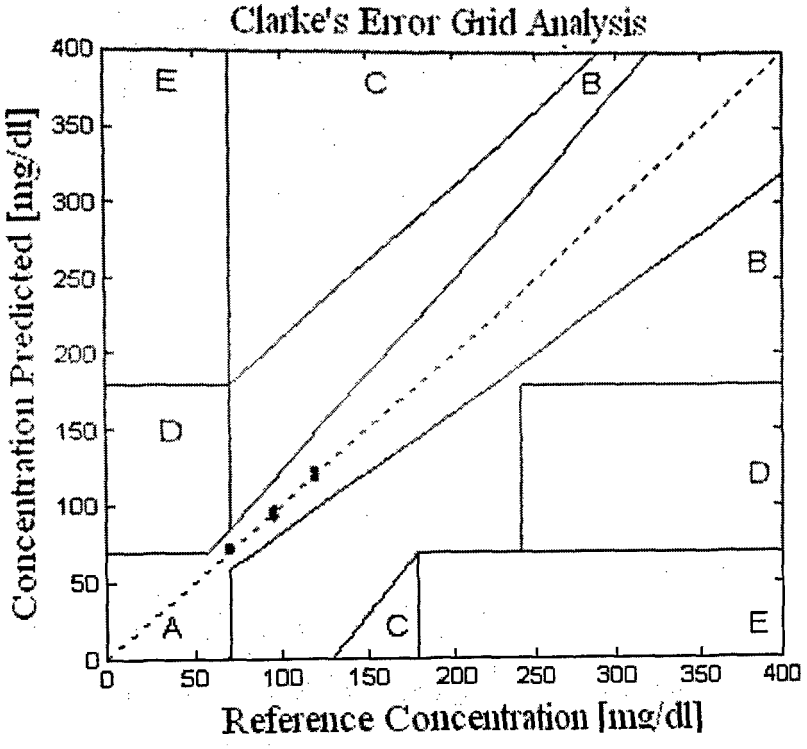

Figure 6.4: Clark error grid plot for glucose in human whole blood

6.1.2 Validation of PLSR model

Validation of PLSR model is decided by SEP, SEC, RMSE and correlation coefficient(r). Table 6.1 gives the values of SEP, SEC, RMSE and correlation coefficient(r) for all the four models discussed in Chapter 5.

Table 6.1: Results from the analysis of spectral data (spectral range 2000 nm to 2500 nm and PLS factor 10)

Sample	RMSE mg/dL	r	SEC mg/dl	SEP mg/dl
Case1: Multivariate model for Human Whole Blood Tissue for Glucose (Lorentz oscillator)	2.459	0.9523	3.345	2.88
Case 2: Multivariate model for Human Whole Blood Tissue for Glucose where spectra are generated using Lorentz oscillator for blood by considering skin colour and temperature along with 5 blood contituents.	2.86	0.9363	3.50	3.26
Case 3: Multivariate model for Human Whole Blood by mixing the 5 blood constituents (Glucose, Urea, Lactate, Ascorbate, Alanine) using standard solutions.	4.143	0.9019	4.77	4.95
Case 4 a: Multivariate model for actual Human Whole Blood Spectra (provided by Y.Shen	2.971	0.9515	3.89	3.49
Case 4 b: Multivariate model for actual Human Whole Blood Spectra (provided by Y.Shen after preprocessing & pre-treatment	2.155	0.9771	3.16	2.46

We have calculated the parameters required (as shown in Table 6.1) to validate the model by taking only 10 PLS factors and spectra are collected in the range 2000 nm to 2500 nm .

Case1: The baseline PLS calibration model prediction performance for the test (monitoring) data yielded SEP of 2.88 mg dl^{-1} for 10 PLS factors with an associated SEC of 3.345 mg dl^{-1} for the training data.

Case2: The baseline PLS calibration model prediction performance for the test data yielded SEP of 3.26 mg dl^{-1} for 10 PLS factors with an associated SEC of 3.50 mg dl^{-1} for the training data.

Case 3: The baseline PLS calibration model prediction performance for the test (after preprocessing & pretreatment) data yielded SEP of 4.957 mg dl^{-1} for 10 PLS factors with an associated SEC of 4.77 mg dl^{-1} for the training data.

Case 4 a: The baseline PLS calibration model prediction performance for the test (after preprocessing & pretreatment) data yielded SEP of 3.49 mg dl^{-1} for 10 PLS factors with an associated SEC of 3.89 mg dl^{-1} for the training data.

Case 4 b: The baseline PLS calibration model prediction performance for the test (after preprocessing & pretreatment) data yielded SEP of 2.46 mg dl^{-1} & SEC of 3.16 mg dl^{-1} for the training data.

By doing the analysis it is found that RMSE, correlation coefficient and prediction errors are improved after applying the preprocessing and pretreatment techniques to the spectral data. The PLSR model has a good correlation coefficient calculated in all 4 cases and is close to 1. The SEC, SEP and RMSE for the prediction of glucose is acceptable as per medical standard.

6.2 Discussion

Accurate non-invasive measurement of in-vivo glucose levels in diabetics by NIR Spectral number spectroscopy has proved to be a very difficult task due to the relatively small influence of glucose at physiological levels and the complexity of human tissue. A large number of researchers and commercial entities are heavily involved in this area.[136] Arnold eta discusses a number of issues that confront those who attempt to measure glucose non-invasively using multivariate calibration with spectral measurements. The ultimate objective of these activities is to provide a mechanism for diabetic patients to accurately and conveniently monitor their glucose levels without the pain and inconvenience associated with current monitoring technology that involves measuring the glucose in blood obtained by pricking the skin.

Most of the models of non-invasive glucose instrumentation have difficulty in satisfying the EGA calibration. This could be due to poor multivariate model. The fine-tuning of the same multivariate model is required by incorporating the various parameters influencing glucose. With proper understanding of the dynamics of the physiology of the human body and the catabolic processes triggered by signals for the alternative path, depending on the situation in the cell, a closer estimate of glucose is possible if all the parameters are taken into consideration.

In general, there are three basic types of absorption processes: electronic, vibrational and rotational. Electronic transition occurs in both atoms and molecules, whereas vibrational and rotational transitions occur only in molecules. PLSR model is more difficult to build because of variation in skin pigments, body temperature, overlapping absorption spectra of other blood analytes etc. It may be noted that even a slight change in temperature, the absorption of the background water spectrum will shift, severely impacting measurement of

the glucose signal.[137][138][139][140][141] The physiological ranges of glucose values seen in the normal human body range is from 80 to 120 mg/dl and should ideally remain around 100 mg/dl (5.5mH). Required accuracy of a useful glucometer is 10mg/dl (0.55mM). For the most identifiable NIR glucose peak at approximately 2.27μm, molar absorptivity is roughly 0.25 $M^{-1}cm^{-1}$. The molar absorptivity of water is 0.41 M^{-1} cm^{-1} and the concentration of the water in typical body tissue is approximately 39 M^{-1} cm^{-1}, considering transmission measurement made through 1 mm of body tissue. The background absorption due to water will be about 1.6 and that due to glucose will be about 1.26 x 10^{-4} M^{-1} cm^{-1}. Further for the accuracy requirement, we must be able to withstand an absorption change of about 1.26 x 10^{-4} on a background of 1.6 and it is evident that even a change in tissue hydration of 1/1000 of a percent would result in a larger signal change than would a 10mg/dl change in glucose concentration. For this reason, high-order multivariate models that incorporate analysis must use entire spectra to extract glucose information.[142] [143]

6.3 Scope of future work

We plan to test the developed PLSR model with minimum wavelength points. Once the successful validation is done by computing SEC, SEP & RMSE, those wavelengths points can be replaced by laser sources. By using the few laser sources in place of white light source and monochromator, we can reduce the size of instrument to achieve the portability.

6.4 Conclusions

Multivariate statistical modeling methods have been applied to NIR spectral data to discriminate glucose concentrations. Specifically, performance levels are compared for PCR and PLSR models based on their SEP. Only the data between 2000 and 2500 nm were used for the calibration model development and validation. Performance results for the PLSR model is shown in Table 3. The Novel embedded DSP architecture is developed and PLSR model validation is done on the sophisticated DSP architecture. The designed glucometer chemo metrics model has around ± 2 % error (Ref. Table 6.1), this error can be minimized if the intra, inter constituents chemistry is known by means of various pathways triggered by the ambient conditions in the process of catabolism of glucose. The RMSE analysis of glucose for the all the 4 cases is found to be satisfactory with the values of 2.459, 2.86, 4.143, 2.971, 2.155 respectively as shown in Table 6.1. If preprocessing and pre-treatment techniques are adopted over the spectra then there is considerable improvement over the RMSE and SEP. This model has potential scope in designing portable, cost effective and accurate non-invasive glucometer based on NIR spectroscopy. This model can be used to predict the concentration of any blood constituents by changing parameter fed to multivariate system. The PLSR model accuracy and validation is also tested so that the model is clinically accepted.

ANNEXURE

ANNEXURE I

```
#include <Philips\LPC2138.h>
#include <stdio.h>
#include "KBD5X5.h"
#include "UART0.h"
void main (void);
void Delay(int ByCount);
void main (void)
{
int ch, ch2, ch1, Initial, scan, R_initial=0, Temp_final, temp_1=0, r, Final, value, step, k,
countfwd=0, countbkwd=0;
        int Init=8192,a=256,c=16 b, nstep, cont;
        b=4212; cont=b*3; k=1;
        PINSEL0 = 0x00000005;
        PINSEL1 = 0x00000000;
        {
       InitUart0();
              kbd_init();
         puts("Enter scan number:\n");
                     puts("enter 1st digit:");
                     ch = rdkbd() ;
                     ch1=ch;
                     printf("Keycode 1st = %02)
                     puts("enter 2nd digit:");
                     ch = rdkbd() ;
                     ch2=ch;
                     printf("Keycode 2nd = %02
                     ch2=ch2<<4;
                     scan=(ch1 | ch2);
                     printf("Scan time= %02X\n\n",scan) ;
        Initial: puts("Enter Initial Wavelength:\n");
              puts("enter 1st digit:");
               ch = rdkbd() ;
               ch1=ch;
```

```
printf("Keycode 1st = %02X\n", ch1) ;
puts("enter 2nd digit:");
ch = rdkbd() ;
ch2=ch;
printf("Keycode 2nd = %02X\n", ch2) ;
ch2=ch2<<4;
nitial=(ch1 | ch2);
printf("InitialWavelength= %02X\n\n",Initial)
```

Final:

```
puts("Enter Final Wavelength:\n");
puts("enter 1st digit:") ;
ch = rdkbd() ;
ch1=ch;
printf("Keycode 1st = %02X\n", ch1) ;
puts("enter 2nd digit:");
ch = rdkbd() ;
ch2=ch;
printf("Keycode 2nd = %02X\n", ch2) ;
ch2=ch2<<4;
Final=(ch1 | ch2);
printf("Final Wavelength = %02X\n\n",Final) ;
```

Resolution:

```
puts("Enter the resolution:\n");
puts("enter 1st digit:") ;
ch = rdkbd() ;
ch1=ch;
printf("Keycode 1st = %02X\n", ch1) ;
puts("enter 2nd digit\n");
ch = rdkbd() ;
ch2=ch;
printf("Keycode 2nd = %02X\n", ch2) ;
ch2=ch2<<4;
r=(ch1 | ch2);
printf("resolution = %02X\n", r) ;
if(Initial>=20)
{
if (Final<38)
```

```
                {
                 Initial=Initial*a;
                Final=Final*a;
                 if(r>=10)
                {
printf("Initial Wavelength=%02Xnm\n", Initial) ;
printf("Final Wavelength= %02X nm\n", Final) ;
                printf("Resolution= %02X nm\n",r) ;
                 while(temp_1<scan)
                 {
                 Temp_final=Initial;
                 R_initial=Initial;
                  R_initial=R_initial+r;
                 step= (cont*r)/(Final-Initial);
                  nstep=step/(Final-Initial);
                   PINSEL0=0x00000000;
                 PINSEL1=0x00000000;
                  IO1DIR=0x000F0000;
          IO0DIR=0xFFFFFFEF;
          while(Init<Initial)
          { IO1PIN=~0x00090000;
                Delay(5000);
                IO1PIN=~0x000A0000;
                Delay(5000);
                 IO1PIN=~0x00060000;
                Delay(5000);
                  IO1PIN=~0x00050000;
                Delay(5000);
                  Init=Init+r;
                 }
                Countfwd =Initial;
                 PINSEL0=0x00000000;
                   PINSEL1=0x00000000;
                  IO1DIR=0x000F0000;
                  IO0DIR=0xFFFFFFEF;
                 do
```

```
{
        IO1PIN=~0x00090000;
        Delay(5000);
        IO1PIN=~0x000A0000;
        Delay(5000);
        IO1PIN=~0x00060000;
       Delay(5000);
        IO1PIN=~0x00050000;
         Delay(5000);
         countfwd=countfwd+4;
         if(countfwd>=R_initial)
         {
         Delay(250000);
       }
         Temp_final=Temp_final+nstep;
         }                                        /*end of do while*/
     while(Temp_final<Final);
       PINSEL0=0x00000000;
      PINSEL1=0x00000000;
      IO1DIR=0x000F0000;
     IO0DIR=0xFFFFFFDF;
    countbkwd=0;
    do
{
       IO1PIN=~0x00050000;
       Delay(1000);
       IO1PIN=~0x00060000;
       Delay(1000);
       IO1PIN=~0x000A0000;
       Delay(1000);
        IO1PIN=~0x00090000;
       Delay(1000);
     }                                  /*end of do while*/
     while (IO0PIN^5==1);
     temp_1=temp_1+1;
   }                                      /*end of while*/
```

```
        }                                   /*end of if*/
      else
      {
         PINSEL0=0x00000005;
          PINSEL1=0x00000000;
          puts("resolution is not within limit");
         goto Resolution;
       }
    }/*end of if*/
    else
    {
    PINSEL0=0x00000005;
          PINSEL1=0x00000000;
          puts("final range is not within limit\n");
         goto Final;
    }
    }                                       /*end of if*/
    else
    {
    PINSEL0=0x00000005;
          PINSEL1=0x00000000;
          puts("Initial range is not within limit\n");
         goto Initial;
        }
              }
              }

void Delay(int ByCount)
{
        int i;
        for(i=0;i<ByCount;i++)
        {}
}
```

ANNEXURE II

```
#include "system.h"
#include "altera_avalon_pio_regs.h"
#include "alt_types.h"
#include <stdio.h>
#define d1 500
#define d2 5000
int keybd(void);
int main (void)
{
 int i,w,fw;
 unsigned int m[3],mm[3],k,l;
 alt_u8 mtr[4] = {0x5,0x6,0xA,0x9};
 volatile int j,a=0,b=0;
 float x,y;

 printf("enter the initial wavelength\n");
 printf("greater than 500nm\n");
 for(i=3;i>=0;i--)
 {

printf(" Wating for 10 secs\n");

 usleep(5000000);
 scan:
 k=keybd();
 if (k<=9)
 {
  m[i]=k;
 printf("\n%d\n",m[i]);
 }
 else{
 goto scan;
 }
```

```
}

w=m[3]*1000+m[2]*100+m[1]*10+m[0];
printf("\nwavelength = %d",w);

usleep(5000000);
//*************************************************
printf("\nenter the final wavelength\n");
printf("Less than 5000nm\n");
for(i=3;i>=0;i--)
{
printf(" Wating for 10 secs\n");

usleep(5000000);
can:
l=keybd();
if (l<=9)
{
 mm[i]=l;
printf("\n%d\n",mm[i]);
}
else{
goto can;
}
}
 fw=mm[3]*1000+mm[2]*100+mm[1]*10+mm[0];
printf("\nwavelength = %d",fw);
for(i=3;i>=0;i--)
{
  printf("\n %d \t",mm[i]);
}

printf("\nfinal wavelength = %d",fw);

//*************************************************************
printf("\nThe End\n Actual wavelength = %d\n Final wavelength = %d\n",w,fw);
```

```
 printf("\nfast 1");
for (x=d1;x<=w;x++)
{ printf("\n for loop 1x=%d",x);
 for(j=0;j<=3;j++)
   {
   IOWR_ALTERA_AVALON_PIO_DATA(MOTOR_BASE, mtr[j]);
   usleep(200);
   }
}
 printf("\nslow");

for (w;w<=fw;w++)
{  printf("\n For loop 2 fw=%d w=%d ",fw,w);
   for(j=0;j<=3;j++)
   {
   IOWR_ALTERA_AVALON_PIO_DATA(MOTOR_BASE, mtr[j]);
   usleep(20000);
   }
}
 printf("\nfast 2");
 for (x=fw;x<=d2;x++)
  {
  printf("\n for loop 3");
   for(j=0;j<=3;j++)
   {
   IOWR_ALTERA_AVALON_PIO_DATA(MOTOR_BASE, mtr[j]);
   usleep(200);
   }
}
printf("\n The End");

 while(1)
{
a= IORD_ALTERA_AVALON_PIO_DATA(READPIN_BASE);
 b= IORD_ALTERA_AVALON_PIO_DATA(SENSE_BASE);
```

```
printf ("a=%d  b=%d\n",a,b);
if ((a==1 && b==0) || (a==0 && b==0))
{
 do {
  for(j=0;j<=3;j++)
  {
  IOWR_ALTERA_AVALON_PIO_DATA(MOTOR_BASE, mtr[j]);
  usleep(20000);
  }
  b = IORD_ALTERA_AVALON_PIO_DATA(SENSE_BASE);
  }while (b==0);
 }
 else if (a==0 && b==1)
 {
 do{
  for(j=3;j>=0;j--)
  {
   IOWR_ALTERA_AVALON_PIO_DATA(MOTOR_BASE, mtr[j]);
   usleep(20000);
  }
  a = IORD_ALTERA_AVALON_PIO_DATA(READPIN_BASE);
  }while (a==0);
 }
 }
}
 int keybd(void)
{
 int j;
 alt_u8 a=0x00;
 alt_u8 b=0x00;

 a= IORD_ALTERA_AVALON_PIO_DATA(CONTROL_BASE);
 //usleep(10000000);
 b= IORD_ALTERA_AVALON_PIO_DATA(SCAN_BASE);
////printf("\n%X \n",a);
if (a==0x01){
```

```
if (b==0x06)
j=3;
if (b==0x05)
j=2;
if (b==0x03)
j=1;

//printf("%d\n",j);
 return (j);
}
if (a==0x02){
if (b==0x06)
j=6;
if (b==0x05)
j=5;
if (b==0x03)
j=4;
 return (j);
}
 if (a==0x03){
 if (b==0x06)
j=9;
 if (b==0x05)
j=8;
 if (b==0x03)
j=7;
 //printf("%d\n",j);
   return (j);
 }
  if (a==0x04){
  if (b==0x06)
 j=0;
  //printf("%d\n",j);
    return (j);
  }
  }
```

ANNEXURE III

```
library IEEE;
use IEEE.STD_LOGIC_1164.ALL;
use IEEE.STD_LOGIC_ARITH.ALL;
use IEEE.STD_LOGIC_UNSIGNED.ALL;

entity adc is
  Port (
   clk     : in std_logic; -- 20 MHz local clock
   reset   : in std_logic; -- Local reset signal
        --      switch   : in std_logic_vector( 7 downto 0);
                smpclk   : out std_logic;
                vary: out std_logic_vector(3 downto 0);

   ---------------------------- For ADC1(7891)
    cs_ad7891                   : out std_logic; --chip select
    convst_ad7891       : out std_logic; --conversion start
    wr_ad7891           : out std_logic; --write
    rd_ad7891           : out std_logic; --read
    eoc_ad7891          : in std_logic;  --end of conversion
    mode_ad7891         : out std_logic; --mode=1 for parallel
       adc_out                  : inout STD_LOGIC_VECTOR(11 DOWNTO 0)
        );

end adc;
architecture Behavioral of adc is
type state_1 is (reset_1, write_cwr, start_conv,read_data);
signal ps_1, ns_1 : state_1;

signal div_adc : std_logic_vector( 15 downto 0 );
signal sampling_clk,wr_s,rd_s,eoc_flag_reset,eoc_flag, convst_ad7891_s : std_logic;
signal adc_out_s : std_logic_vector( 11 downto 0 );
signal adc_out_IN : std_logic_vector( 11 downto 0 );
signal dac_out_s,dac_out_ss,adc_out_ss : std_logic_vector( 11 downto 0 );
```

```
begin
--=================== AD7891_1 Interface=====================
process(clk, reset)
begin
        if(reset = '1') then
                div_adc <= (others => '0');
        elsif(clk'event and clk = '1') then
                div_adc <= div_adc + 1;
        end if;
end process;
sampling_clk <= div_adc(2) ;
--sampling_clk <= clk;
smpclk <= sampling_clk;
-------------------------------------------------------------------
process(reset, sampling_clk)
begin
        if(reset = '1' ) then
                ps_1 <= reset_1;
        elsif(sampling_clk'event and sampling_clk = '1') then
                ps_1 <= ns_1;
        end if;
end process;
-------------------------------------------------------------------
process(ps_1)
begin
        case ps_1 is
        when reset_1 =>
          ns_1 <= write_cwr;
     vary <="1111";
        when write_cwr =>
           ns_1 <= start_conv;
                vary <="0011";
        when start_conv =>
                ns_1 <= read_data       ;
        vary <="0110";
        when read_data =>
```

```
            ns_1 <= reset_1;
                vary <="0111";
        end case;
end process;
cs_ad7891 <= '0' when (ps_1 = read_data or ps_1 = write_cwr) else  '1';
wr_s <= '0' when (ps_1 = write_cwr) else '1';
wr_ad7891 <= wr_s;
rd_s <= '0'when (ps_1 = read_data) else  '1';
rd_ad7891 <= rd_s;
mode_ad7891 <= '1'; -- set parallel mode of ADC

adc_out(5 downto 0) <= '0' &"00" & "001" when wr_s = '0' else
                                (others => 'Z');
----------------------------convst----------------------
process(reset, sampling_clk)
begin
        if(reset = '1') then
                convst_ad7891_s <= '0';
         elsif(sampling_clk'event and sampling_clk = '1') then
            convst_ad7891_s <= wr_s;
        end if;
end process;
convst_ad7891 <= convst_ad7891_s;
-------------------------read adc-------------------------
process(reset, sampling_clk,rd_s)
begin
        if(reset = '1') then
                adc_out_s <= (others => '0');
        elsif(sampling_clk'event and sampling_clk = '1') then
          if(rd_s = '0') then
                 adc_out_s <= adc_out;
           end if;
        end if;
end process;
end Behavioral;
```

ANNEXURE IV

```
#include <stdio.h>
#include <math.h>
#include <float.h>
#define ROW1 4
#define COL1 4
#define ROW2 4
#define COL2 4
#define N 4

double** minus(double** ,double**,int );
double addition(double** ,int ,int);
double** wpq(double** ,int ,int);
double**divide(double**, int,int,double);
double** column(double**,int,int);
void Jacobi_Cyclic_Method(double eigenvalues[COL1], double
*eigenvectors[COL1][COL1],double *A, int n);
double** identity(int);
double** transpose(double**,int,int);
double** init(double**,int,int);
double** set(double**,int,int);
void get(double**,int,int);
double** mul(double**,double**,int,int,int);
void main()
{
int i,j
double**matrix1,**matrix2,**AO,**MO,**trans,**CO,**AO_trans,**g,M[COL1][COL1];
        double eigenvalues[COL1],**qh,**Wh,**Wh_mat,**Ch,**W,**ph,**p,**q,**vh;
        double eigenvectors[COL1][COL1],Ch_sq,m=2.0,**X_pre;

double **v_trans,**C1,**p_trans,**M1,**A1,**q_trans,**B,**T,av_vh;
        clrscr();
matrix1=init(matrix1,ROW1,COL1);
        matrix2=init(matrix2,COL2,COL2);
```

```
        set(matrix1,ROW1,COL1);
 set(matrix2,ROW2,COL2);
clrscr();
trans=transpose(matrix1,COL1,ROW1);
AO=mul(trans,matrix2,COL1,COL2,ROW1);
MO=mul(trans,matrix1,COL1,COL1,ROW1);
CO=identity(COL1);
AO_trans=transpose(AO,COL2,COL1);
g=mul(AO_trans,AO,COL2,COL2,COL1);
        for(i=0;i<COL1;i++)
         {
          for(j=0;j<COL1;j++)
          {
           M[i][j]=*(*(g+i)+j);
          }
         }


Jacobi_Cyclic_Method(eigenvalues,*eigenvectors,*M,COL1);
qh=init(qh,COL1,COL1);
 for(i=0;i<COL1;i++)
        {
         for(j=0;j<COL1;j++)
         {
          if(i==j)
           qh[i][j]=eigenvalues[i];
          else
           qh[i][j]=0.0;
         }
        }
         Wh=mul(AO,qh,COL1,COL1,COL2);
         Wh_mat=column(Wh,COL1,COL1);
         Ch=transpose(Wh_mat,1,COL1);
         Ch=mul(Ch,MO,1,COL1,COL1);
         Ch=mul(Ch,Wh_mat,1,1,COL1);
```

```
            Ch_sq=sqrt(**Ch);
Wh_mat=divide(Wh_mat,COL1,1,Ch_sq);
            W=wpq(Wh_mat,COL1,1);

            Wh_mat=column(W,COL1,1);
            ph=mul(MO,Wh_mat,COL1,1,COL1);
            p=wpq(ph,COL1,1);

      Wh_mat=column(W,COL1,1);
      qh=mul(AO_trans,Wh_mat,COL2,1,COL1);
      q=wpq(qh,COL2,1);
            ph=column(p,COL1,1);
            vh=mul(CO,ph,COL1,1,COL1);
            av_vh=addition(vh,COL1,1);
            av_vh=av_vh/m;
            vh=divide(vh,COL1,1,av_vh);
            v_trans=transpose(vh,1,COL1);
           C1=mul(vh,v_trans,COL1,COL1,1);
           C1=minus(CO,C1,COL1);
            p_trans=transpose(ph,1,COL1);
     M1=mul(ph,p_trans,COL1,COL1,1);
            M1=minus(MO,M1,COL1);
     A1=mul(CO,AO,COL1,COL2,COL1);
            q_trans=transpose(q,1,COL1);
            B=mul(W,q_trans,COL1,COL1,1);
            T=mul(matrix1,W,ROW1,1,COL1);
            get(T,ROW1,1);
             ph=transpose(p,1,COL1);
             X_pre=mul(T,ph,ROW1,COL1,1);
             matrix1=transpose(matrix1,COL1,ROW1);
             X_pre=transpose(X_pre,COL1,ROW1);
             get(X_pre,COL1,ROW1);
    printf("\n\t\t Thanks ");
            getch();
            free(matrix1);
            free(matrix2);
```

```
} /* end main */



double** init(double** arr,int row,int col)
{
 int i=0,j=0;
 arr=(double**)malloc(sizeof(double)*row*col);
    for(i=0;i<row;i++)
    {
          for(j=0;j<col;j++)
          {
*((arr+i)+j)=(double*)malloc(sizeof(double));
           *(*(arr+i)+j)=0.0;
          }
    }
 return arr;
}


double** set(double** arr,int row,int col)
{
 int i=0,j=0;
 double val=0.0;
 for(i=0;i<row;i++)
    {
          for(j=0;j<col;j++)
          {
 printf("Enter value for row %d col %d  :",(i+1),(j+1));
        scanf("%lf",&val);
        *(*(arr+i)+j)=val;
          }
    }
    return arr;
}
```

```
void get(double** arr,int row,int col)
{
    int i=0,j=0;

   for(i=0;i<row;i++)
    {
         for(j=0;j<col;j++)
         {
          printf("%lf\t",*(*(arr+i)+j));
         }
        printf("\n");
    }
}
double** mul(double** arr1,double** arr2,int row,int col,int col1)
{
 double  **result;
 int i=0,j=0,k=0;
 result=init(result,row,col);
  for(i=0;i<row;i++)
    {
         for(j=0;j<col;j++)
         {
              for(k=0;k<col1;k++)
              {
                *(*(result+i)+j)+=(*(*(arr1+i)+k))*(*(*(arr2+k)+j));
                if (k!=(col1-1))
                printf("+");
              }
            printf("\t");
         }
     printf("\n");
    }
 return (result);
}
```

```
double** transpose(double** arr,int row1,int col1)
{
double **trans;
int i,j;
trans=init(trans,row1,col1);
for(i=0;i<col1;i++)
{
 for(j=0;j<row1;j++)
 *(*(trans+j)+i)=*(*(arr+i)+j);
}
return trans;
}

double** identity(int dim)
{
double **CO;
int i,j;
CO=init(CO,dim,dim);
for(i=0;i<dim;i++)
{
 for(j=0;j<dim;j++)
 {
 if(i==j)
 {
 CO[i][j]=1.0;
 }
 else
 {
 CO[i][j]=0.0;
 }
 }
 }
 return CO;
 }
```

```
Void Jacobi_Cyclic_Method (double eigenvalues[N], double*eigenvectors[N][N],double
*A, int n)
{
int row, i, j, k, m;
double *pAk, *pAm, *p_r, *p_e;
double threshold_norm;
double threshold;
double tan_phi, sin_phi, cos_phi, tan2_phi, sin2_phi, cos2_phi;
double sin_2phi, cos_2phi, cot_2phi;
double dum1;
double dum2;
double dum3;
double r;
double max;
 if ( n < 1) return;
 if ( n == 1) {
  eigenvalues[0] = *A;
 *eigenvectors[0][0] = 1.0;
  return;
 }

 for (p_e = eigenvectors, i = 0; i < n; i++)
   for (j = 0; j < n; p_e++, j++)
     if (i == j)
     *p_e = 1.0; else *p_e = 0.0;
 for (threshold = 0.0, pAk = A, i = 0; i < ( n - 1 ); pAk += n, i++)
   for (j = i + 1; j < n; j++) threshold += *(pAk + j) * *(pAk + j);
 threshold = sqrt(threshold + threshold);
 threshold_norm = threshold * DBL_EPSILON;
 max = threshold + 1.0;
 while (threshold > threshold_norm) {
   threshold /= 10.0;
   if (max < threshold) continue;
   max = 0.0;
   for (pAk = A, k = 0; k < (n-1); pAk += n, k++) {
for (pAm = pAk + n, m = k + 1; m < n; pAm += n, m++) {
```

```
 if ( fabs(*(pAk + m)) < threshold ) continue;
cot_2phi = 0.5 * ( *(pAk + k) - *(pAm + m) ) / *(pAk + m);
        dum1 = sqrt( cot_2phi * cot_2phi + 1.0);
        if (cot_2phi < 0.0) dum1 = -dum1;
        tan_phi = -cot_2phi + dum1;
        tan2_phi = tan_phi * tan_phi;
        sin2_phi = tan2_phi / (1.0 + tan2_phi);
        cos2_phi = 1.0 - sin2_phi;
        sin_phi = sqrt(sin2_phi);
        if (tan_phi < 0.0) sin_phi = - sin_phi;
        cos_phi = sqrt(cos2_phi);
        sin_2phi = 2.0 * sin_phi * cos_phi;
        cos_2phi = cos2_phi - sin2_phi;
        p_r = A;
        dum1 = *(pAk + k);
        dum2 = *(pAm + m);
        dum3 = *(pAk + m);
        *(pAk + k) = dum1 * cos2_phi + dum2 * sin2_phi + dum3 * sin_2phi;
        *(pAm + m) = dum1 * sin2_phi + dum2 * cos2_phi - dum3 * sin_2phi;
        *(pAk + m) = 0.0;
        *(pAm + k) = 0.0;
        for (i = 0; i < n; p_r += n, i++) {
          if ( (i == k) || (i == m) ) continue;
          if ( i < k ) dum1 = *(p_r + k);
           else
             dum1 = *(pAk + i);
          if ( i < m ) dum2 = *(p_r + m); else dum2 = *(pAm + i);
          dum3 = dum1 * cos_phi + dum2 * sin_phi;
          if ( i < k ) *(p_r + k) = dum3; else *(pAk + i) = dum3;
          dum3 = - dum1 * sin_phi + dum2 * cos_phi;
          if ( i < m ) *(p_r + m) = dum3; else *(pAm + i) = dum3;
        }
        for (p_e = eigenvectors, i = 0; i < n; p_e += n, i++) {
          dum1 = *(p_e + k);
          dum2 = *(p_e + m);
          *(p_e + k) = dum1 * cos_phi + dum2 * sin_phi;
```

```
            *(p_e + m) = - dum1 * sin_phi + dum2 * cos_phi;
          }
        }
        for (i = 0; i < n; i++)
          if ( i == k ) continue;
          else if ( max < fabs(*(pAk + i))) max = fabs(*(pAk + i));
      }
    }
    for (pAk = A, k = 0; k < n; pAk += n, k++) eigenvalues[k] = *(pAk + k);
}
double** column(double** matrix,int row,int col)
{
int i,j,k=0;
double **column;
column=init(column,row,col);
for(i=0,j=(col-1);i<row;i++)
{
*(*(column+i)+k)=*(*(matrix+i)+j);
}
return column;
}
double** divide(double** matrix,int row,int col,double Ch_sq)
{
int i,j,k=0;
double **divide;
divide=init(column,row,col);
for(i=0,j=(col-1);i<row;i++)
{
*(*(divide+i)+k)=*(*(matrix+i)+j) / Ch_sq;
}
return divide;
}
double** wpq(double** matrix,int row,int col)
{
int i,j,k=0;
double **wpq;
```

```
wpq=init(wpq,row,col);
for(i=0;i<row;i++)
{
*(*(wpq+i)+k)= *(*(matrix+i)+k);
}
return wpq;
}
double addition(double** matrix,int row,int col)
{
int i,j=col-1;
double add=0.0;
for(i=0;i<row;i++)
add+= *(*(matrix+i)+j);
return add;
}
double** minus(double** matrix1,double** matrix2,int col)
{
int i,j;
double **minus;
minus=init(minus,col,col);
for(i=0;i<col;i++)
{
 for(j=0;j<col;j++)
 *(*(minus+i)+j)=( *(*(matrix1+i)+j) - *(*(matrix2+i)+j) );
}
return minus;
}
```

ANNEXURE V

```
#include <stdio.h>
#include <string.h>
int main()
{
   FILE* fp;
   fp = fopen("/dev/uart", "w+");
  if(fp){
 printf("UART open. \n");
   }
 else{
 printf("UART closed. \n");
  return 0;
   }
    printf("\n now type on the console\n");
   fprintf(fp,"PM:LAMBDA 2000");
   fclose(fp);
   return 0;
}
```

ANNEXURE VI

Lorentz oscillator modeling for eight oscillators for spectra's for samples.

```
fre= [2000; 2050; 2150; 2200; 2280; 2300; 2320; 2400; 2430; 2500];
line= [20.1;    10.8; 30.3;  20.5;  50.3;  10.8;  30.3;  15.8;  15.0;  30.0;];
fid = fopen('Lortzpls_cali.txt','wt') ;
fid = fopen('Lortzpls_cali.txt','at');
count1 = fprintf (fid,'%s\t','Tem');
count1 = fprintf (fid,'%s\t','SColx');
count1 = fprintf(fid,'%s\t','c1');
count1 = fprintf(fid,'%s\t','c2');
count1 = fprintf(fid,'%s\t','c3');
count1 = fprintf(fid,'%s\t','c4');
count1 = fprintf(fid,'%s\t','c5');
count1 = fprintf(fid,'%s\t','c6');
count1 = fprintf(fid,'%s\t','c7');
%count1 = fprintf(fid,'%s\t','c8');
for j=2000:2:2500
fid = fopen('Lortzpls_cali.txt','at');
count = fprintf(fid,'%d ',j);
count3= fprintf(fid,'%s\t', ' ');
end
count3 = fprintf(fid,'\n')
initialwave=2000;
finalwave=2500;
resolution=(finalwave-initialwave)/50;
%resolution=30;
o_str1=0;o_str2=0;o_str3=0;o_str4=0;o_str5=0;o_str6=0;
a = 10; b = 50;
x = a + (b-a) * rand(5)
%o_str1=a+ (b-a)*rand(1,resolution);
%o_str2=a+ (b-a)*rand(1,resolution);
%o_str3=a+ (b-a)*rand(1,resolution);
```

```
%o_str4=a+ (b-a)*rand(1,resolution);
%o_str5=a+ (b-a)*rand(1,resolution);
%o_str6=a+ (b-a)*rand(1,resolution);
%o_str7=a+ (b-a)*rand(1,resolution);
o_str1=rand(1,resolution);
o_str2=rand(1,resolution);
o_str3=rand(1,resolution);
o_str4=rand(1,resolution);
o_str5=rand(1,resolution);
o_str6=rand(1,resolution);
o_str7=rand(1,resolution);
fid = fopen('Lortzpls_cali.txt','at');

l=1;
fre_line=0;
n1=0;
% c1= Glucose(70-110 mgm/dl); c2= Serum Cholesterol(130-220 mgm/dl);
 %c3=Serum Urea(10-45 mgm/dl), c4=serum triglycerides(65-160 mgm/dl),
 %c5=HDL cholesterol(35-60 mgm/dl), c6=LDL Cholesterol(130-150),
 %c7=LDL(130-150mgm/dl) and lambda= 0.4 to 0.7
 %Temperature t=25-40 degrees, Skin complexion s = 0.2 - 0.4 .

for t=0.25:0.05:0.25
   for s=0.2:0.1:0.2
     for c1 =90:10:100
  for c2 =145:30:180
      for c3 =30:5:40
         for c4 =70:20:100
            for c5 =45:5:50
            for c6 =140:10:150
               for c7 =145:5:150

   count3 = fprintf(fid,'%d',t);
   count3 = fprintf(fid,'\t%d',s);
   count3 = fprintf(fid,'\t%d',c1);
   count3 = fprintf(fid,'\t%d',c2);
```

```
   count3 = fprintf(fid,'\t%d',c3);
   count3 = fprintf(fid,'\t%d',c4);
   count3 = fprintf(fid,'\t%d',c5);
   count3 = fprintf(fid,'\t%d',c6);
   count3 = fprintf(fid,'\t%d',c7);
   count3 = fprintf(fid,'\t%d',' ');
   o_str1=t*s*c1*o_str1/10;
   o_str2=t*s*c2*o_str2/10;
   o_str3=t*s*c3*o_str3/10;
   o_str4=t*s*c4*o_str4/10;
   o_str5=t*s*c5*o_str5/10;
   o_str6=t*s*c6*o_str6/10;
   o_str7=t*s*c7*o_str7/10;

Epsilon=1;
k=1;
for j=2000:2:2500
sum1=0;sum2=0;sum3=0;sum4=0;sum5=0;sum6=0;sum7=0;
for i=1:1:10
      sum1 = sum1 + ((o_str1(1,i)*fre(i,1)^2)/((fre(i,1)^2)-(j^2)-(sqrt(-1)*j*line(i,1))));
      sum2 = sum2 + ((o_str2(1,i)*fre(i,1)^2)/((fre(i,1)^2)-(j^2)-(sqrt(-1)*j*line(i,1))));
      sum3 = sum3 + ((o_str3(1,i)*fre(i,1)^2)/((fre(i,1)^2)-(j^2)-(sqrt(-1)*j*line(i,1))));
      sum4 = sum4 + ((o_str4(1,i)*fre(i,1)^2)/((fre(i,1)^2)-(j^2)-(sqrt(-1)*j*line(i,1))));
      sum5 = sum5 + ((o_str5(1,i)*fre(i,1)^2)/((fre(i,1)^2)-(j^2)-(sqrt(-1)*j*line(i,1))));
      sum6 = sum6 + ((o_str6(1,i)*fre(i,1)^2)/((fre(i,1)^2)-(j^2)-(sqrt(-1)*j*line(i,1))));
      sum7 = sum7 + ((o_str7(1,i)*fre(i,1)^2)/((fre(i,1)^2)-(j^2)-(sqrt(-1)*j*line(i,1))));
end
sum1 = sqrt(Epsilon + sum1);%n1(1,k)=sum1/15;
sum2 = sqrt(Epsilon + sum2);%n2(1,k)=sum2/15;
sum3 = sqrt(Epsilon + sum3);%n3(1,k)=sum3/15;
sum4 = sqrt(Epsilon + sum4);%n4(1,k)=sum4/15;
sum5 = sqrt(Epsilon + sum5);%n5(1,k)=sum5/15;
sum6 = sqrt(Epsilon + sum6);%n6(1,k)=sum6/15;
sum7 = sqrt(Epsilon + sum7);%n7(1,k)=sum7/15;
%fid = fopen('specLortzdata4.txt','at');
%count1 = fprintf(fid,'\t%d ',sum);
```

```
%sum = sum1;
%w = conv(u,v)
%sum=sum1
sum=sum1+sum2+sum3+sum4+sum5+sum6+sum7;
%fid = fopen('specLortzdata1.txt','at');
n1(k,l)=sum/500;
fre_line(k,l)=j;
   count3 = fprintf(fid,'\t%d',sum);

%count3= fprintf(fid,'%s\t',sum);
k=k+1;
end
l=l+1;

%plotyy(fre_line,n1,fre_line,n2,fre_line,n3,fre_line,n4,fre_line,n5,fre_line,n6,fre_line,n7)
%plot(fre_line,n1,n2,n3,n4,n5,n6,n7);
count3 = fprintf(fid,'\n');
                    end
                end
              end
            end
          end
        end
        end
        end
      end
     end
plot(fre_line,n1);
status=fclose(fid);
```

(Note: Single Spectra can be generated just by customizing the concentration control structure.)

ANNEXURE VII:

```
if nargin==0
 error('clarke:Inputs','There are no inputs.')
end
if length(yp) ~= length(y)
   error('clarke:Inputs','Vectors y and yp must be the same length.')
end
if (max(y) > 400) || (max(yp) > 400) || (min(y) < 0) || (min(yp) < 0)
   error('clarke:Inputs','Vectors y and yp are not in the physiological range of glucose
(<400mg/dl).')
end
scrsz = get(0,'ScreenSize')-[0 -5 0 72];
n = length(y);
figure
h = plot(y,yp,'ko','MarkerSize',4,'MarkerFaceColor','k','MarkerEdgeColor','k');
xlabel('Reference Concentration [mg/dl]');
ylabel ('Predicted Concentration [mg/dl]');
ylabel ('Concentracion Predicha [mg/dl]');
title('Clarke"s Error Grid Analysis');
set(gca,'XLim',[0 400]);
set(gca,'YLim',[0 400]);
axis square
hold on
plot([0 400],[0 400],'k:')              % Theoretical 45° regression line
plot([0 175/3],[70 70],'k-')
plot([175/3 320],[70 400],'k-')
plot([70 70],[84 400],'k-')
plot([0 70],[180 180],'k-')
plot([70 290],[180 400],'k-')           % Corrected upper B-C boundary
plot([70 70],[0 175/3],'k-')
plot([70 400],[175/3 320],'k-')
plot([180 180],[0 70],'k-')
plot([180 400],[70 70],'k-')
plot([240 240],[70 180],'k-')
plot([240 400],[180 180],'k-')
plot([130 180],[0 70],'k-')             % Lower B-C boundary slope OK
```

```
text(30,20,'A','FontSize',12);
text(30,150,'D','FontSize',12);
text(30,380,'E','FontSize',12);
text(150,380,'C','FontSize',12);
text(160,20,'C','FontSize',12);
text(380,20,'E','FontSize',12);
text(380,120,'D','FontSize',12);
text(380,260,'B','FontSize',12);
text(280,380,'B','FontSize',12);
set(gcf, 'color', 'white');              % sets the color to white
%print(gcf,'-dmeta','Clarke_EGA');
total = zeros(5,1);
percentage = zeros(5,1);                 % Initializes output
for i=1:n,
  if (yp(i) <= 70 && y(i) <= 70) || (yp(i) <= 1.2*y(i) && yp(i) >= 0.8*y(i))
    total(1) = total(1) + 1;             % Zone A
  else
    if ( (y(i) >= 180) && (yp(i) <= 70) ) || ( (y(i) <= 70) && yp(i) >= 180 )
      total(5) = total(5) + 1;           % Zone E
    else
      if ((y(i) >= 70 && y(i) <= 290) && (yp(i) >= y(i) + 110) ) || ((y(i) >= 130 && y(i)
<= 180)&& (yp(i) <= (7/5)*y(i) - 182))
        total(3) = total(3) + 1;         % Zone C
      else
  if ((y(i) >= 240) && ((yp(i) >= 70) && (yp(i) <= 180))) || (y(i) <= 175/3 && (yp(i) <= 180) &&
(yp(i) >= 70)) || ((y(i) >= 175/3 && y(i) <= 70) && (yp(i) >= (6/5)*y(i)))
          total(4) = total(4) + 1;% Zone D
        else
          total(2) = total(2) + 1;% Zone B
        end                              % End of 4th if
      end                                % End of 3rd if
    end                                  % End of 2nd if
  end                                    % End of 1st if
end                                      % End of for loop
percentage = (total./n)*100;
```

REFERNCES

REFERENCES

[1] Wilfrid G. Oakley, Transactions of the Medical Society of London, 78:16, (1962).

[2] Zimmet P,Alberti KGMM and Shaw J,"Global and societal implications of the diabetes epidemic." Nature, vol.414, 2001, pp.782-787.

[3] The Silver Book: Chronic Disease and Medical Innovation in an Aging Nation, Advancing Science, Enhancing Life.

[4] Centers for Disease Control and Prevention, National Diabetes Fact Sheet, 2005.

[5] Goldman et al., The Value of Elderly Disease Prevention,2005.

[6] American Diabetes Association, Federal Legislative Priorities for the 109th Congress.

[7] Diabetes Atlas 3rd Edition, International Diabetes Federation, 2006.

[8] American Diabetes Association, "All About Diabetes." November 2006.

[9] Merriam-Webster's Medical Dictionary. Springfield, Massachusetts: Merriam-Webster, Inc., 2006.

[10] Renard E. "Monitoring glycemic control: the importance of self-monitoring of blood glucose." Am J Med. 2005; vol.118:12S-19S.

[11] Heise, H. M. Glucose, In Vivo Assay of. In: Meyers, R.A. Encyclopedia of analytical chemistry, John Wiley Press, vol. 1, p. 56-83, 2000.

[12] National Diabetes Statistics, 2007 Bethesda, MD: U.S. Department of Health and Human Services, National Institutes of Health, 2008.

[13] How to Control Diabetes Through Yoga, Articlebase, Aug 2009.

[14] Jonathon T. Olesberg, Lingzhi Liu, Valerie Van Zee, and Mark A. Arnold,"In Vivo Near-Infrared Spectroscopy of Rat Skin Tissue with Varying Blood Glucose Levels" , Anal. Chem., 2006, vol.78 (1), pp. 215–223

[15] American Diabetes Association, "Economic Costs of Diabetes in the U.S. in 2002," inDiabetes Care, 2003, vol. 26, pp. 917-932.

[16] Arthur C. Guyton & John E. Hall, Textbook on Medical Physiology, Pub: W B Saunders Co, July 2005.

[17] Jo McEntyre, Bethesda, "The Genetic Landscape of Diabetes", National Center for Biotechnology Information (US); 2004.

[18] Norman Endocrine Surgery Clinic, "Normal Regulation of Blood Glucose, " Norman Endocrine Surgery Clinic, 2002.

[19] Vickers TJ, Mann CK. Quantitative analysis by Raman spectroscopy. Garassili JG Bulkin BJ eds. Analytical Raman spectroscopy 1991:107-135 Wiley New York.

[20] Lombardi DJ, Wang C, Sun B, Fountain AW, III, Vickers JJ, Mann CK, et al. "Quantitative and qualitative analysis of some inorganic compounds by Raman spectroscopy", Appl Spectrosc 1994, vol.48, pp.875-883.

[21] Tanaka K, Pacheco MTT, Brennan JF, III, Itzkan I, Berge AJ, Dasari RR, Feld MS. "Compound parabolic concentrator probe for efficient light collection in spectroscopy of biological tissues", Appl Opt 1996, vol. 35, pp. 758-763.

[22] Wickramasinghe Y., Yang Y., Spencer S.A. Current problems and potential techniques in in-vivo glucose monitoring. Journal of Fluorescence 2004, vol.14, pp. 513-520.

[23] Allen. T.J., Cox B.T, Beard P.C," Generating photoacoustic signals using high peak power laser diodes", Proceedings of the SPIE 2005, vol. 5697, pp. 233-242.

[24] Glucon, "A personal, non-invasive, real-time and continuous blood glucose monitoring"

[25] Emilio Squillante , "Applications of Fiber-Optic Evanescent Wave Spectroscopy", Taylor and Francis Group ,1998, vol.24(12), pp. 1163 – 1175.

[26] Pickup. JC., Hussain F., Evans N. D., Sachedina N. In vivo glucose monitoring:the clinical reality and the promise. Biosensors and Bioelectronics, 2005, vol. 20, pp.1897-1902.

[27] Khalil O.S. "Non-invasive glucose measurement technologies: an update from 1999 to the dawn of the new millennium", Diabetes Technology & Therapeutics, 2004, vol. 6, pp. 660-697.

[28] Malchoff C.D, Shoukri K, Landau J.I, Buchert J.M, "A novel non-invasive blood glucose monitor", Diabetes Care 2002, vol. 25, pp. 2268–2275.

[29] Leboulanger B, Guy R.H, Delgado-Charro M.B,"Reverse iontophoresis for non-invasive transdermal monitoring", Physiological Measurement, 2004, vol.25, pp.35-50.

[30] Potts R.L O, Tamada J.A, Tierney M. J,"Glucose monitoring by reverse iontophoresis", Diabetes Metabolism Research and Reviews, 2002, vol. 18, pp. S49-S53.

[31] Burmeister J.J, Arnold M.A,"Evaluation of measurement sites for non-invasive bloodglucose sensing with near-infrared transmission spectroscopy", Clinical Chemestry, vol. 45.

[32] Caduff A, Dewarrat, F., Talary, M., Stalder, G., Heinemann L, Feldman Y ," Non-invasive glucose monitoring in patients with diabetes: A novel system based on impedance spectroscopy" , Biosense Bioelectron 2006, vol. 22, pp. 598-604.

[33] Advait V. Badkar,Alan M. Smith,Jonathan A. Eppstein and Ajay K. Banga" Transdermal Delivery of Interferon Alpha-2B using Microporation and Iontophoresis in Hairless Rats, Springer 2007

[34] Yuzhakov V.V., Smith A., "Numerical Modeling of Skin Microporation for Continuous Transdermal Insulin Delivery with PassPort Patch", Invited Presentation at Georgia Tech Symposium on Computing Systems and Networking Technologies, Atlanta GA, February 18, 2005.

[35] Kirill V. Larin, Mohsen S. Eledrisi,Massoud Motamedi, PHD and Rinat O. Esenaliev,"Non-invasive Blood Glucose Monitoring With Optical Coherence Tomography, A pilot study in human subjects", Diabetes care.

[36] Kyung Cho,Yoon Ok Kim,1 Hiroshi Mitsumaki,Katsuhiko Kuwa," Noninvasive Measurement of Glucose by Metabolic Heat Conformation Method", Clinical Chemistry 2004, vol.50(10), pp.1894–1898.

[37] Choul-Gyun Lee, "Calculation of light penetration depth in photobioreactors", Biotechnology and Bioprocess Engineering, springer 1999,vol.4,pp.78-81.

[38] Leonid Fukshansky," Absorption statistics in turbid media", Journal of Quantitative Spectroscopy and Radiative Transfer, 1987, vol.38(5), pp. 389-406.

[39] R. R. Anderson and J. A. Parrish, "The optics of human skin", J. Invest. Dermatol. , 1981, vol. 77, pp.13-19.

[40] Handbook of Near-Infrared Analysis, Marcel Dekker, Inc., New York (2001).

[41] Infrared and Raman Spectroscopy of Biological Materials, Marcel Dekker, Inc., New York (2000).

[42] H. Zeller, P. Novak,P. Landgraf, "Blood glucose measurement by infrared spectroscopy," Int. J. Artif. Organs, 1989, vol.12(2), pp. 129-135.

[43] P. Bhandare, Y. Mendelson, A. Robert, G¨unther Janantsch, J¨urgen D. Kruse-Jarres, Ralf Marbach, and Michael H. Heise, "Multivariate Determination of Glucose in Whole Blood Using Partial Least-Squares and Artificial Neural Networks Based on Mid-Infrared Spectroscopy," Appl. Spectrosc.,1993,vol.47(8), pp. 1214-1221.

[44] H. M. Heise , A. Bittner, "Investigation of Experimental Errors in the Quantitative Analysis of Glucose in Human Blood Plasma by ATR-IR Spectroscopy", J. Mol. Struct., 1995,vol.348, pp. 21-24.

[45] H. M. Heise , R. Marbach, "Human Oral Mucosa Studies with Varying Blood Glucose Concentration by Non-Invasive ATR-FT-IR spectroscopy", Cellular and Molecular. Biol., 1999,vol.44(6), pp. 899-912.

[46] Kenneth J. Ward, David M. Haaland, M. Ries Robinson, R. Philip Eaton, "Post-Prandial Blood Glucose Determination by Quantitative Mid- Infrared Spectroscopy," Appl. Spectrosc., 1992, vol.46 (6), pp. 959-965.

[47] Jason J. Burmeister and Mark A. Arnold, "Evaluation of Measurement Sites for Noninvasive Blood Glucose Sensing with Near-Infrared Transmission Spectroscopy," Clin. Chem., 1999, vol. 45(9), pp. 1621-1627.

[48] H. Chung, Mark A. Arnold, M. Rhiel, David W. M, "Simultaneous Measurements of Glucose, Glutamina, Ammonia, Lactate, and Glutamate in Aqueous Solutions by Near-Infrared Spectroscopy," Appl. Spectrosc., 1996,vol.50(2), pp. 270-276 .

[49] Kevin H. Hazen, Mark A. Arnold, and Gary W. Small, "Temperature- Insensitive Near-Infrared Spectroscopic Measurement of Glucose in Aqueous Solutions," Appl. Spectrosc., 1994, vol.48(4), pp. 477-483 .

[50] R. Vonach, J. Buschmann, R. Falkowski, R. Schindler, B. Lendl, and R. Kellner, "Application of Mid-Infrared Transmission Spectrometry to the Direct Determination of Glucose in Whole Blood," Appl. Spectrosc., 1999, vol.52(6), pp. 820-822.

[51] T. Yano, T. Funats,K. Suehara, Y. Nakano, "Measurement of the concentrations of glucose and citric acid in the aqueous solution of a blood anticoagulant using near infrared spectroscopy," J. Near Infrared Spectrosc., 2001, vol.9, pp. 43-48.

[52] Gilwon Yoon, Yoen-Joo Kim, and Sangjoon Hahn, "Determination of glucose in whole blood samples by mid-infrared spectroscopy," Appl. Opt., 2003,vol.42(4).

[53] Elaine N. N. Marieb, "Human Anatomy And Physiology", Benjamin-cummings Publishing Company, 1995, **ISBN:** 0805343229.

[54] George M. Hale and Marvin R. Querry, "Optical Constants of Water in the 200-nm to 200-μm Wavelength Region",Applied Optics,1973,vol. 12(3), pp. 555-563.

[55] Phelan MK, Barlow CH, Kelley JJ, Jinguji TM, Callis JB. Measurement of caustic and caustic brine solutions by spectroscopic detection of the hydroxide ion in the near-infrared region 700–1150 nm", Anal Chem, 1989,vol.61,pp.1419-1424.

[56] Lin J, Brown CW. Near-IR spectroscopic determination of NaCl in aqueous solutions. Appl Spectrosc, 1992,vol.46,pp.1809–15.

[57] Lin J, Brown CW, " Spectroscopic measurement of NaCl and sea water salinity in the near-IR region of 680–1230 nm", Appl Spectrosc, 1993,vol.47,pp.239-241.

[58] Lin J, Brown CW, "Near-IR fiber optic temperature sensor", Appl Spectrosc, 1993,vol. 47,pp.62-68.

[59] Lin J, Brown CW, "Universal approach for determination of physical and chemical properties of water by near-IR spectroscopy",Appl Spectrosc,1993,vol.47, pp.1720-1727.

[60] Kelley JJ, Kelley KA, Barlow CH, "Tissue temperature by near-infrared spectroscopy", SPIE Proc 1995, vol.2389,pp.818–28.

[61] Wheeler OH. "Near-IR spectra of organic compounds. ", Chem Rev 1959, vol.59, pp.629-666.

[62] Vasko PD, Blackwell J,Koenig JL, "Infrared and Raman spectroscopy of carbohydrates. I. Identification of O-H and C-H vibrational modes for D-glucose, maltose, cellobiose, and dextran by deuterium substitution methods." Carbohydr Res, 1971,vol.19, pp.297-310.

[63] Vasko PD, Blackwell J,Koenig JL," Infrared and Raman spectroscopy of arbohydrates. II.Normal coordinate analysis of α-D-glucose." Carbohydr Res 1972, vol. 23, pp.407-417.

[64] Cael JJ, Koenig JL, Blackwell J. Infrared and Raman spectroscopy of carbohydrates. IV. Identification of configuration and conformation sensitive modes for D-glucose by normal coordinate analysis.", Carbohydr Res, 1974,vol.32,pp.79-91.

[65] Low MJD, Yang RT. "The measurement of infrared spectra of aqueous solutions using Fourier transform spectroscopy", Spectrochem Acta ,1973,vol.20A,pp.1761-1772.

[66] Hall JW, Quaresima V, Ferrari M. "Can we get more tissue biochemistry information from in vivo near-infrared spectra?." SPIE Proc ,1995,vol.2387,pp.225-231.

[67] Marquardt LA, Arnold MA, Small GW. "Near-infrared spectroscopic measurement of glucose in a protein matrix.", Anal Chem, 1993,vol.65,pp.3271-3278.

[68] Hazen KH, Arnold MA, Small GW. Temperature-insensitive near-infrared spectroscopic measurements of glucose in aqueous solutions. Appl Spectrosc ,1994,vol.48,pp.477-483.

[69] Small GW, Arnold MA, Marquardt LA. "Strategies for coupling digital filtering with partial least-squares regression: application to the determination of glucose in plasma by Fourier transform near-infrared spectroscopy",Anal Chem ,1993,vol.65,pp.3279-3289.

[70] Arnold MA. "Non-invasive glucose monitoring." Curr Opin Biotechnol,1996,vol.7, pp. 46-49.

[71] Arnold MA. "New developments and clinical impact of non-invasive monitoring." Clinical laboratory automation, robotics and knowledge optimization, Jhon Willey1995, pp.631-647 ,

[72] Chung S, Arnold MA, Rhiel M, Murhammer DW. "Simultaneous measurement of glucose and glutamine in aqueous solutions by near infrared spectroscopy." Appl Biochem Biotechnol, 1995,vol.40,pp.109-125.

[73] Tuchin V "Tissue Optics: light scattering methods and instruments for medical diagnosis." SPIE Press, 2000.

[74] Jacques SL ,"Origins of tissue optical properties in the UVA, visible and NIR regions" OSA TOPS on advances in optical imaging and photon migration ,1996, vol.2,pp. 364-371.

[75] Cope M, "The Application of Near Infrared Spectroscopy to Non-Invasive Monitoring of Cerebral Oxygenation of the Newborn Infant" Department of Medical Physics and Bioengineering, University College London,1991,pp.214–223.

[76] S. Haddad, P. Poulin and K. Krishnan "Relative lipid content as the sole mechanistic determinant of the adipose tissue:blood partition coefficients of highly lipophilic organic chemicals" Chemosphere,2000,vol.40(8), pp. 839-843.

[77] Ginsberg BH. "An overview of minimally invasive technologies." Clin Chem, 1992, vol.38,pp.1596-1600.

[78] Klonoff DC "Non-invasive blood glucose monitoring" Diabetes Care, 1997,vol.20, pp.433-437.

[79] Heise HM. "Non-invasive monitoring of metabolites using near infrared spectroscopy: state of the art." Horm Metab Res, 1996, vol.28,pp.527-534.

[80] Coté GL. "Non-invasive optical glucose sensing–an overview." J Clin Eng, 1997, vol.22,pp.253-259.

[81] Heise HM, Bittner AB. "Blood glucose assays based on infrared spectroscopy: alternatives for medical diagnostics." SPIE Proc, 1998, vol.3257,pp.2-12.

[82] Rajanish KK, Santosh SA, Vinod SG . "Unleash the System On Chip using FPGAs and Handel C", Springer, 2009.

[83] Messerschmitt DG "Echo cancellation in speech and data transmission" IEEE, J. on selected areas in communication,1984, vol.2, pp.283-297.

[84] Mishra, P. and Dutt, N., "Architectural description languages for programmable embedded systems", IEE Proceedings of Computers and Digital Techniques, 2005, pp. 285–297.

[85] Coelo Jr, C. J. N., Da Silva Jr., D. C., Fernandes, A. O. "Hardware software codesign of embedded systems", Proceedings of the 11th Brazilian Symposium on Integrated Circuit Design, January 1998, pp.2–8.

[86] Ernst R. "Codesign of embedded systems: status and trends", Proceedings of IEEE Design and Test, 1998, pp.45–54.

[87] Altera Corporation Website, June 2006.

[88] "NIOS II Processor Handbook", Altera Corporation, October 2005.

[89] "MicroBlaze Processor Reference Guide", Xilinx Corporation, 2005.

[90] PicoBlaze 8-bit Embedded Microcontroller User Guide", Xilinx Corporation.

[91] "Tensilica Diamond Standard Series Product Brief", Tensilica Incorporated, 2006.

[92] Tom R. Halfhill, "Tensilica's Preconfigured Cores", Microprocessor Report, 2006.

[93] Xtensa Overview, www.tensilica.com/products/overview.htm, June 2006

[94] Create TIE, www.tensilica.com/products/create tie.htm, Septembe 2006.

[95] XPRESS Compiler, http://www.tensilica.com/products/xpres.htm,September 2006.

[96] Opencores.org Website, www.opencores.org, June 2006.

[97] UT NIOS Homepage, www.eecg.toronto.edu/~plavec/utnios.html, June2006.

[98] "GRLIB IP Core User's Manual", Gaisler Research, February 2006.

[99] SOPC Builder Applications ALTERA 2005.

[100] Lee DS, Jeon CO, Park JM, Chang KS. "Hybrid neural network modelling of a full-scale industrial wastewater treatment process." Biotechnol Bioeng, 2002,vol.78, pp.670–82.

[101] Lee DS, Park JM, Vanrolleghem PA. "Adaptive multiscale principal component analysis for on-line monitoring of a sequencing batch reactor" J Biotechnol, 2005,vol.116, pp.195–210.

[102] Lee DS, Vanrolleghem PA."Monitoring of a sequencing batch reactor using adaptive multiblock pricipal component analysis" Biotechnol Bioeng,2003,vol.82(4), pp.489–97.

[103] MacGregor JF, Kourti T. "Statistical process control of multivariate processes" Control Eng Pract ,1995,vol.3,pp.403–14.

[104] Wise BM, Gallagher NB. "The process chemometrics approach to process monitoring and fault detection" J Proc Control, 1996, vol.6,pp.329–348.

[105] Geladi P, Kowalski BR. "Partial least-squares regression: a tutorial." Anal Chim Acta, 1986,vol.185,pp.1–17.

[106] Wold S, Ruhe A, Wold H, Dunn WJ. "The Collinearity problem in linear regression. The partial least squares approach to generalized inverse." SIAM J Sci Stat Comput, 1984, vol.3,pp.735–743.

[107] H. Martens and T. Naes, Multivariate Calibration, John Wiley & Sons,New York, 2nd edn., 1991.

[108] de Jong, S. "SIMPLS: an alternative approach to partial least squares regression" Chemometrics and Intelligent Laboratory Systems, 1993,vol.18,pp.251–263.

[109] Randall T.D. "An Introduction to Partial Least Squares Regression" SUGI Proceedings,1995.

[110] Ham F.M, Cohen G.M, Kostanic, I., Gooch, B.R. "Multivariate determination of glucose concentrations from optimally filtered frequencywarped NIR spectra of human blood serum" Physiological Measurement,1996, vol. 17, pp. 1-20.

[111] Leger M.N, Ryder A.G. "Comparison of Derivative Preprocessing and Automated Polynomial Baseline Correction Method for Classification and Quantification of Narcotics in Solid Mixtures" Applied Spectroscopy, 2006,vol. 60, pp. 182-193.

[112] Günzler H, Gremlich H.U "IR Spectroscopy: An Introduction" Wiley, 2002, Weinheim, Germany.

[113] Vickers T.J, Wambles R.E, Mann C.K. "Curve fitting and linearity: Data processing in Raman spectroscopy" Applied Spectroscopy, 2001,vol. 55, pp. 389-393.

[114] Mendelson, Y. "Optical Sensors, in The Biomedical Engineering Handbook" CRC, 1995, pp. 764–778.

[115] Small G.W., Arnold M.A., Marquardt L.A. "Strategies for Coupling Digital Filtering with Partial Least-Squares Regression: Application to the Determination of Glucose in Plasma by Fourier Transform Near-Infrared Spectroscopy" Analytical Chemistry, 1993,vol. 65, pp. 3279-3289.

[116] Shen Y C, Linfield E H, Davies A G, Taday P F, Arnone D D and Elsey T S, "Determination of glucose concentration in whole blood using Fourier-transform infrared transmission spectroscopy", 2003,Journal of Biological Physics, vol.29, pp. 129-133.

[117] M. P. Fuller, G. L. Ritter, and C. S. Draper, " Partial Least-Squares Quantitative Analysis of Infrared Spectroscopic Data. Part I: Algorithm Implementation," Appl. Spectrosc,1988, vol.42, pp.217-227

[118] Chance B, "Optical method" Annu. Rev. Biophys. Chem., 1991, vol.20(1).

[119] Tuchin, V. V. , Ed., Handbook of Optical Biomedical Diagnostics, PM107, SPIE Press, 2002,Bellingham, WA.

[120] Goetz MJ Jr, Cote GL, March WE, Erckens R, Motamedi M, "Application of a multivariate technique to Raman spectra for quantification of body chemicals", IEEE Trans Biomed Eng,1995,vol.42(7), pp.728-731.

[121] Arnold, *et al.*, Analytical Chemistry, 1998,vol.70, pp.1773.

[122] MacKenzie HA, Ashton HS, Spiers S, Shen Y, Freeborn SS, Hannigan J, Lindberg J, Rae P, "Advances in photoacoustic noninvasive glucose testing", Clin Chem,1999,vol.45(9), pp.1587-1595.

[123] Shen Y C, Davies A G, Linfield E H, Elsey T S, Taday P F and Arnone D D, "The use of Fourier-transform infrared spectroscopy for the quantitive determination of glucose concentration in whole blood", Physics in Medicine and Biology, 2003,vol.28,pp. 2023-2032.

[124] Arnold, MA; Liu, L; Olesberg, JT "Selectivity assessment of noninvasive glucose measurements based on analysis of multivariate calibration vectors" Journal of Diabetes Science and Technology, 2007, vol.1(4), pp.454-462.

[125] Ren, M; Arnold, MA; "Comparison of multivariate calibration models for glucose, lactate and urea from near infrared and Raman spectra" Analytical and Bioanalytical Chemistry, 2007,vol.387, pp.879-888.

[126] Amerov, AK; Small, GW; Arnold, MA "Selective multivariate analysis of blood glucose with near infrared spectral range" SPIE Proceedings, 2005, pp.180-189.

[127] Chen, J; Arnold, MA; Small, GW "Comparison of combination and first overtone spectral regions for near infrared calibration models for glucose and other biomolecules in aqueous solutions" Analytical Chemistry, 2004,vol.*76*, pp.5405-5413.

[128] Arnold MA, "Review of the monograph Chemometrics in Analytical Spectroscopy", Journal of the American Chemical Society, 2004,vol.126, pp.14678-14679.

[129] Pan S, Chung H, Arnold MA, Small GW, "Near-infrared spectroscopic measurement of physiological glucose levels in variable matrices of protein and triglycerides", Anal Chem, 1996, vol.68(7), pp.1124-1135.

[130] Schugerl , K. , "Progress in monitoring , modeling and control of bioprocesses during the last 20 years" J. Biotechnolol, 200,vol.85, pp.149.

[131] Clarke WL, Cox D, Gonder-Frederick LA ,Carter W, Pohl SL" Evaluating clinical accuracy of systems for self-monitoring of blood glucose" Diabetes Care,1987, vol.10,pp.622–628.

[132] W L Clarke, D Cox, L A Gonder-Frederick, W Carter and S L Pohl "Evaluating clinical accuracy of systems for self-monitoring of blood glucose" Diabetes Care,1987, vol. 10 (5),pp. 622-628.

[133] A. Maran et al. "Continuous Subcutaneous Glucose Monitoring in Diabetic Patients" Diabetes Care, 2002,vol.25(2).

[134] B.P. Kovatchev et al. "Evaluating the Accuracy of Continuous Glucose-Monitoring Sensors"Diabetes Journal ,2004.

[135] Mark A. Arnold, Jason J. Burmeister, and Gary W. Small "Phantom Glucose Calibration Models from Simulated Noninvasive Human Near-Infrared Spectra" Anal. Chem. ,1998, vol.70, pp.1773-1781.

[136] Heise, H. M. "Near-infrared Spectrometry for in vivo Glucose Sensing" in Biosensors in the Body: Continuous in vivo Monitoring , John Wiley, 1997.

[137] Nilsson, A. M. K., Lucassen, G. W. , Verkruysee, W. , AndersssonEngels, S. and van Gemert, M.J.C., Changes in optical properties of human whle blood in vitro due to slow heating, Photochem. Photobiol.,1997, vol. 65(2),pp.366.

[138] Gabriely I, Wozniak R, Mevorach M, Kaplan J, Aharon Y, Shamoon H, "Transcutaneous glucose measurement using near-infrared spectroscopy during hypoglycemia", Diabetes Care, 1999,vol.22(12), pp.2026-2032.

[139] Robinson MR, Eaton RP, Haaland DM, Koepp GW, Thomas EV, Stallard BR, Robinson PL, "Noninvasive glucose monitoring in diabetic patients: a preliminary evaluation", Clin Chem,1992,vol.38(9), pp.1618-1622.

[140] Maier JS, Walker SA, Fantini S, Franceschini MA, Gratton E, "Possible correlation between blood glucose concentration and the reduced scattering coefficient of tissue in the near infrared", Optics Lett 19,1994, pp. 2062-2064.

[141] Angelopoulou, Elli. "The Uniqueness of the Color of Human Skin." Electronic Imaging, SPIE Press, 2001,vol.11(2),pp. 5.

[142] McClure, G. L., "Computerized Quantitative Infrared Analysis" American Society for Testing and Materials, 1987,Philadelphia, PA.

[143] Martens, H. and Naes, T., "Multivariate Calibration" John Wiley & Sons ,1989, New York.